Functional analysis of the neurodevelopmental disorder candidate gene *RUFY4* in *Drosophila melanogaster*

Doctoral thesis

to obtain a doctorate (PhD)

from the Faculty of Medicine

of the University of Bonn

Peiyun Yu

from Hubei, China

2025

Written with authorization of

the Faculty of Medicine of the University of Bonn

First reviewer: Prof. Dr. Peter Soba

Second reviewer: Prof. Dr. Ilona Grunwald Kadow

Day of oral examination: 10.04.2025

From the Life & Medical Science Institute (LIMES)

Table of Contents

List of abbreviations

ADHD	Attention-deficit/hyperactivity disorder
AEL	After egg laying
AM	N-amyl-acetate
AMPK	AMP-activated protein kinase
ARID1B	AT-rich interactive domain 1B
ASD	Autism spectrum disorder
BDSC	Bloomington Drosophila stock center
Brp	Bruchpilot
$CaCl_2$	Calcium chloride
CD	Communication disorders
CDC	Centers for Disease Control and Prevention
cm	Centimeter
CNVs	Copy number variants
d	Day
DNA	Deoxyribonucleic acid
FXS	Fragile X syndrome
GABA	γ-Aminobutyric acid
GFP	Green fluorescent protein
h	Hour
ID	Intellectual disability
IL	Interleukin
IQ	Intelligence quotient
KCl	Potassium chloride
L	Liter
LD	Learning disorders

LED	Light emitting diode
LI	Learning index
M	Mole
MD	Motor disorders
$MgCl_2$	Magnesium chloride
mGluR	Metabotropic glutamate receptor
ml	Milliliter
mm	Millimeter
mM	Millimole
mN	Milli-Newton
mTOR	Mammalian target of rapamycin
NaCl	Sodium chloride
NaH_2PO_4	Monosodium phosphate
$NaHCO_3$	Sodium bicarbonate
NDDS	Neurodevelopmental disorders
nm	Nanometer
PBS	Phosphate-buffered saline
PFA	Paraformaldehyde
PI3K	Phosphatidylinositol (3, 4, 5)-trisphosphate
PKC	Protein kinase C
$PM_{2.5}$	2.5-micrometer particulate matter
PNS	Peripheral nervous system
PtdIns(3)P	Phosphatidylinositol 3-phosphate
RNAi	RNA interference
RUFY	RUN and FYVE domain
SEM	Standard error of mean

Tb	Tubby
TD	Tic disorders
TLR	Toll-like receptors
TNF-α	Tumor necrosis factor-α
TREM2	Myeloid cells 2
TRKA+	Tropomyosin receptor kinase A positive
TS	Tourette syndrome
VNC	Ventral nerve cord
WDR5	WD-repeat domain 5
WES	Whole exome sequencing
µl	Microliter
µW	Microwatt

1. Introduction

1.1 Overview of neurodevelopmental disorders

Neurodevelopmental disorders (NDDs) are a group of conditions that affect the development of the nervous system, leading to impairments in brain development and function variably affecting cognition, motor function, and social adaptability and behavioral regulation (Morris-Rosendahl and Crocq, 2020; Mullin et al., 2013). These disorders generally appear early in development, usually before children enter school, and can impact day-to-day functioning throughout an individual's life.

According to the Diagnostic and Statistical Manual of Mental Disorders, Fifth Edition (DSM-5) published in 2013 (Halter et al., 2013), NDDs are primarily categorized into seven groups: 1. Intellectual disability (ID); 2. Communication disorders (CD); 3. Autism spectrum disorder (ASD); 4. Attention-deficit/hyperactivity disorder (ADHD); 5. Learning disorders (LD); 6. Motor disorders (MD); 7. Tic disorders (TD).

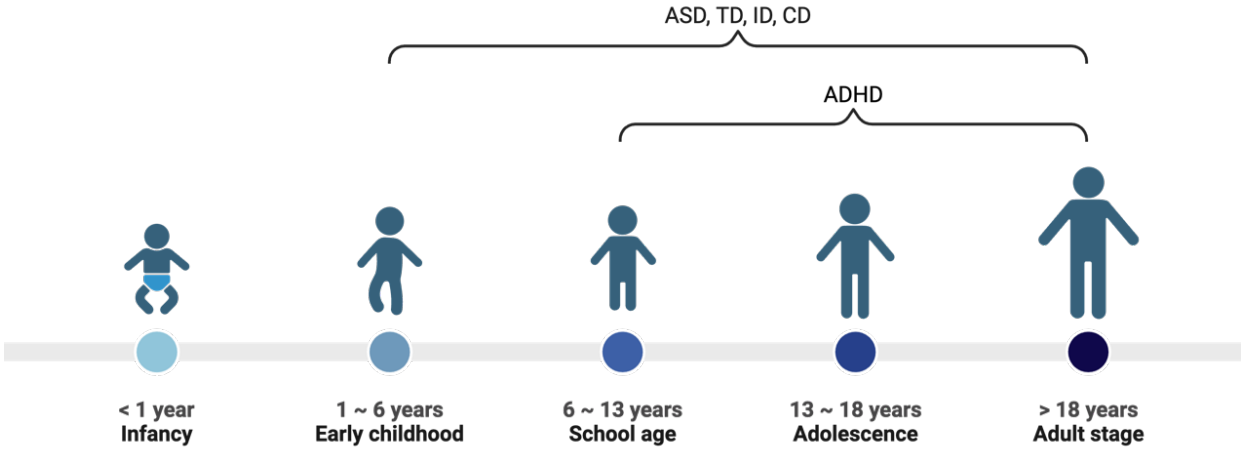

Fig. 1: Typical ages for the initial appearance of neurodevelopmental disorder symptoms. Neurodevelopmental disorders encompass a diverse set of conditions that affect children's development and can continue into adulthood. (ASD) Autism spectrum disorder; (TD) Tic disorders; (ID) Intellectual disability; (CD) Communication disorders; (ADHD) Attention-deficit/hyperactivity disorder (made with BioRender).

The symptoms associated with neurodevelopmental disorders (NDDs) are notably intricate and differ widely in their severity, exerting a significant effect on every aspect of the affected individuals' lives. Key common characteristics of NDDs include:

1) They typically manifest early in a person's life, usually during childhood (Fig. 1). Symptoms and the resulting functional difficulties can continue into adulthood (Antolini and Colizzi, 2023).
2) NDDs are common, affecting about 15 % of the global child and adolescent population (Gidziela et al., 2023). Among these, ADHD is the most prevalent, with about 7.2 % of children diagnosed (Thomas et al., 2015). Autism Spectrum Disorder (ASD) is also a widespread NDD, with a prevalence rate of around 2.8 % (Maenner et al., 2023).
3) NDDs present a variety of developmental abnormalities, resulting in challenges with cognitive, motor, and emotional skills, along with social, academic, and occupational abilities. The level of impairment can range from specific learning limitations to extensive difficulties with social interaction or intellectual functioning.
4) The occurrence of NDDs is more common in males than females. For ADHD, the male-to-female ratio is approximately 4~9:1 (Homberg et al., 2016), for ASD it is about 4:1 (Halter et al., 2013), and for ID it is around 1.3:1 (Piton et al., 2013). Tourette Syndrome (TS), a recognized tic disorder, has a male-to-female diagnosis ratio of 4.3:1 (Freeman et al., 2000).
5) It is not uncommon for various NDD features to coexist within a single individual and to present alongside other conditions, such as anxiety disorders (Hansen et al., 2018), creating a complex array of neuropsychiatric comorbidities. It is estimated that about 30-80 % of individuals with ASD also have some degree of ID (McClain et al., 2017).
6) The etiology of NDDs is multifaceted (Fig. 2) and largely remains elusive. Both neurobiological and environmental factors are thought to play roles in the development of these disorders, either separately or in combination.
7) Currently, there are no definitive targeted treatments for most NDDs. Treatment is primarily symptomatic and varies significantly in effectiveness, requiring a multidisciplinary approach to diagnosis and treatment.

The causes of neurodevelopmental disorders (NDDs) are highly intricate, stemming from a mixture of genetic, environmental, immunological, metabolic, and other influences (Fig.

2). Among these, genetic factors are considered to be the most significant contributors to NDDs.

Genetic factors include a spectrum of anomalies such as chromosomal aberrations, copy number variants (CNVs), monogenic conditions, polygenic mutations, epigenetic modifications, mitochondrial changes, and other genetic mutations that are linked to the development of NDDs. For example, CNVs (D'Arrigo et al., 2016; Zahir and Friedman, 2007) and point mutations (Ropers, 2010) are known to account for certain instances of ID. Epigenetic modifications like DNA methylation (Gropman and Batshaw, 2002) are implicated in conditions such as Fragile X Syndrome (FXS), a leading genetic cause of intellectual disability. CNVs have also been associated with ASD (Jacquemont et al., 2006; Sebat et al., 2007), with duplications in the 15q11.2-11.3 region and microdeletions and duplications in the 16p11.2 region (Weiss et al., 2008) being among the most common. Additionally, single gene mutations are critical to the etiology of ASD-related syndromes, with genes like FMR1 (Fyke and Velinov, 2021), MeCP2 (LaSalle and Yasui, 2009; Sandweiss et al., 2020), and SHANK3 (Zhou et al., 2019) identified as monogenic risk factors. Synaptic mitochondrial dysfunction has been associated with ASD and ID as well (Rojas-Charry wt al., 2021). Remarkably, there is a significant overlap in gene mutations related to ASD and those associated with ID (Vissers et al., 2016), indicating shared molecular pathways among different NDDs.

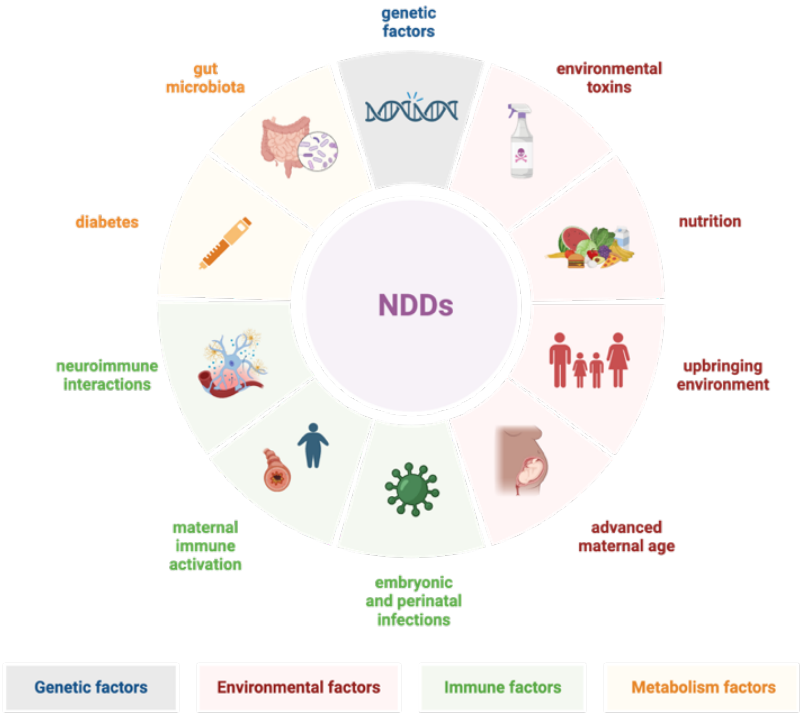

Fig. 2: Causes of neurodevelopmental disorders (NDDs). The origins of neurodevelopmental disorders are multifaceted and frequently elusive, encompassing genetic, environmental, immunological, and metabolic influences among others. In-depth studies into how these various factors—genetic, immune, metabolic, and environmental—interact and impact the onset and progression of neurodevelopmental disorders will be instrumental in enhancing early detection, therapeutic intervention, and prognosis evaluation for these conditions (made with BioRender).

The immune system also plays a major role, with maternal immune activation during pregnancy potentially leading to NDDs in the offspring (Han et al., 2021). A range of maternal inflammatory conditions, such as infections, obesity, asthma, diabetes, autoimmune diseases, and stress, can impact fetal neurodevelopment through various signaling pathway, raising the risk of the child developing NDDs like ADHD, ASD, and TD (Han et al., 2022) . Additionally, neuroimmune interactions are involved in the etiology of NDDs. For instance, deletion of the TREM2 gene is associated with microglial phagocytic dysfunction, impaired synaptic pruning, increased excitatory neurotransmission, and reduced long-range functional connectivity in early neurodevelopment, which can lead to ASD (Filipello et al., 2018). Systemic immunity is another factor, as evidenced by changes in cytokines, chemokines, adhesion molecules, and growth factors in the brain tissues of individuals with ASD (Shen et al., 2018), and elevated levels of pro-inflammatory cytokines

like TNF-α, IL-6, and IL-12 in the peripheral blood of patients with tic disorders (Parker-Athill et al., 2015).

Metabolic factors also play an important role. When a mother has phenylketonuria, it can disrupt the fetal brain development, increasing the likelihood of intellectual disability (Lee et al., 2005). Additionally, the consumption of trace elements (Sharma et al., 2018) and the homeostasis of gut microbiota (Dan et al., 2020; Strati et al., 2017) have been linked to the development of ASD.

Environmental factors from the parents, such as being of an advanced maternal age of 35 years or older, risks during the birth period like fetal distress, and post-birth issues such as a lower birth weight, are connected with the emergence of NDDs (Wang et al., 2017). Exposure to environmental pollutants like lead, organophosphorus pesticides, or fine particulate matter ($PM_{2.5}$) during pregnancy or early childhood is considered to be a risk factor for ADHD (Saxena et al., 2020). Nutritional imbalances in mothers and infants, including both deficiencies and excesses, are associated with the risk of developing NDDs.

Due to the largely unknown causes of most NDDs, treatment tends to be symptomatic, utilizing both pharmacological and non-pharmacological approaches. For example, drugs for treating ADHD are mainly divided into stimulants and non-stimulants, and the efficacy can reach 70 % (Khan et al., 2019). Non-pharmacological interventions often include rehabilitative therapies such as cognitive-behavioral therapy, psychological therapy, and psychological education (Antolini and Colizzi, 2023).

1.2 Consanguineous populations provide a prime opportunity for identifying novel autosomal recessive genes implicated in neurodevelopmental disorders

Intellectual disability (ID) refers to an intelligence quotient (IQ) below 70 and impairments in conceptual, social, and practical adaptive skills starting before 18 years of age (Patel et al., 2020). ID affects 1-3 % of the global population (Moeschler et al., 2014). Given its prevalence, ID poses significant public health challenges. ID frequently co-occurs with other NDDs, for instance, about 40% of individuals with ID are also diagnosed with ASD (Matson and Shoemaker, 2009), and ID is present in 30% to 80% of those diagnosed with ASD (McClain et al., 2017). Similar to the phenotypic overlap seen between ID and other

NDDs, genetic overlap is also evident: mutations in *SHANK2* (Berkel et al., 2010) and *NLGN4* (Laumonnier et al., 2004) genes have been identified in both ID and ASD cases. The overlap indicates a shared molecular basis of NDDs at the single-gene level.

NDDs with ID has a wide array of origins, encompassing environmental influences and genetic variations. Although both non-genetic and genetic factors can cause ID of varying severity, environmental influences tend to be associated with milder forms of ID (Patel et al., 2010), with the level of impact often correlating to the duration and intensity of exposure. In contrast, genetic causes are predominantly linked to moderate to severe cases of ID (van Bokhoven, 2011), indicating a higher genetic contribution in more severe cases. Studies over the last decade suggest an increasing recognition of the genetic component in ID, to date estimated to represent between a quarter to a half of all ID cases (Srour and Shevell, 2014). This proportion may rise to as much as 65% in individuals with moderate to severe ID (van Bokhoven, 2011). Unfortunately, a substantial proportion of ID-causative genes remain unidentified. As of now, the genetic etiology of about 60% of ID cases has yet to be determined (Rauch et al., 2006).

The SysID database, curated by Kochinke et al. (Kochinke et al., 2016), encompasses 1396 verified ID-causing genes along with 1218 potential candidate genes as of November 2020. The majority of genes listed in this database were reported to be implicated in autosomal recessive forms of ID. It is estimated that over 2500 autosomal genes are involved in NDDs with ID, with the majority exhibiting a recessive pattern of inheritance (Musante and Ropers, 2014). Notably, in communities with high rates of consanguineous marriages, autosomal recessive ID represents approximately 30% to 60% of cases (Ataei et al., 2019). In outbred populations as well, recessive genetic factors play a critical role in the development of NDDs. Research by Papuc et al. has shown that inherited recessive variants are significantly implicated in epileptic encephalopathies (Papuc et al., 2019). Furthermore, a whole-genome sequencing study by Palmer et al. has underlined the relevance of recognizing autosomal recessive inheritance in diagnosing developmental and epileptic encephalopathies (Palmer et al., 2021).

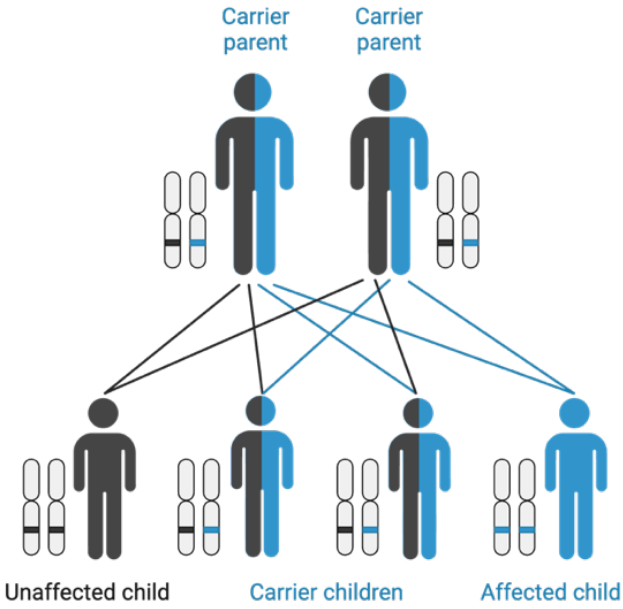

Fig. 3: Schematic diagram of autosomal recessive inheritance. While de novo chromosomal abnormalities and point mutations are often behind severe sporadic intellectual disability in outbred populations, it's typically autosomal recessive inheritance is suspected to be the predominant cause in children from consanguineous families (made with BioRender).

Consanguineous populations are those where marriages among relatives are customary, often for traditional, societal, or financial motives (Alkuraya, 2013). Globally distributed, consanguineous marriages are notably widespread in areas including North Africa, West Asia, and the Middle East (Hamamy, 2012). Consanguinity can increase the likelihood of genetic disorders since the practice heightens the chance of recessive genetic conditions due to increased risk of homozygosity (Fig. 3). Research by Hu et al. involving over 400 such families, primarily from Iran, with multiple children experiencing genetic disorders, indicates a vast genetic diversity with little overlap of the genes affected across various regions like Iran, Pakistan, and the Arab countries (Hu et al., 2019). This diversity suggests the need for extensive genetic sequencing in consanguineous populations to thoroughly explore the complexity of recessive genetic disorders related to NDDs and ID.

1.3 Function and NDDs association of RUFY family proteins

The collaborative team from the Department of Human Genetics at FAU Erlangen in this project has been dedicated to discovering candidate genes linked to NDDs by studying 100 consanguineous Turkish families with at least two affected offspring. Their efforts have

uncovered a number of promising novel candidate genes and variants, including *RUFY4, MDH1B, GEMIN5, PPL, and NR2C1*.

The current study was focused on *RUFY4* as a novel NDD candidate gene. *RUFY4* is a member of the RUN and FYVE domain (RUFY) family, which derived their name from the presence of respective domains within each family member. Typically, the structural architecture of these proteins includes a RUN domain, one or more coiled-coil domains, and a FYVE domain (Char and Pierre, 2020).

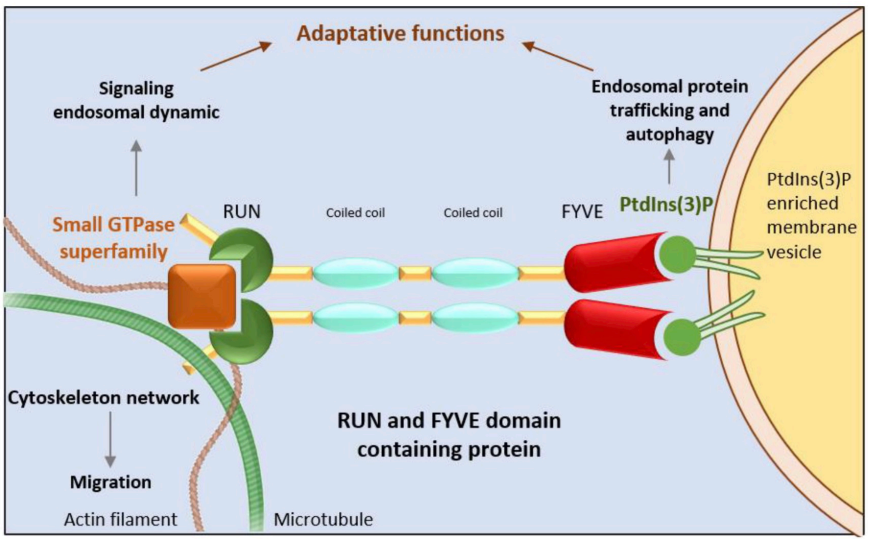

Fig. 4: Schematic diagram of the structure of RUFY proteins. They comprise an amino-terminal RUN domain which binds to the small GTPase superfamily, one or several coiled-coil domains, and a carboxyl-terminal FYVE domain which interacts with PtdIns(3)P (illustration adapted from Char and Pierre (2020)).

RUN domains derive their name from the proteins RPIP8, UNC-14, and NESCA (Callebaut et al., 2001). RUN domains are typically found at the amino-terminal ends of proteins and bind members of the small GTPase superfamily, which includes Rab and Rap family proteins (Yoshida et al., 2011). Rab proteins constitute a significant subset of GTPases that are integral to intracellular membrane trafficking (Lamb et al., 2016). Rab GTPases regulate vesicle trafficking by acting as molecular switches, alternating between an active GTP-bound state and an inactive GDP-bound state. This switching mechanism is crucial for various vesicular processes, such as the budding, movement, docking, and fusion of vesicles (Stenmark, 2009). Given their extensive involvement in the organization and control of membrane trafficking, the large family of GTPases play a vital role in several

cellular functions, including endocytosis and autophagy (Ao et al., 2014; Langemeyer et al., 2018). The FYVE domain, structured as a zinc finger motif (Kutateladze and Overduin, 2001), was named for Fab1, YOTB/ZK632.12, Vac1, and EEA1 proteins (Hayakawa et al., 2007). This domain is typically found at the proteins' carboxyl terminus and binds to phosphatidylinositol 3-phosphate (PtdIns(3)P) (Yang et al., 2002). PtdIns(3)P is known to accumulate on the membrane of early endosomes and autophagosomes, playing a crucial role in the processes of endocytosis and autophagy (Nascimbeni et al., 2017). The combination of the amino-terminal RUN domain and the carboxyl-terminal FYVE domain in RUFY proteins enables them to coordinate endocytosis and autophagy by simultaneously interacting with small GTPases and PtdIns(3)P (Fig. 4).

The *RUFY* gene family comprises four distinct genes, referred to as *RUFY1* through *RUFY4* (Kitagishi and Matsuda, 2013). These genes have been conserved throughout evolution but are absent in prokaryotes and fungi. Specifically, *RUFY4* is exclusive to mammals, suggesting that it emerged following the divergence of the evolutionary path leading to mammals, making it a relatively recent addition to the gene family in comparison to the other RUFY genes which are present in a broader range of species (Char and Pierre, 2020). Arthropods possess a gene analogous to the *RUFY* family, identified as *CG31064* (Char and Pierre, 2020). In this thesis, this arthropod ortholog was investigated experimentally in the *Drosophila* model.

RUFY1 is characterized by the presence of a RUN domain and a FYVE domain, separated by a pair of coiled-coil repeats (Mari et al., 2001). It is primarily expressed in the brain, lungs, kidneys, testes, and placenta (Char and Pierre, 2020). RUFY2 shares a similar structural makeup with RUFY1, including a RUN domain, a FYVE domain, and two intermediate coiled-coil domains (Miao et al., 2022). Its expression is prominent in the brain, lungs, liver, and gastrointestinal system (Yang et al., 2002). RUFY3, which is the smallest in the RUFY protein family, and is predominantly expressed in neurons (Char and Pierre, 2020). Neuronal RUFY3 has an atypical structure because it comprises only a RUN domain (Mori et al., 2007) and is classified in the RUFY family primarily due to its significant sequence similarities within the RUN and coiled-coil domains with other members (Char and Pierre, 2020). Recently, longer isoforms of RUFY3 (RUFY3XL) have been identified which possess a RUN domain along with a C-terminal FYVE domain (Char

and Pierre, 2020). Lastly, RUFY4 is unique among its counterparts as it has one fewer coiled-coil domain (Terawaki et al., 2015) and is primarily expressed in the lungs and lymphoid tissues (Char and Pierre, 2020).

RUFY family members have been implicated in the onset and progression of several neurological disorders, particularly those involving neurodegeneration. RUFY1 is recognized as a gene associated with early-onset Alzheimer's Disease, potentially playing a role in its emergence (Kunkle et al., 2017). The work of Bofill-De Ros and colleagues suggested that RUFY2 is involved in the characteristics of Down syndrome that depend on the hippocampus, and it may also relate to the changes seen in Alzheimer's and similar neurological disorders (Bofill-De Ros et al., 2015). RUFY3 has been reported to be linked to major depressive disorder (Aberg et al., 2020), amyotrophic lateral sclerosis (Arosio et al., 2016), and Alzheimer's Disease (Zelaya et al., 2015).

RUFY4 has been recognized as a positive regulator of autophagy, where its increased expression enhances autophagic flux via interaction with interleukin-4 (IL-4) (Terawaki et al., 2015). RUFY4 teams up with Rab7 to regulate the positioning of endosomes and autophagosomes in dendritic cells, thereby improving immune responses (Terawaki et al., 2015, 2016). Given its roles in intracellular trafficking and immune regulation, RUFY4 was reported to be a prognostic biomarker in clear cell renal cell carcinoma (Miao et al., 2022), and has potential as a therapeutic target for preventing pathological bone loss in conditions such as osteoporosis (Kim et al., 2024). A recent study revealed that in hippocampal neurons, RUFY4 plays a significant role in the retrograde transport of endolysosomal vesicles along microtubules. Specifically, RUFY4, along with RUFY3, functions as an effector of the small GTPase ARL8, promoting the coupling of endolysosomes to the dynein-dynactin motor complex. This action facilitates the movement of endolysosomes from the axon back to the soma in hippocampal neurons (Keren-Kaplan et al., 2022).

1.4 Drosophila melanogaster is a powerful model organism for exploring the genetic and molecular foundations underlying NDDs

Conducting functional studies using animal models is crucial to determine the involvement of identified genes in neural development and to confirm the disease-causing potential of

genetic variations.

Drosophila melanogaster, commonly known as the fruit fly, features a rapid life cycle, with a span of merely 9 to 10 days required to progress from a fertilized egg to a mature adult fly (Hales et al., 2015). Additionally, they are economical to care for, breed prolifically, and are capable of producing a substantial number of descendants in a compressed timeframe (Ma et al., 2022). These attributes render the fruit fly a highly efficient organism for genetic research, facilitating the swift accumulation of experimental data.

For a considerable number of genes associated with human diseases, functional orthologs can be found in *Drosophila*, with a majority of cellular and molecular mechanisms conserved between humans and fruit flies (Bellen and Yamamoto, 2015; Bier, 2005; Pandey and Nichols, 2011; Rajan and Perrimon, 2013; Reiter et al., 2001; Shih et al., 2014). In particular, pathways regulating brain development are highly conserved between humans and *Drosophila*, and *Drosophila* brain undergoes many developmental processes that are similar to those in the human brain (Link and Bellen, 2020). This conservation positions *Drosophila* as a powerful model for investigating the genetic roots of neurodevelopmental disorders. Nearly 75 % of human disease-causative genes have homologues in *Drosophila* (Link and Bellen, 2020). Specifically, for genes linked to human ID, studies have shown that approximately 73 % have corresponding homologues in fruit flies (Oortveld et al., 2013). FlyBase, accessible at http://flybase.org, offers a comprehensive database for information on *Drosophila* genes and genomes. It encompasses over 2.5 million pages and consolidates information from upwards of 42000 primary research articles and large-scale genomic studies (St Pierre et al., 2014).

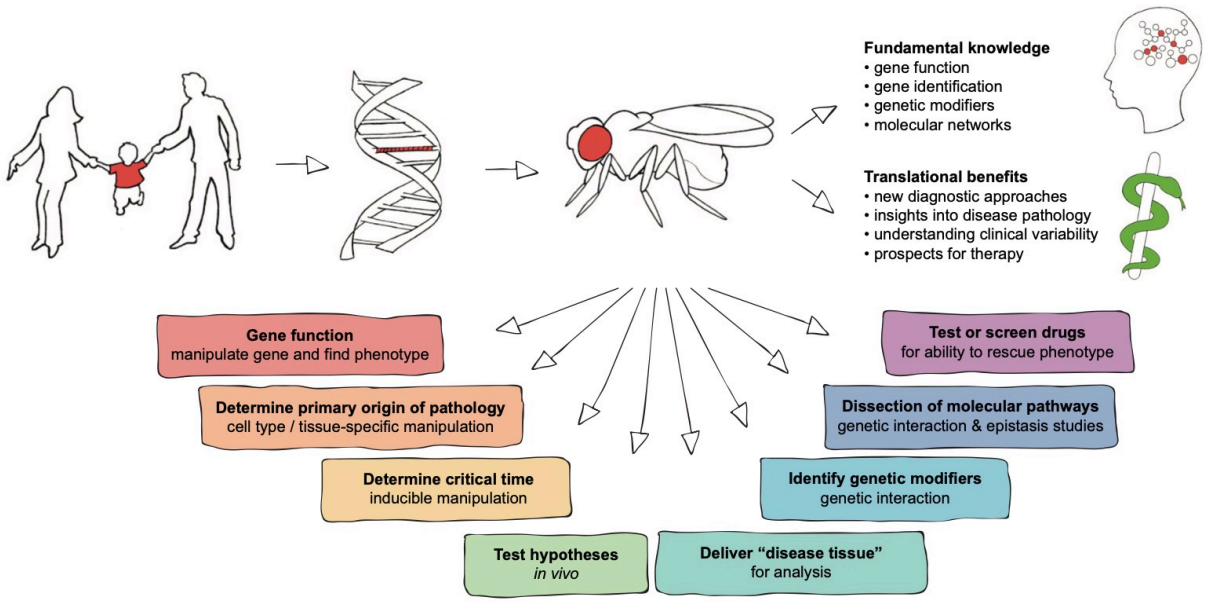

Fig. 5: The advantages and uses of *Drosophila* as a model for disease research are manifold. A variety of methods for studying abnormalities in neural structure and function positions the fruit fly as an excellent resource for enhancing basic understanding in the study of intellectual disability (figure adapted from van der Voet et al. (2014)).

A wide range of genetic tools and techniques that have been developed and refined over the years, including P-element-mediated transformation for the creation of various mutant lines (Rabin and Spradling, 1982), binary expression systems such as the Gal4/UAS (Brand and Perrimon, 1993) and LexA/LexA operator systems (Lai and Lee, 2006) which enable precise spatial and temporal gene expression regulation, CRISPR/Cas9 for precise genomic editing (Bassett and Liu, 2014; Bier et al., 2018), RNA interference (RNAi) to downregulate specific genes (Hannon, 2002), and the use of balancer chromosomes to retain lethal mutations in a heterozygous state (Muller HJ, 1918). Gal4/UAS and LexA/LexA operator binary expression systems are widely and commonly used together allowing independent expression in different cells. For example, Gal4 drivers are used to drive the UAS-RNAi against the gene of interest to knockdown the gene in specific neurons or tissues (Şentürk and Bellen, 2018). Gal4 drivers are also used to activate the UAS-human reference cDNA or variant within the background of *Drosophila* mutant or gene knockdown. This approach allows researchers to assess whether the human reference cDNA or variant can compensate for the effects of gene loss, thereby assessing the functional conservation of the gene and validating the pathogenicity of patient-derived mutation (Link and Bellen, 2020). Researchers can acquire *Drosophila* mutants, gene

knockdown, or overexpression lines from public repositories like the Bloomington *Drosophila* Stock Center (BDSC), or they can generate new strains utilizing these established tools (van der Voet et al., 2014).

Impaired sensory reactivity is a common symptom in many NDDs (Hudac et al., 2024), for example, somatosensory hypersensitivity is a core feature of ASD patients (Orefice et al., 2019). *Drosophila* larval dendritic arborization (da) neurons in the peripheral nervous system (PNS) have served as an outstanding model for assessing the somatosensory function. Da neurons innervate the entire larval epidermis and are categorized into four distinct classes (I-IV) based on the complexity of their dendritic trees (Grueber et al., 2002), each serving different sensory functions. Class I da neurons have relatively simple dendritic trees and primarily function in proprioception—helping the larvae sense its body position and movements; class II da neurons have slightly more complex dendritic trees than class I and are thought to play a role in mechanosensation, detecting gentle or subtle stimuli; class III da neurons have even more complex dendritic trees and are sensitive to mechanical and noxious cold stimuli; class IV da neurons have the most complex dendritic arborizations and are involved in detecting harsh mechanical, chemical, and heat stimuli, such as noxious or damaging sensations (Kilo et al., 2021). Class IV da neurons, also known as C4da neurons, thus function as peripheral nociceptors, which oupon activation by noxious stimuli trigger a series of responses designed to protect the larva, such as rolling or crawling away from the source of irritation or potential harm (Yoshino et al., 2017). Their axons extend into the ventral nerve cord (VNC), where they form synaptic connections with various second-order interneurons, including DnB, Basin, A08n, and mCSI neurons (Hu et al., 2017; Ohyama et al., 2015). These connections are essential for the transmission of sensory information from the peripheral sensory receptors to the central nervous system, culminating in coordinated escape behaviors. The integration of potentially harmful sensory information to produce appropriate behavioral responses involves surprisingly complex neural circuitry that ensures the larvae can react swiftly and appropriately to avoid damage (Kilo et al., 2021).

Abnormal dendritic morphology and synaptic structures play crucial roles in the pathogenesis of NDDs. For instance, several studies have revealed consistent findings of reduced dendritic branching and abnormal dendritic spine morphology across multiple ID-

associated disorders (Benítez-Bribiesca et al., 1999; Cordero et al., 1993; DeLong, 1993). Furthermore, numerous studies have documented a decline in synaptic connections across different models of ID, indicating that synaptic deficits are a prevalent feature of these neurodevelopmental disorders (Jung et al., 2017; Pfeiffer and Huber, 2007). The Drosophila da neurons system enables researchers to gain detailed insights into dendritic and synaptic morphology. C4da neurons, in particular, continue to generate higher-order branches during larval stage to maintain complete coverage of their receptive fields (Hu er al., 2020). This characteristic renders C4da neurons an excellent model for exploring the mechanisms underlying dendritic development in vivo. A08n neurons have been demonstrated to be major postsynaptic partners of C4da neurons, essential for eliciting nociceptive behavior (Hu et al., 2017; Kaneko et al., 2017; Vogelstein et al., 2014). Similar to the scaling growth of C4da dendrites, previous research conducted in our lab has shown that during *Drosophila* larval development, the quantity of presynaptic and postsynaptic sites, along with the connectivity within C4da-A08n nociceptive circuits, proportionally increases with larval size (Tenedini et al., 2019). Therefore, the C4da-A08n nociceptive circuit is an excellent model to investigate the regulation of synapses morphogenesis.

Furthermore, *Drosophila* laboratories have developed various straightforward behavioral assays to investigate the effects of manipulating NDDs risk gene homologues within specific tissues or cells. For example, climbing assays (Manjila and Hasan, 2018) are a simple and efficient test for assessing motor function, which is commonly compromised in NDDs patients. Ube3a mutant files, a *Drosophila* model for Angelman syndrome, display abnormal climbing behaviors. This impaired motor function is similar to the aberrant motor coordination observed in Angelman syndrome patients (Wu et al., 2008). Additionally, impaired social interaction is one of main clinical manifestations of NDDs patients. *Drosophila* stands out among invertebrate genetic model organisms because it displays both courtship and aggression, which are critical aspects of social behaviors (Dankert et al., 2009). *Cyfip* heterozygous mutant flies, used as a *Drosophila* model for ASD, exhibit fewer social interactions in food competition assays, reduced courtship behavior towards female flies, excessive grooming behavior, and increased social distance from the nearest fly compared with controls (Kanellopoulos et al., 2020). These altered behaviors observed

in fly social behavioral assays reflect social deficits, a core symptom of ASD patients. Given that patients with NDDs typically exhibit cognitive impairments, particularly in learning and memory, the fly model further provides opportunities to investigate the contribution of NDD gene homologs to these cognitive functions. Behavioral experiments such as odor-taste learning (Gerber et al., 2013) and courtship conditioning (Koemans et al., 2017; McBride et al., 2005) are frequently employed to assess deficits in learning and memory.

1.5 Aims of the project

Our collaborators from the Department of Human Genetics at FAU Erlangen have discovered candidate genes linked to NDDs by study 100 consanguineous Turkish families with at least two affected offspring. One promising novel candidate NDD gene was *RUFY4*, where a potentially pathogenic variant was discovered in a family with three affected children displaying intellectual disability and developmental delay, typical signs of NDDs. As *RUFY4* plays a pivotal role in autophagy and endocytosis (Terawaki et al., 2015), which are important for neuronal development, it stands out as a strong NDD candidate gene. As the RUFY family is conserved in *Drosophila*, but has not been studied so far, the aims for this project included:

1) Investigate specific functions of the *Drosophila RUFY* family ortholog *CG31064* in neuronal development and function.
2) Investigate the functional conservation between *CG31064* and *RUFY4*.
3) Validating the disease-causing potential of the variant found in the *RUFY4* patient.

2. Material and methods

2.1 *Drosophila* stocks and transgenic constructs

All *Drosophila* stocks were maintained in vials (wide, K-Resin) containing standard cornmeal/molasses food at 25 °C under a 12-hour light/dark cycle with a 70 % relative humidity. All Drosophila stocks, unless otherwise specified, used in this study were sourced from the Bloomington Drosophila Stock Center (BDSC). To rule out potential background effects, the respective genetic backgrounds were employed as controls. All experiments were consistently conducted at a room temperature of 25 °C, with a relative humidity range of 75 % to 80 %.

Alleles and transgenic lines used in this thesis were as follows: *CG31064^{KG01739}* (BDSC # 14165), *CG31064^{RNAi}* #1 (chromosome 3rd) (BDSC # 51494), *CG31064^{RNAi}* #2 (chromosome 2nd) (BDSC # 60496) (in result 3.4 where C4da neuron dendrites were imaged, both #51494 and #60496 *CG31064^{RNAi}* lines were used (Fig. 14), the rest part in results, only #51494 *CG31064^{RNAi}* line was used), *5-40-Gal4* (Hu et al., 2020), *21-7-Gal4* (Hu et al., 2020), *27H06-LexA* (BDSC # 54751) (Tenedini et al., 2019), *82E12-Gal4* (Tenedini et al., 2019), *82E12-LexA* (BDSC # 54417) (Tenedini et al., 2019), *82E12-Gal4^{AD}; 6.14.3-Gal4^{DBD}* (Tenedini et al., 2019), *ppk-Gal4* (BDSC # 32079) (Tenedini et al., 2019), *ppk-CD4-tdTomato* (Hu et al., 2020), *LexAop-CsChrimson* (BDSC # 55138) (Tenedini et al., 2019), *LexAop-Brp^{short}-mCherry* (Tenedini et al., 2019), *UAS-Drep2-GFP* (Tenedini et al., 2019), *LexAop-Drep2-GFP* (Tenedini et al., 2019), *UAS-Brp^{short}-mCherry* (Tenedini et al., 2019), *UAS-GFP-mCherry-Atg8* (BDSC # 37749), *Rab4-ATG-Gal4-KO* (provided by Hiesinger lab) (Kohrs et al., 2021). *UAS-hRUFY4 WT* and *Q432** variant were generated by cloning into the pUAST-AttB vector and phiC31-mediated transgenesis into the VK37 locus on the 2nd chromosome (FlyORF injection service, Zurich, Switzerland).

2.2 Mechanonociception assays

2.2.1 Tool preparation

To facilitate the induction of stereotyped rolling escape behavior in the larvae, it was imperative to fabricate a suitable tool for the experiment. Initially, a segment of

monofilament fishing line (Shakespeare, diameter 0.009 inch [0.23 mm]) measuring 18 mm in length was prepared. Subsequently, 10 mm of this filament was securely affixed to one end of a toothpick, leaving the remaining 8 mm exposed. To ensure precise control, the filament was calibrated using an electronic scale, ensuring it applied a force within the range of 45 to 50 milli-Newtons (mN) (Hoyer et al., 2018). Furthermore, in order to avoid puncturing the body wall of the experimental animals, the filament's tip was inspected under a stereoscope for excessive sharpness, and gently polished it if necessary.

2.2.2 Preparation of experimental animals

The staging process was commenced by selecting 25-30 vigorous and healthy virgin flies along with 10-15 males, and transferred them into a vial supplied with fly food to initiate genetic crossing. Prior to staging, which occurred three days later, these flies were transferred into a new vial containing fresh food to facilitate a controlled egg-laying period lasting 4 to 6 hours, at an environmental condition of 25 °C and 70 % relative humidity. Once this period was over, the flies were transferred to another vial with fresh food. Then the vial used for staging was maintained under the same temperature and humidity conditions, within a 12-hour light/dark cycle. For experimental purposes, only 3rd instar larvae that were 96 ± 3 hours after egg laying (AEL) were used, ensuring they were at the foraging stage and have not yet left from the fly food.

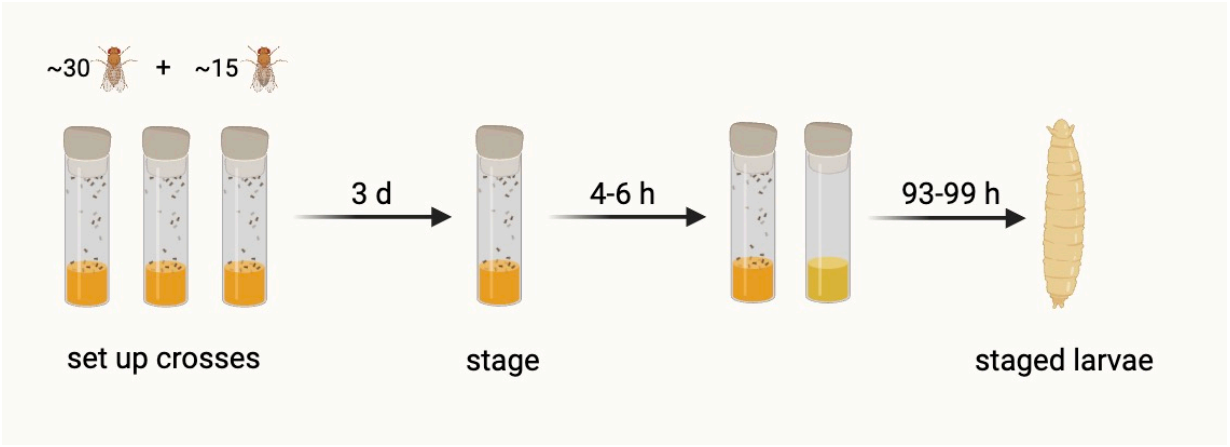

Fig. 6: Schematic of the staging procedure of the *Drosophila* larvae. Proper and precise staging gives rise to healthy L3 animals at 96 hours after egg laying, which have processed the food very well and remain within it, instead of migrating towards the vial's wall (made with BioRender).

Before initiating the experiment, the staged larvae were carefully extracted from the fly food using a brush. Subsequently, larvae were rinsed once or twice with double distilled water to eliminate any food residue. It was ensured that the larvae selected for the experiment were uniform in size and appear healthy and active. Then the selected larvae with Tubby (Tb) balancer or green fluorescent protein (GFP) would be screened out.

2.2.3 Experimental procedure

Approximately 30 minutes prior to the experiments, 2 % agar plates (100 × 15 mm petri dish) were removed from the refrigerator. This step was crucial to bring the plates to room temperature, ensuring that the cooler surface does not influence larval behavior. 1 ml of double distilled water was added to the plate to create a smooth, moist surface that facilitates unimpeded larval movement. Approximately 15 staged larvae were then carefully transferred onto the agar plate carefully using a brush.

Under the stereoscope, mid-abdominal segments 4, 5, or 6 of the larva were precisely target. Mechanical pressure was quickly exert using the previously calibrated von-Frey filament on the dorsal side. It was ensured that this mechanical stimulus was delivered swiftly and lasted no more than 1 second before removal, to prompt an escape response from the larva. After a brief interval of 2 to 3 seconds, the same procedure was conduct again on the same larva. At least 60 larvae were sampled for each experiment to achieve adequate statistical significance. A positive rolling response, indicative of nociception, was recorded when the larva completed at least one full 360 ° rotation around its body axis following mechanical stimulation. Other observed behaviors, classified as non-nociceptive responses, included no response, stop, stop and turn, and bending. These responses were assigned scores as follows: no response = 1, stop = 2, stop and turn = 3, bending = 4, and rolling = 5. Behavioral reactions were immediately documented on a scoring sheet. For the purpose of analysis and graphical representation, only the behaviors elicited by the second stimulus were considered.

2.3 Gentle touch assays

2.3.1 Tool preparation

The base of an eyelash was carefully affixed to the end of a toothpick, ensuring that the eyelash extended freely. This would enable the experimenter to apply an innocuous force to the larvae.

2.3.2 Preparation of experimental animals

Refer to section 2.2.2 for details.

2.3.3 Experimental procedure

Roughly 30 minutes prior to the assay, 2 % agar plates (100 × 15 mm petri dish) were removed from the refrigerator. It's important to normalize the plate to room temperature to prevent the cold surface from affecting the larvae's behavior. The plate was moistened by spreading distilled water onto it with a brush, creating a sufficiently wet surface for the larvae to crawl. Then, using the brush with care, about 15 third instar staged larvae were transfer to the agar plate, allowing them to adjust to their new environment for three minutes.

While observing through the stereoscope, the head segment of the larva was lightly touched with the tool when it exhibited continuous motion. The elicited response was record. Wait for the larva to resume a direct forward movement before applying another touch. This process was repeat a total of four times, pausing for a duration of one to two seconds between each touch. It was ensured that at least 60 larvae are sampled for each experiment to achieve adequate statistical significance. Larval responses were quantified using the Kernan et al. (Kernan et al., 1994) scale where '0' denoted no response; '1' indicated a halt in movement; '2' was assigned for a combination of stopping and contracting / turning; '3' corresponded to a single reverse contraction wave; and '4' represented multiple contraction waves.

2.4 Thermo-nociception assays

2.4.1 Preparation of experimental animals

Refer to section 2.2.2 for details.

2.4.2 Experimental procedure

2 % agar plates (100 x 15 mm petri dish) were removed from the refrigerator about 30 minutes prior to the assay to ensure the plates reached room temperature. 250 µl of double distilled water was evenly spread on the agar plate to create a thin film, facilitating uninhibited crawling and escape rolling behavior of the larvae. Around 20 third instar staged larvae were carefully placed onto the plate using a brush, then they were given three minutes to adjust to the environment.

Temperature control device (custom built, ZMNH, Hamburg (Petersen et al., 2018)) was activated and the probe's temperature was adjusted to 46 °C, allowing time for the temperature to stabilize. The petri dish containing the larvae was positioned under the stereoscope that was equipped with a camera (Basler ac1960gm), and recording was started using a capture software (Pylon Viewer).

When the larva moved forward, the 46 °C hot probe was used to provide stimulation laterally at the 4th to 6th abdominal segments. This stimulation was maintained for a duration of no less than 10 seconds, or until the larva exhibited the escape rolling behavior. Immediately after the experiment, the larva was removed from the plate to prevent retesting. For each experiment, at least 80 larvae were tested to ensure the results have sufficient statistical power.

Following the completion of the experiment, the recorded videos were reviewed to evaluate the outcomes. Time delay from the moment the larvae were subjected to the heat stimulus to the onset of their escape rolling behavior was calculated.

2.5 In vivo confocal microscopy

2.5.1 Preparation of experimental animals

Refer to section 2.2.2 for details.

2.5.2 Experimental procedure

A measured quantity of 50 % glycerol was placed on a microscope slide, and third instar larva (96 h ± 3 h AEL) were carefully positioned onto the glycerol, dorsal side up. A small amount of adhesive was added to the four corners of a coverslip, then the coverslip was gently set over the larva to secure it in place. Class IV dendritic arborization (C4da) neurons of the *Drosophila* larvae were imaged using live confocal microscopy (Carl Zeiss, LSM700) with a 20x/NA0.8 air objective lens. It was ensured that the complete dendritic architecture of the C4da neurons was captured for each larva. To obtain statistically reliable data, a minimum of six larvae were imaged for each genotype.

2.6 Optogenetic behavioral assays

2.6.1 Preparation of experimental animals

The general method followed the same steps as outlined in section 2.2.2, with the exception that for this specific assay, the flies should be housed and developed inside a cage that includes a grape-agar plate. After the stage was completed, any remaining yeast paste on the grape-agar plate must be replaced with a yeast paste that had been mixed with all-trans retinal (prepared by combining 1 ml of distilled water, 5 µl of all-trans Retinal (Sigma, # R2500; 0.1 M in ethanol), and 0.5 g of yeast). It was essential to keep the staged larvae in complete darkness prior to beginning the experiments.

2.6.2 Experimental procedure

A piece of 2 % agar was set on a clear glass plate that was connected to a camera, and 1 ml of double-distilled water was spread onto the agar to create a thin layer of water. This ensured that the larvae could move without restraint and exhibited various behaviors. With a soft brush, approximately 30 third instar larvae (96 h ± 3 h AEL) were carefully transferred onto the agar and they were spaced out evenly. A LED source device was

positioned overhead so that the larvae were situated in the central area beneath the device.

The recording was started using a capture software (Pylon Viewer). Light source was switch on to activate the CsChrimson (Klapoetke et al., 2014) with a 625 nm red light (760 μW/cm^2, max. 24 V). The exposure sequence was as follows: started with a 5 s illumination, after a pause for 10 s, proceeded with a 10 s illumination, and concluded with a 5 s pause. To ensure the results were statistically significant, a minimum of 100 larvae per genotype should be subjected to this test. The experimental procedure described was conducted in darkness.

Post-experiment, the responses of the larvae were assessed using the Fiji cell counter plugin (ImageJ, NIH, Bethesda). The behaviors to be documented included rolling, bending, and turning. A full 360 ° rotation qualified as an escape rolling behavior. Bending was characterized as an incomplete rolling action, where the rotation was less than 360 degrees. A turning response was defined by a change in the initial crawling direction of the larva.

2.7 Climbing assay

2.7.1 Preparation of experimental animals

Newly eclosed, non-mated *Drosophila* flies were collected and relocated into individual vials, each containing fresh food and accommodating 10 flies of the same gender—either all female or all male. These collected flies were kept at a stable environment of 25 °C with 70 % humidity, under a 12-hour light-dark cycle. The flies were then utilized for experimental purposes when they reached an age of three to four days.

2.7.2 Experimental procedure

A clear plastic cylinder measuring 30 cm in length and 2.5 cm in diameter was set up. The midpoint was marked on the tube at 15 cm from the base. Prior to use, the cylinder was cleansed thoroughly to eliminate any residual scents. Then the tube was positioned vertically on a flat surface and a lighting apparatus was arranged centrally above the top of the cylinder.

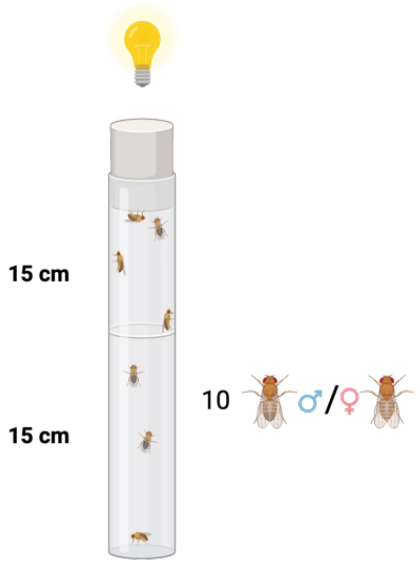

Fig. 7: Schematic of the settings of climbing assay. A 30 cm long, 2.5 cm diameter clear plastic tube is prepared, marked at the midpoint. The tube is positioned upright and illuminated from above. Ten flies are introduced into the tube. Following a tap to gather the flies at the bottom, the number crossing the midpoint is timed and counted in 15 seconds. This procedure is repeated five times with 3-minute intervals. Ten groups per sex per genotype are tested, and the rates of crossing the midpoint are averaged (created with BioRender).

The light was turned on before starting the experiments. A group of 10 flies were gently introduced into the cylinder, taking care to avoid their escape. The flies were allowed to acclimate to the environment for 5 minutes. Cylinder was tapped lightly to ensure all flies fall to the bottom, then the stopwatch was promptly started. The number of flies that pass the midpoint mark within 15 seconds was recorded. This assessment was performed five times with the same batch of flies, spacing each trial by about 3 minutes. 10 separate groups of 10 flies were tested for each sex of each genotype, and the average passage rate over the mark was calculated.

2.8 Odor-taste learning assay

2.8.1 Preparation of experimental animals

Refer to section 2.2.2 for details.

2.8.2 Experimental procedure

1 % agar plates were set up, as well as plates containing 1 % agar with 2 M fructose added. It was ensured that there were twice as many normal agar dishes as sugar agar dishes, and they were marked distinctly to prevent mix-ups. Covers of all plates were replaced with perforated ones during the experiment.

A 1 : 50 dilution of 99 % n-amyl-acetate (AM) was created with double-distilled water. Before the experiment began, 10 µl of this diluted AM solution was introduced into the designated scent containers. Two containers with AM were placed on each dish approximately 8 mm from the plate's perimeter for the training phase.

The training setup was designed to be reciprocal, meaning the arrangement of dishes associated with the AM scent is reversed for different groups. Third instar larvae (96 h ± 3 h AEL) were separated into two groups of 30 each. One group was placed in the center of a fructose-containing agar plate with two AM-filled containers using a brush. Post a 5-minute training interval, they were moved to a plain 1 % agar dish without odor containers for 5 minutes. Then, they were returned to the initial dish for another training session. This process was repeated three times. The other group received the opposite training sequence, starting in a plain agar dish with scent containers for 5 minutes, followed by transfer to a fructose dish without AM for another interval. This was also done for three total rounds.

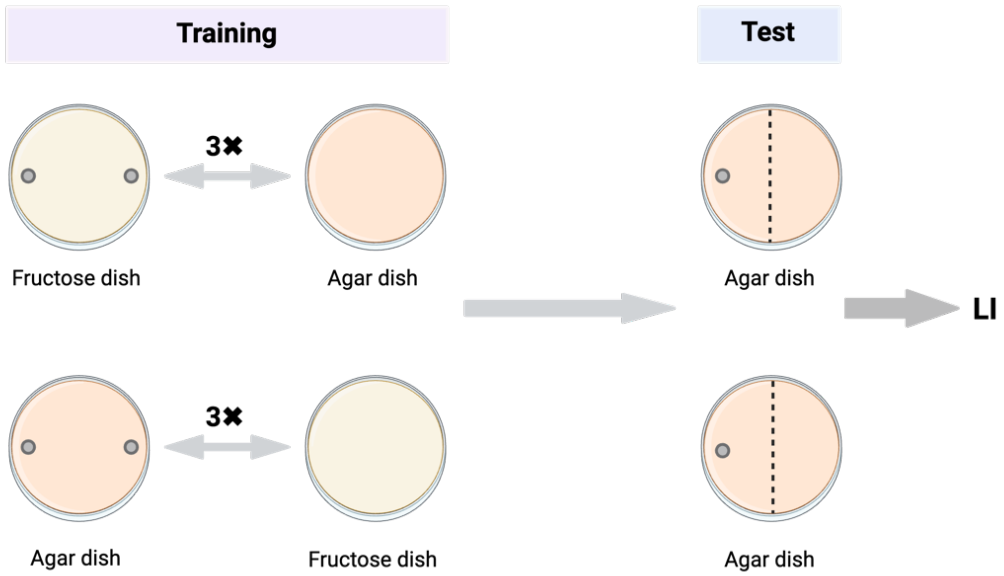

Fig. 8: Schematic of the experimental design of Odor-taste learning assays. This assay involves training *Drosophila* larvae using reciprocal setups with odor containers on agar dishes, testing their learned response to an odor (n-amyl-acetate). Larvae are trained in groups with and without an odor paired with fructose, and then tested for their preference, with a calculated learning index reflecting their ability to associate odor with sugar reward (created with BioRender).

Immediately after training the larvae, they were proceeded to the testing phase. While the last training session was underway, dishes for testing were prepared, which would only use 1 % agar. An odor container with 10 µl of AM was placed on the left side of each test dish. A line was drawn in the middle of each plate to divide it into two equal halves. All the trained larvae were gently moved to the center of these plates. After 3 minutes, the number of larvae on each half was counted. The preference for AM was calculated by subtracting the number of larvae on the non-AM side from those on the AM side, then divided by the total number of larvae. To determine the learning index (LI), AM preference score of the second group was subtracted from that of the first group and divided by two. 10 batches of larvae were trained and tested for each genotype to complete the study.

Several key points should be taken into account for this assay. Firstly, it's important to use fresh dishes for each experimental round, and the odor liquid in the containers must be replenished with a new batch. Secondly, at the end of each day's experiments, both the containers and the perforated lids must be thoroughly cleaned to ensure their readiness

for subsequent use.

2.9 Food competition assay

2.9.1 Preparation of experimental animals

Newly eclosed, non-mated male *Drosophila* flies were collected and relocated into individual vials, each containing fresh food and accommodating 8 flies. These collected flies were kept at a stable environment of 25 °C with 70 % humidity, under a 12-hour light-dark cycle. The flies were then tested when they reached an age of three to four days.

2.9.2 Experimental procedure

Before starting the experiment, adult male flies were taken out of the incubator and transferred to clean empty vials without food to starve them for one and a half hours. Meanwhile, fresh food was prepared and placed on plugs of another set of empty vials. Once the starvation process was over, the food-deprived flies were transferred to the vials containing fresh food. It was ensured that each vial contained eight healthy and active flies. The flies were allowed some time to adjust to the new conditions before the start of videotaping, and then their activities were recorded by a cellphone. Physical contact was considered social interaction and usually in the form of head-to-head contact. The number of social interactions among the flies was counted within a two-minute period. For each genotype, at least 8 batches of male flies were tested.

2.10 Synaptic imaging

2.10.1 Preparation of experimental animals

Refer to section 2.2.2 for details. To maintain uniformity in larval brain size, it's important to limit the staging period to a strict 4-hour window.

2.10.2 Mounting of larval brain specimens

The dissection buffer was composed of various components with the following concentrations: sodium chloride (NaCl) at 108 mM/L, potassium chloride (KCl) at 5 mM/L, sodium bicarbonate ($NaHCO_3$) at 4 mM/L, monosodium phosphate (NaH_2PO_4) at 1 mM/L,

Trehalose at 5 mM/L, Sucrose at 10 mM/L, HEPES at 5 mM/L, magnesium chloride ($MgCl_2$) at 8.2 mM/L, and calcium chloride ($CaCl_2$) at 2 mM/L.

Uniformity in larval size was critical for both experimental and control brain specimens. The dissection process involved immersing the live larvae in the dissection buffer, using forceps to stabilize the larval head, and removing the body wall to reveal the brain. The brain was then carefully detached from the head capsule and cleared of adjacent tissue. Fixed in 4 % paraformaldehyde (PFA) solution for 15 min, the brain specimens were subsequently rinsed three times with 1x PBS for five minutes per wash.

For mounting, coverslips should be prepared with a poly-L-lysine (Sigma) coating, allowed to air dry. Reuse of poly-L-lysine was acceptable. An appropriate amount of antifade solution (SlowFade™ Gold Antifade Mountant, Thermo Fisher, USA) was applied to the prepared coverslip. Each brain was placed into the antifade medium and arranged neatly. Brains from both experimental and control groups, dissected on the same day, were mounted together on a single coverslip. The coverslip was then inverted onto a clean glass slide with care. Any air surrounding the brain tissue was displaced with antifade medium, and the slide was sealed using transparent nail polish.

Once the nail polish was thoroughly dry, the specimen's inherent fluorescence can be observed under a confocal microscope with AiryScan function (Carl Zeiss, LSM900AS2). Each experiment was conducted a minimum of three times to ensure reproducibility. Subsequently, the outcomes of these repeated trials were analyzed for consistency.

2.10.3 Synaptic marker co-localization analysis

Synaptic markers Brp^{short}-mCherry (magenta) and Drep2-GFP (green) were used to visualize C4da presynapses and A08n postsynapses, respectively (*82E12-LexA > LexAop-Drep2-GFP; ppk-Gal4 > UAS-*Brp^{short}*-mCherry* or *27H06-LexA > LexAop-*Brp^{short}*-mCherry; 82E12-Gal4 > UAS-Drep2-GFP*). Imaris software (Bitplane AG, Zurich, Switzerland) was employed to assess both the presynaptic and postsynaptic puncta. Images that were not clear will be disregarded, ensuring only those of superior quality were considered for further processing and evaluation.

For each larval brain, the four hemisegments in abdominal segments 5 and 6 were set as a region of interest. A high-quality image from the control group was chosen to calibrate the detection thresholds for both presynaptic and postsynaptic puncta, using the software's automatic threshold setting as a baseline. These established thresholds were then consistently applied to all subsequent image processing. After subtraction of background, presynaptic C4da and postsynaptic A08n puncta were automatically identified within a region of interest using the Imaris spot function, configured with a size setting of 200 nm. The distance threshold for C4da and A08n neuron synapses was defined as 0.35 μm, and a spot colocalization function was used to detect C4da-A08n synaptic connections.

2.11 Statistical analysis

Statistical analysis was conducted using Prism 10 software (RRID: SCR_002798, GraphPad). Details on sample sizes and the types of statistical tests employed were provided in the legends accompanying the figures. I used Kruskal-Wallis one-way ANOVA, Mann-Whitney test, or Fisher’s exact test to assess statistical significance. Where multiple group comparisons were necessary, Dunn’s *post hoc* test and Bonferroni correction test were applied to evaluate differences between several groups and a control group. Statistical significance was established at P values less than 0.05, denoted as $*p < 0.05$, $**p < 0.01$, $***p < 0.001$, $****p < 0.0001$, with “ns” indicating non-significance.

2.12 Utilization of AI language model

In the preparation of this thesis, I used the ChatGPT to assist in rephrasing sentences and polishing the language. English is not my first language, and my use of this tool was strictly limited to linguistic adjustments to ensure clarity and readability of the content. The research and analysis of this thesis were conducted independently.

3. Results

3.1 Analysis of the homology of *dRUFY* and *RUFY4*

The *RUFY* genes are relatively conserved across species. Arthropods have one orthologous gene named *CG31064* (Char and Pierre, 2020), referred to as *dRUFY* in this study. Both human *RUFY4* and *dRUFY* feature an N-terminal RUN domain and a C-terminal FYVE domain (Fig. 9A). A stop-gain mutation identified in the *RUFY4* gene of the patient truncates the *RUFY4* protein at position 432 (*hRUFY4*^{Q432*}) in which results in the loss of the C-terminal 139 amino acids including the FYVE domain (Fig. 9A). The phylogenetic analysis of human and fly *RUFY* family proteins indicates that *dRUFY* is evolutionarily most closely related to human *RUFY2* within the *RUFY* protein family (Fig. 9B).

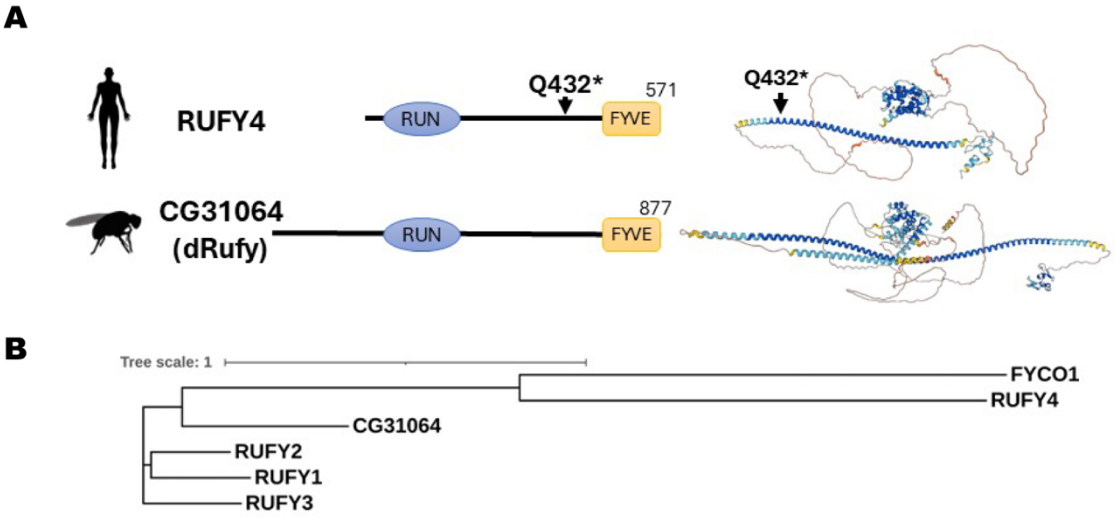

Fig. 9: Comparison of human *RUFY* and the fly orthologue *CG31064* (*dRUFY*). (A) Schematic diagram of domain structure and structural prediction by Alphafold of human *RUFY4* and *CG31064* (*dRUFY*). The position of the stop-gain variant (Q432*) found in the *RUFY4* patient is indicated. (B) Phylogenetic tree of *RUFY* family proteins. Human *RUFYs* (1,2,3,4 and the paralog *FYCO1*) and *Drosophila CG31064* protein sequences were aligned using MUSCLE (SnapGene Inc.), then analyzed with the Simple Phylogeny tool (EBI: https://www.ebi.ac.uk/jdispatcher/phylogeny/simple_phylogeny, Phylip tree with distance correction excluding gaps, using neighbor-joining clustering, then visualized using iTOL, https://itol.embl.de).

To assess *dRUFY* function in flies, which was not studied before, I obtained available

reagents allowing the genetic manipulation of *dRUFY*. A survey of the FlyBase database revealed that the *dRUFY* genomic locus features six putative isoforms with alternative 5' and 3' exons (Fig. 10). Two isoforms (isoform B and G) contain the C-terminal FYVE domain. I could identify a putative *dRUFY* mutant allele (*dRUFY*^{KG01739}) featuring a P-element insertion in the 5'-UTR/enhancer region that could affect *dRUFY* expression (Fig. 10, red dotted box). Additionally, a transgenic RNAi line targeting coding exon 4 (Fig. 10, green dotted box), which is common to all putative isoforms, was available from the stock center. I used these tools to assess the function of *dRUFY* in nervous system development in subsequent structural, functional and behavioral analyses.

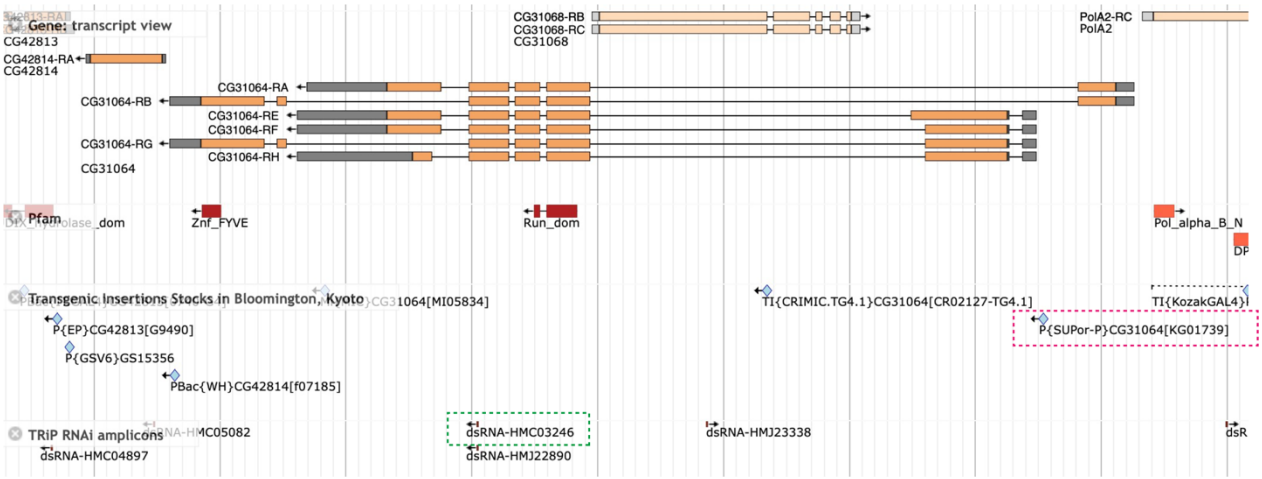

Fig. 10: Structure of the *dRUFY* gene. The insertion location of the *KG01739* mutant allele (*dRUFY*^{KG01739}) and the RNAi targeting region (dsRNA-HMC03246) are indicated by pink and green dotted lines, respectively. Source: FlyBase (https://flybase.org).

3.2 Loss of *dRUFY* function leads to memory and social impairments in *Drosophila*

Adaptive impairment is a crucial aspect in defining intellectual disability (36). Given that the human *RUFY4* gene variant was identified in the offspring of a consanguineous family showing signs of intellectual disability, I wanted to explore the functional implications of its *Drosophila* homolog, *dRUFY*, in relation to adaptive skills.

To ascertain the role of *dRUFY* in learning and memory, I employed associative learning paradigms using *dRUFY* (*dRUFY*^{KG01739}) mutant *Drosophila* larvae. While memory is not traditionally categorized as an adaptive skill, it is impaired in ID and significantly underpins the development and application of adaptive skills. Initially, control assays were conducted

to determine if the *dRUFY* mutant larvae displayed changes in inherent preferences for odor (n-amyl-acetate) or taste (fructose) (Fig. 11A). Subsequently, I performed odor-taste learning assays to assess the larval capacity to associate an odor (n-amyl-acetate) with the appetitive stimulus fructose (Fig. 11B).

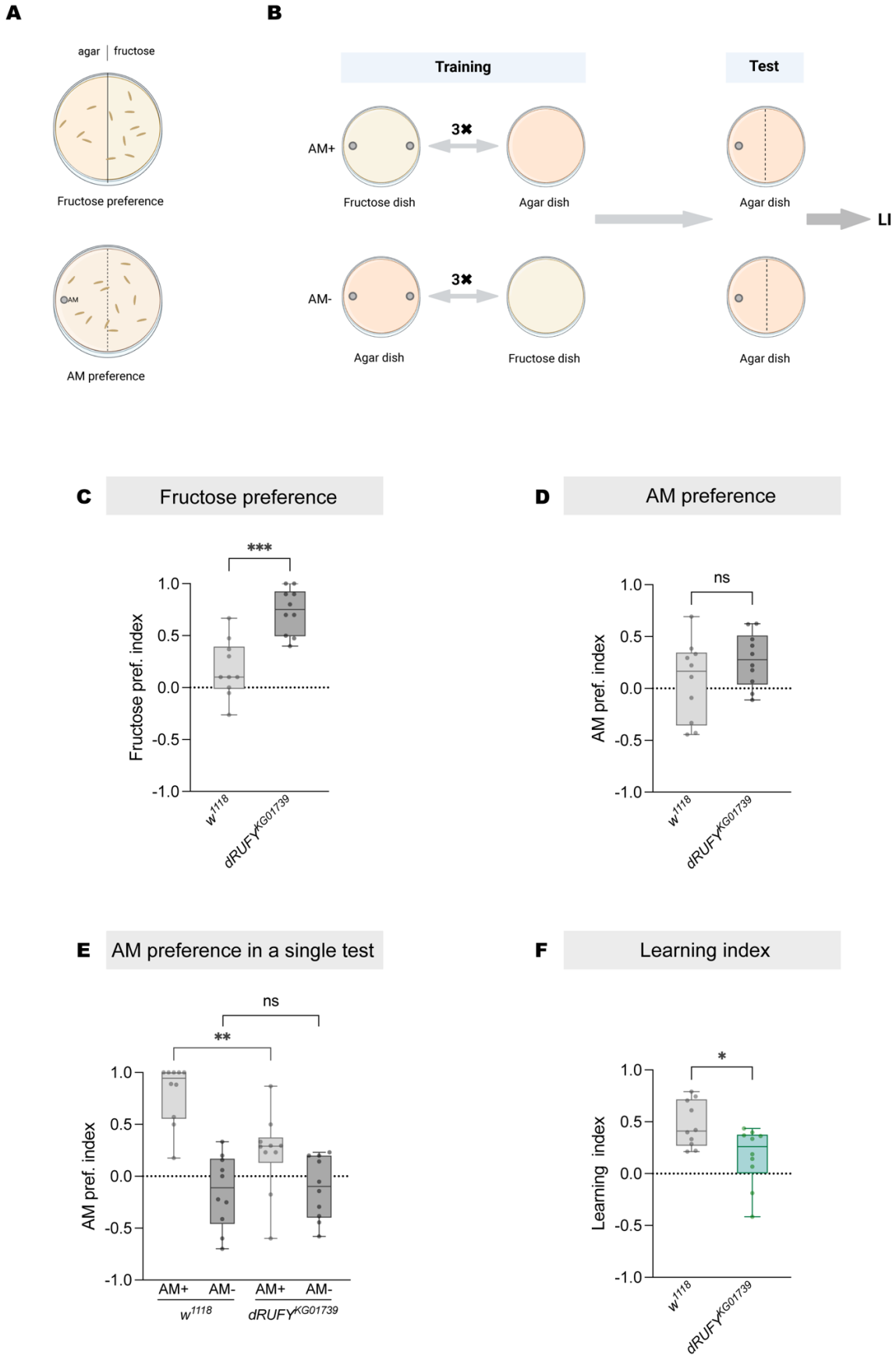
A
agar
fructose
Fructose preference
AM
AM preference
B
Training
Test
AM+
3✖
Fructose dish
Agar dish
Agar dish
LI
AM-
3✖
Agar dish
Fructose dish
Agar dish
C
Fructose preference
***
Fructose pref. index
1.0
0.5
0.0
-0.5
-1.0
w1118
dRUFYKG01739
D
AM preference
ns
AM pref. index
1.0
0.5
0.0
-0.5
-1.0
w1118
dRUFYKG01739
E
AM preference in a single test
ns
**
AM pref. index
1.0
0.5
0.0
-0.5
-1.0
AM+
AM-
AM+
AM-
w1118
dRUFYKG01739
F
Learning index
*
Learning index
1.0
0.5
0.0
-0.5
-1.0
w1118
dRUFYKG01739

Fig. 11: Impact of *dRUFY* deficiency on innate and learned behaviors in *Drosophila*. (A) Top, schematic diagram showing the fructose preference assay. In each trial, a group of 25 larvae is placed along the midline of a partitioned Petri dish, with one half containing plain agar and the other half containing agar mixed with fructose. After 3 minutes, the number of larvae on each side is counted to calculate the fructose preference index. Bottom, schematic illustrating the n-amyl-acetate (AM) preference assay. Similarly, 25 larvae are placed along the midline of a standard agar plate. A container holding 10 µl of AM is placed on one half of the plate. After 3 minutes, the larvae on each side are counted to determine the AM preference index (made with BioRender). (B) Schematic of the experimental design of Odor-taste learning assays. This assay involves training Drosophila larvae using reciprocal setups with odor containers on agar dishes, testing their learned response to an odor (n-amyl-acetate). Larvae are trained in groups with and without an odor paired with fructose, and then tested for their preference, with a calculated learning index reflecting their ability to associate odor with sugar reward (made with BioRender). (C, D) Preference scores for fructose (C) and n-amyl acetate (D) in third instar (96 h AEL) larvae of control (w^{1118}) and $dRUFY^{KG01739}$ mutant. n = 10 groups of 25 larvae each. (E) AM preference scores for control larvae (w^{1118}) and $dRUFY^{KG01739}$ mutant larvae receiving a sugar reward in the presence of AM (AM+) or in the absence of AM (AM-) in odor-taste learning assays. n = 10 groups of 30 larvae each. (F) Learning index (LI) for third instar larvae of control (w^{1118}) and $dRUFY^{KG01739}$ mutant. n = 10 groups of 30 larvae each. All data presented using box-and-whisker plots, where the median is marked with the line inside the box and box boundaries represent the 75 % quartiles. *$p < 0.05$, **$p < 0.01$, ***$p < 0.001$, ns $p \geq 0.05$, Mann-Whitney test.

In the control tests, where the odor was not associated with a sugar reward, larvae were assessed for their innate preference for n-amyl-acetate (AM) or fructose, respectively (Fig. 11A). Results revealed that *dRUFY* mutant larvae showed an increased preference for fructose, but no change in preference for n-amyl-acetate when compared to control larvae (Fig. 11C, D). This suggests that the *dRUFY* allele may heighten fructose sensitivity and/or carbohydrate preference. Subsequent odor-taste associative learning assays indicated that the *dRUFY* mutants displayed a reduced learning index, indicating memory deficits, compared to control larvae (Fig. 11B, E, F). The lower learning index observed in *dRUFY* mutants was due to their decreased preference for AM following sugar reward training with AM exposure, compared to control larvae (Fig. 11E). Loss of *dRUFY* appears to impair the associative learning capabilities of the larvae, potentially indicating a role of this gene in memory and learning functions within the adaptive skill framework.

Motor abilities are not just necessary for everyday tasks and self-care, but they also play a significant role in an individual's adaptive behavior. I examined the motor abilities of *dRUFY* mutant flies to investigate if motor deficits appear when this gene is disrupted. The

climbing assays used in this study, which test the ability of flies to climb a vertical surface, showed no detectable defects in climbing ability comparing *dRUFY* mutant flies to control flies (Fig. 12A, B). This finding suggests that the loss of *dRUFY* function may not impair basic motor functions as measured by this assay.

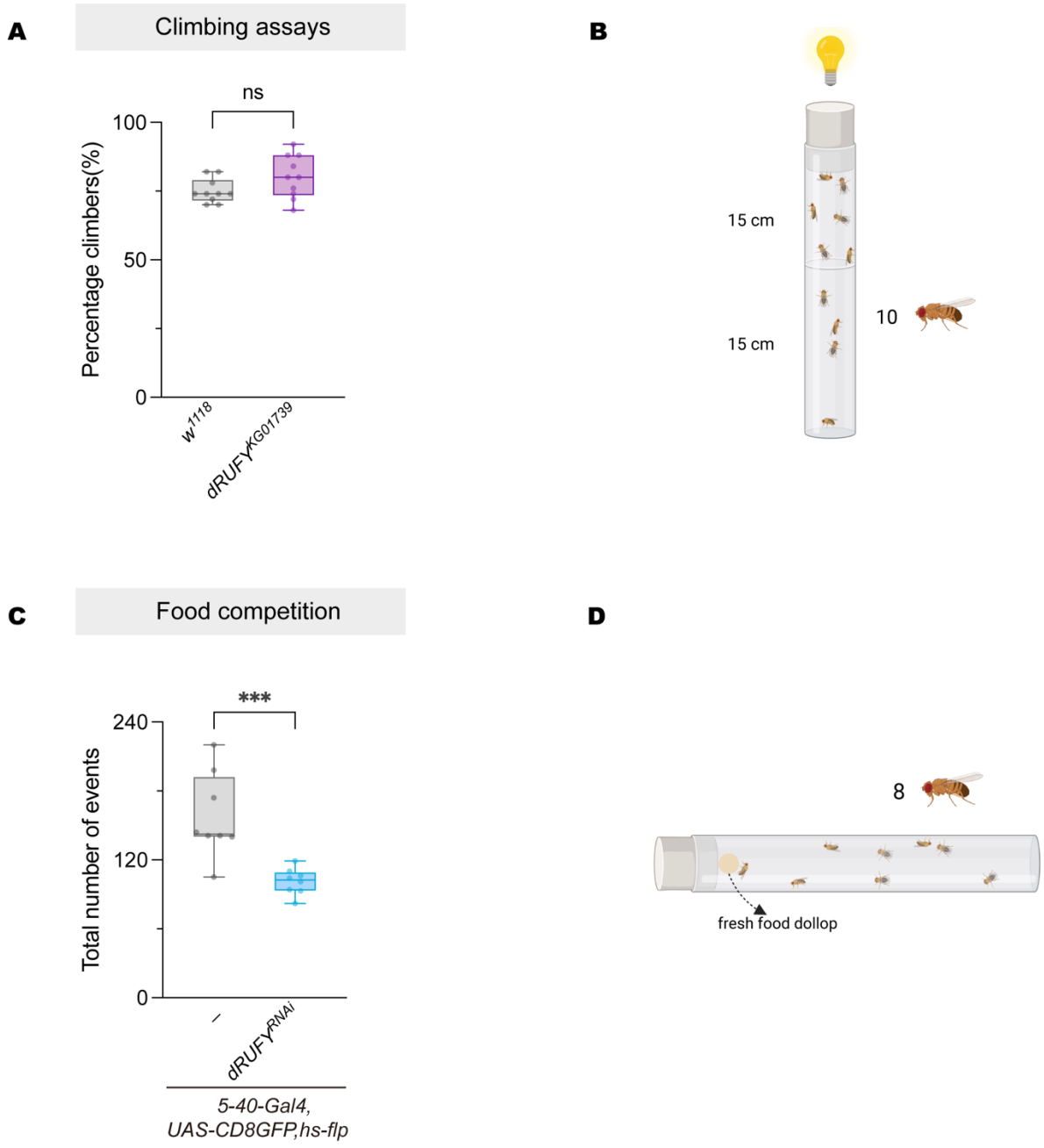

Fig. 12: Impact of *dRUFY* deficiency on motor and social behaviors in *Drosophila*. (A) Percentage of adult flies crossing a 15 cm threshold within 15 seconds, comparing control (w^{1118}) with $dRUFY^{KG01739}$ mutants. n = 10 groups of 10 flies each. (B) Schematic of the climbing assay. 30 cm long, 2.5 cm diameter clear plastic tube with 10 male flies were marked at the midpoint and illuminated from above. After tapping the tube to gather the flies at the bottom, flies crossing the midpoint in 15 seconds were counted (made with BioRender) . (C) Total number of social interactions during food competition assays between control male flies and male flies with sensory neuron-specific *dRUFY* knockdown. n = 8 groups of 8 flies each. (D) Schematic of the food competition assay. 8 adult male flies, which have been deprived of food for 1.5 hours, were placed in a tube containing a small amount of fresh food. Over a two-minute period, the number of social interactions among the flies was recorded (made with BioRender). All data presented using box-and-whisker plots, where the median is marked with the line inside the box and box boundaries represent the 75 % quartiles. ***$p < 0.001$, ns $p \geq 0.05$, Mann-Whitney test.

I then examined whether *dRUFY* plays a role in social behavior using food competition assays (Kanellopoulos et al., 2020), where the average number of social events was recorded within a 2-minute period. Specifically, RNAi-mediated knockdown of *dRUFY* in somatosensory neurons of male flies resulted in fewer social interactions compared to their control counterparts (Fig. 12C, D), suggesting that the absence of *dRUFY* in the somatosensory system leads to deficits in social interaction.

3.3 Disruption of *dRUFY* alters sensory responses in the larval dendritic arborization neuron system

The patient with the identified *RUFY4* variant clinically exhibited sensory hypersensitivity to light and touch. Sensory hypersensitivity refers to an excessive or heightened response to sensory stimuli, a phenotype commonly observed in ASD. This finding suggested a potential link between the *RUFY4* vatiant and typical ASD characteristics, suggesting co-morbidity of ID and ASD in this case. ID and ASD frequently co-occur and current studies suggest that about 30% to 80% of children affected by ASD also fulfill the diagnostic criteria for ID (Ben Itzchak et al., 2008; Leyfer et al., 2006). Conversely, ASD-related symptoms such as difficulties with social interaction, communication challenges, and repetitive behaviors are commonly observed in individuals diagnosed with ID.

I explored the potential effects of *dRUFY* disruption on the somatosensory system of *Drosophila* larvae. Specifically, I conducted a series of sensory behavioral assays on third instar *dRUFY* mutant larvae. Using a calibrated *von Frey* filament exerting a force of 50

mN, I assessed the mutant larvae's response to mechanonociceptive stimuli. Notably, these mutants demonstrated an increase in nociceptive rolling behaviors when subjected to noxious mechanical stimuli, showing a heightened response compared to the control group (Fig. 13A). Further investigations into the sensitivity of these mutants to less intense stimuli were conducted using gentle touch assays. Here, an eyelash was employed as the stimulant, and the results showed that *dRUFY* mutant larvae exhibited a substantial increase in their touch scores (Kernan et al., 1994), indicating enhanced sensitivity to the mild touch stimuli (Fig. 13B). The thermal sensitivity of these mutants was also tested using a hot probe heated to 46 °C probing thermonociceptive response (Petersen et al., 2018). The findings indicated that the rolling latency—the time it takes for larvae to begin rolling in response to the heat—was significantly reduced in the *dRUFY* mutant larvae compared to controls (Fig. 13C). This suggested an increased thermal responsiveness due to the *dRUFY* mutation.

To further investigate the specific role of *dRUFY* in sensory da neurons, I employed $dRUFY^{RNAi}$ to selectively knockdown this gene in Class I-IV da neurons and repeated the behavioral assays. When assessing the effects of *dRUFY* knockdown in mechanonociception or gentle touch assays, I observed no significant behavioral alterations compared to control larvae (Fig. 13D, E). However, *Drosophila* larvae with $dRUFY^{RNAi}$ in da neurons displayed a decreased rolling latency in response to noxious heat (Fig. 13F).

The increased sensitivity of larvae to heat upon *dRUFY* knockdown indicated sensitization of C4da neuron responses, which are required for heat-induced escape behavior. Therefore, I investigated the effects of directly activating C4da neurons with red light using CsChrimson, a red-light-shifted channelrhodopsin (Klapoetke et al., 2014). By specifically expressing $dRUFY^{RNAi}$ and CsChrimson in C4da neurons and stimulating them with red light, I observed that the escape rolling responses of the larvae were significantly enhanced, in line with sensory behavioral results (Fig. 13G). These results indicate that the loss of *dRUFY* in da neurons heightens the output of sensory neurons, in particular C4da, in response to somatosensory stimuli.

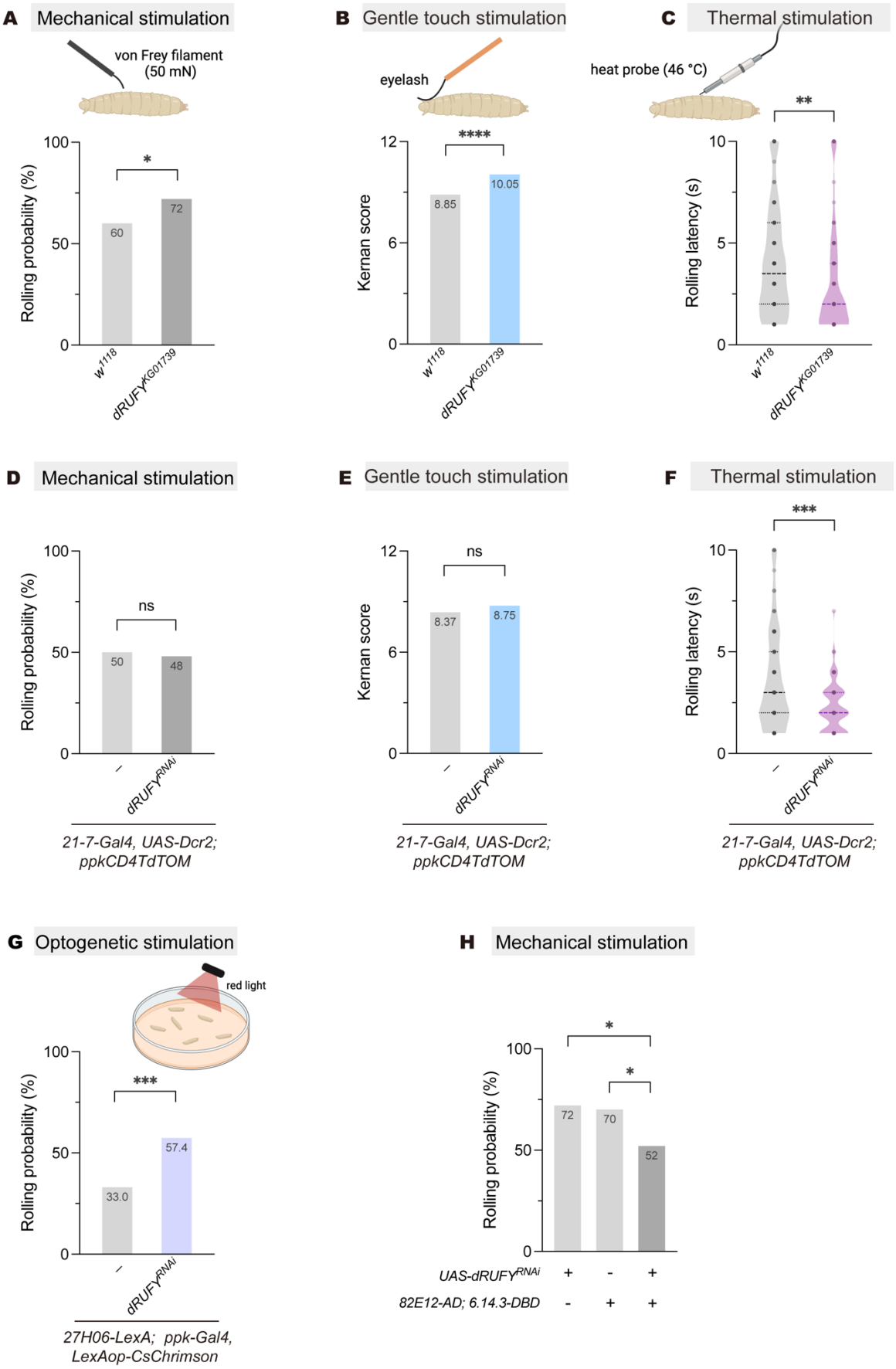
A
Mechanical stimulation
von Frey filament
(50 mN)
Rolling probability (%)
100
50
0
*
60
72
w1118
dRUFYKG01739
B
Gentle touch stimulation
eyelash
Kernan score
12
6
0
****
8.85
10.05
w1118
dRUFYKG01739
C
Thermal stimulation
heat probe (46 °C)
**
Rolling latency (s)
10
5
0
w1118
dRUFYKG01739
D
Mechanical stimulation
Rolling probability (%)
100
50
0
ns
50
48
–
dRUFYRNAi
21-7-Gal4, UAS-Dcr2;
ppkCD4TdTOM
E
Gentle touch stimulation
Kernan score
12
6
0
ns
8.37
8.75
–
dRUFYRNAi
21-7-Gal4, UAS-Dcr2;
ppkCD4TdTOM
F
Thermal stimulation
***
Rolling latency (s)
10
5
0
–
dRUFYRNAi
21-7-Gal4, UAS-Dcr2;
ppkCD4TdTOM
G
Optogenetic stimulation
red light
Rolling probability (%)
100
50
0
***
33.0
57.4
–
dRUFYRNAi
27H06-LexA; ppk-Gal4,
LexAop-CsChrimson
H
Mechanical stimulation
Rolling probability (%)
100
50
0
*
*
72
70
52
UAS-dRUFYRNAi + - +
82E12-AD; 6.14.3-DBD - + +

Fig. 13: Altered sensory behaviors in larvae lacking *dRUFY* in the da neuron system. (A) Top, schematic diagram illustrating a larva being stimulated by a von Frey filament applying a force of 50 mN (made with BioRender). Bottom, probability of mechano-nociceptive rolling after a second force application in third instar (96 h AEL) $dRUFY^{KG01739}$ mutant larvae. Both groups tested with n = 60. *p < 0.05, Fisher's exact test. (B) Top, diagram showing a larva being stimulated by an eyelash attached to a toothpick on the head segment (made with BioRender). Bottom, gentle touch response (Kernan score) in third instar $dRUFY^{KG01739}$ mutant larvae. Control (w^{1118}) n = 60, $dRUFY^{KG01739}$ n = 58. ****p < 0.0001, Fisher's exact test. (C) Top, schematic diagram showing a third instar larva stimulated by a 46-degree hot probe laterally (made with BioRender). Bottom, latency to initiate thermo-nociceptive rolling in third instar $dRUFY^{KG01739}$ mutant larvae. Control (w^{1118}) n = 80, $dRUFY^{KG01739}$ n = 80. Thick and thin dotted lines represent median and quartiles, respectively. **p < 0.01, Mann-Whitney test. (D) Mechano-nociceptive rolling probability post-second force application in third instar larvae with C1-4da neuron-specific knockdown of *dRUFY* ($dRUFY^{RNAi}$). Control n = 60, $dRUFY^{RNAi}$ n = 60. ns $p \geq 0.05$, Fisher's exact test. (E) Kernan score in gentle touch assays of third instar larvae following C1-4da neuron-specific knockdown of *dRUFY* ($dRUFY^{RNAi}$). Control n = 60, $dRUFY^{RNAi}$ n = 60. ns $p \geq 0.05$, Fisher's exact test. (F) Thermo-nociceptive rolling latency in third instar larvae after C1-4da neuron-specific knockdown of *dRUFY* ($dRUFY^{RNAi}$). Control n = 80, $dRUFY^{RNAi}$ n = 80. Thick and thin dotted lines represent median and quartiles, respectively. ***p < 0.001, Mann-Whitney test. (G) Top, diagram showing larvae expressing CsChrimson in C4da neurons being stimulated with red light (made with BioRender). Bottom, rolling probability induced optogenetically in third instar larvae after C4da neuron-specific knockdown of *dRUFY* ($dRUFY^{RNAi}$). Control n = 100, $dRUFY^{RNAi}$ n = 101. ***p < 0.001, Fisher's exact test. (H) Mechano-nociceptive rolling probability after second force application in third instar larvae post A08n neuron-specific knockdown of *dRUFY*. Control (*UAS-dRUFY*^{RNAi}) n = 60, control (*82E12-AD; 6.14.3-DBD*) n= 60, *UAS-dRUFY*^{RNAi} + *82E12-AD; 6.14.3-DBD* n = 60. *p < 0.05, Fisher's exact test with Bonferroni correction.

Lastly, I examined the role of A08n neurons, which are well-established postsynaptic partners of C4da neurons known to be required for nociceptive escape responses of downstream of C4da neurons (Tenedini et al., 2019). By specifically knocking down *dRUFY* in A08n neurons and subjecting them to mechanonociceptive assays using a 50 mN *von Frey* filament, I found that these larvae exhibited reduced nociceptive rolling behavior after harsh touch stimulation compared to controls (Fig. 13H). In conclusion, while perturbation of *dRUFY* in sensory neurons seems to sensitize larvae to sensory stimuli, specific manipulation of connected downstream neurons desensitizes behavioral responses.

3.4 *dRUFY* loss of function impacts the number of A08n postsynapses and the synaptic connections between C4da and A08n neurons

Abnormal dendritic morphology and synaptic structures play crucial roles in the pathogenesis of ID (Benítez-Bribiesca et al., 1999; Cordero et al., 1993; DeLong, 1993).

To investigate the influence of *dRUFY* on dendritic morphology, I employed two distinct RNAi lines targeting *dRUFY*, inserted either on the second or third chromosomes, to specifically knockdown *dRUFY* expression in C4da neurons. Qualitative analysis revealed no notable alterations in dendritic phenotypes in these neurons when compared to control C4da neurons (Fig. 14), suggesting no major impact of *dRUFY* on C4da neuron dendritic morphology.

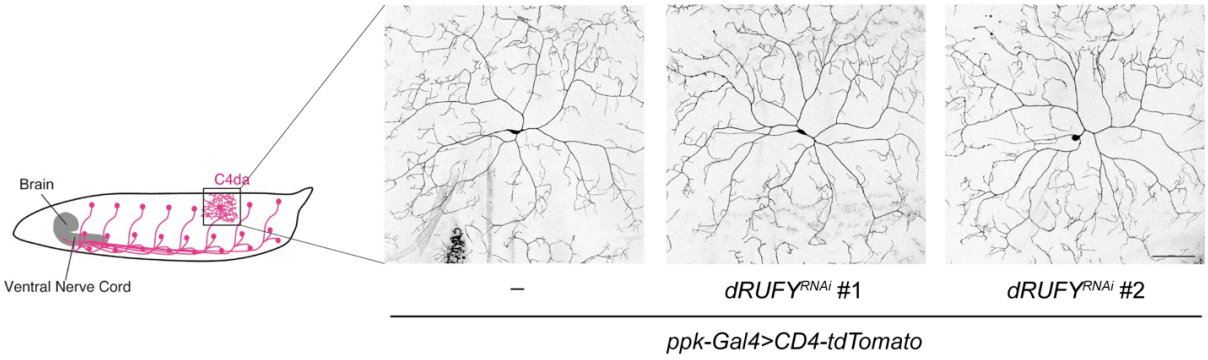

Fig. 14: *dRUFY* has no impact on C4da dendritic phenotypes. Left, schematic lateral view showing dendritic arborization and axonal projections of C4da neurons in third instar larvae (96 h AEL) (Yoshino et al., 2017). Right, representative images showing dendritic phenotypes upon knockdown of *dRUFY* in C4da neurons (*ppk-Gal4>CD4-tdTomato*). Scale bar = 100 µm.

As perturbation of *dRUFY* in C4da neurons affected sensory function but not their dendritic morphology, I examined the impact of *dRUFY* on synaptic structures within the C4da-A08n nociceptive circuit. I applied RNAi-mediated knockdown of *dRUFY* specifically in C4da or A08n neurons and visualized their pre- and postsynaptic compartments by expressing Brp^{short}-mCherry and Drep2-GFP, respectively (Tenedini et al., 2019). Quantitative analysis of synaptic structures showed that *dRUFY* knockdown in C4da neurons led to a significant increase in both the number of A08n postsynapses as well as of C4da-A08n synaptic connections, whereas there were no changes observed in the presynapse numbers in C4da neurons (Fig. 15A, C-E). Conversely, A08n-specific

knockdown of *dRUFY* markedly decreased both the A08n postsynapses and synaptic connections within the C4da-A08n circuit, without affecting the presynaptic configuration of C4da neurons (Fig. 16A, C-E). These findings underscore the critical, neuronal or compartment-specific role of *dRUFY* in synaptogenesis. Moreover, the observed synaptic modifications align with the results from sensory behavioral assays, which indicated that knocking down *dRUFY* in da neurons enhances sensory responsiveness, while its knockdown in A08n neurons leads to a diminished reaction to noxious touch stimuli.

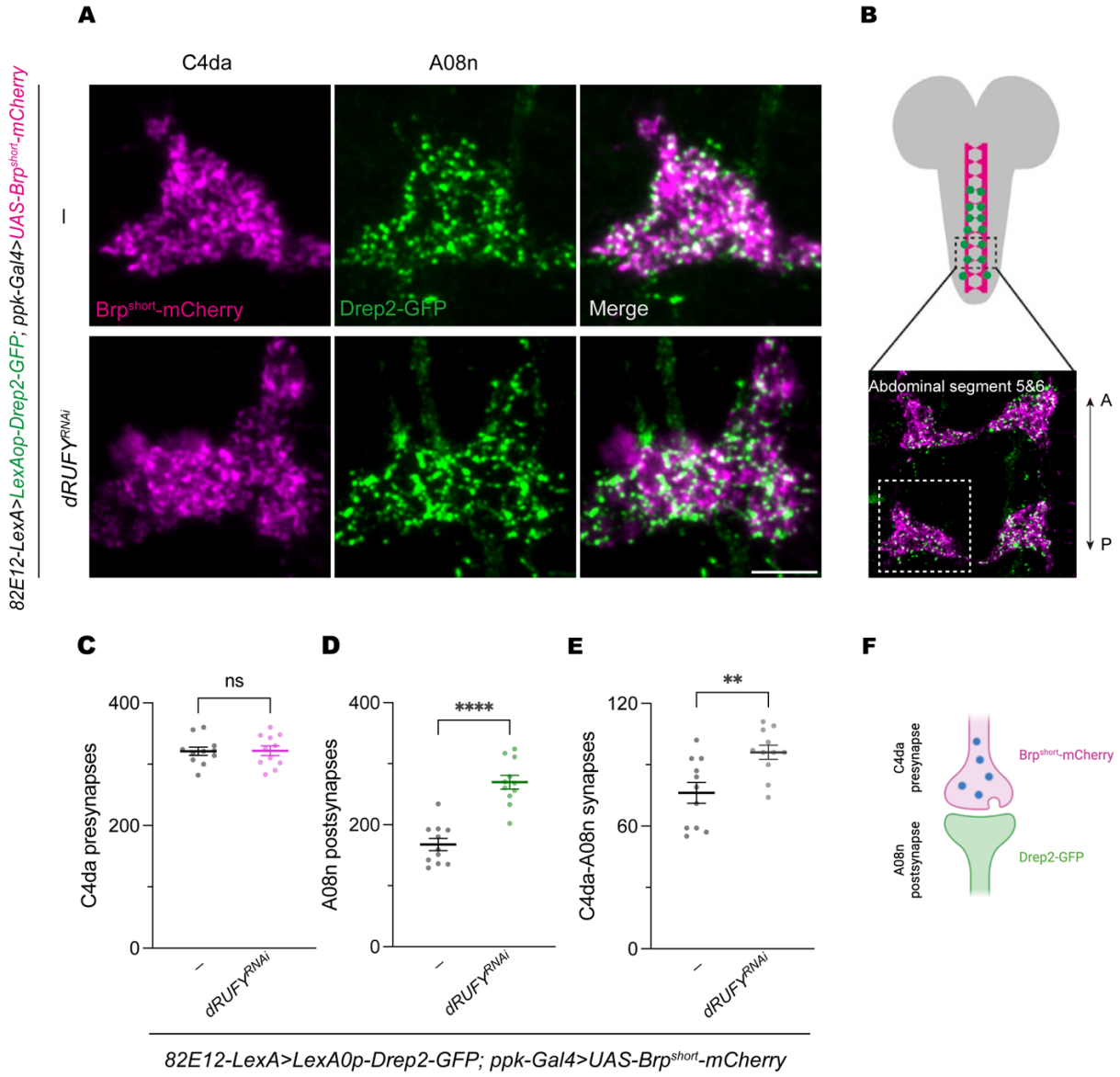

Fig. 15: *dRUFY* affects A08n postsynapse development and C4da-A08n synaptic connections. (A) Confocal microscopy images of hemisegments under control conditions and with *dRUFY*^{RNAi} expression in C4da neurons. Synaptic markers Brp^{short}-mCherry (magenta) and Drep2-GFP (green) are used to label C4da presynapses and A08n postsynapses, respectively. Scale bar = 5 µm. (B) Top, enlarged schematic representation of abdominal segments 5 and 6 (outlined by dotted lines) in the VNC (Yoshino et al., 2017). Bottom, representative confocal image showing C4da presynaptic (magenta) and A08n postsynaptic (green) markers in abdominal segments 5 and 6. A: Anterior, P: Posterior. (C-E) Quantification of (C) C4da presynaptic, (D) A08n postsynaptic, and (E) colocalized C4da-A08n synaptic markers in controls or upon *dRUFY*^{RNAi} expression in C4da neurons. Control n = 11, *dRUFY*^{RNAi} n = 11. Horizontal line and error bars represent mean and standard error of mean (SEM), respectively. $^{**}p < 0.01$, $^{****}p < 0.0001$, ns $p \geq 0.05$, Mann-Whitney test. (F) Schematic model of the expression of C4da presynaptic (Brp^{short}-mCherry) and A08n postsynaptic (Drep2-GFP) markers (made with BioRender).

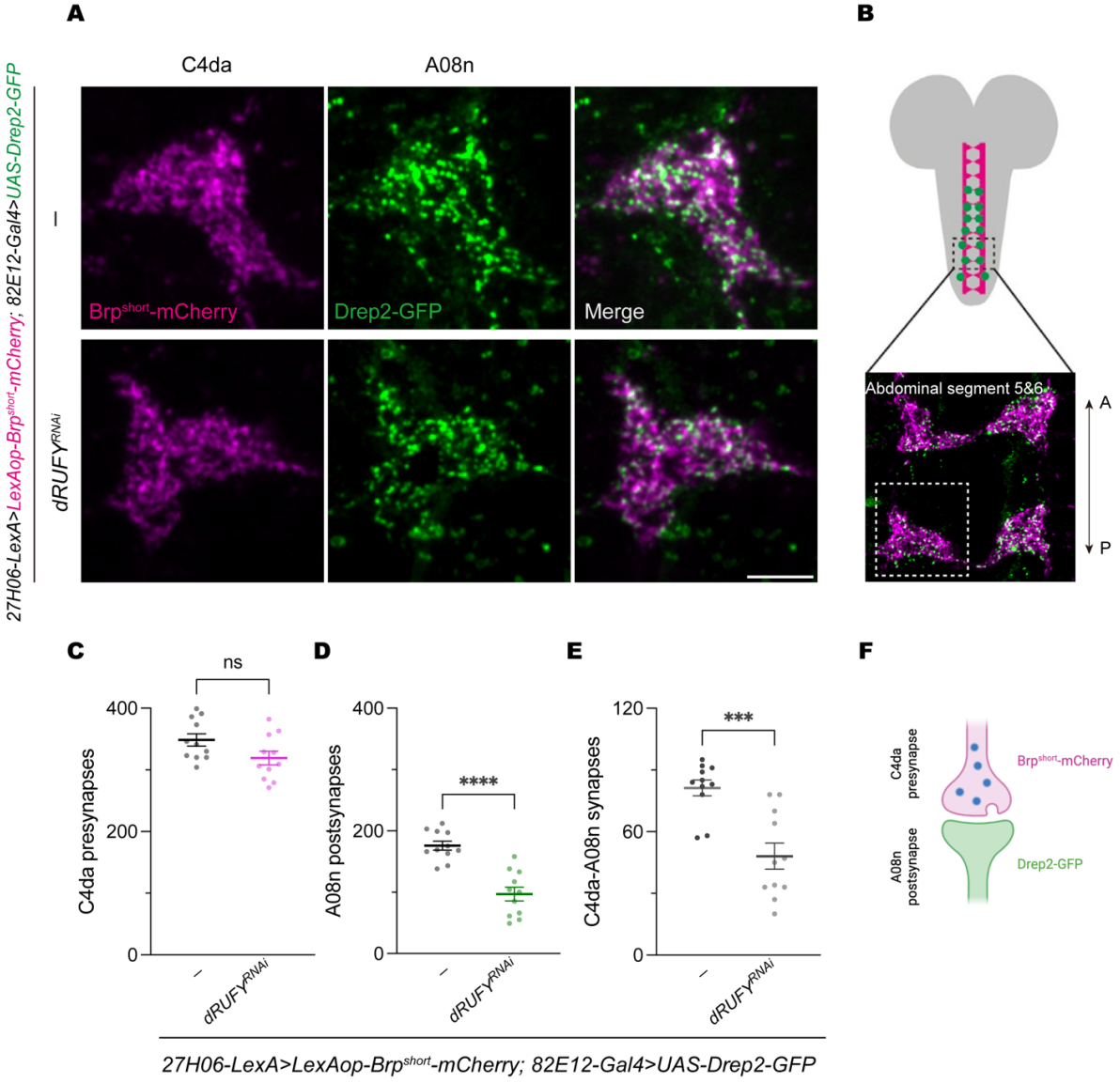

Fig. 16: *dRUFY* affects A08n postsynapse development and C4da-A08n synaptic connections. (A) Confocal microscopy images illustrating synaptic markers labeling in hemisegments, comparing controls to *dRUFY*^{RNAi} in A08n neurons. Synaptic markers Brp^{short}-mCherry (magenta) and Drep2-GFP (green) are used to label C4da presynapses and A08n postsynapses, respectively. Scale bar = 5 µm. (B) Top, enlarged schematic representation of abdominal segments 5 and 6 (outlined by dotted lines) in the VNC (Yoshino et al., 2017). Bottom, representative confocal image showing C4da presynaptic (magenta) and A08n postsynaptic (green) markers in abdominal segments 5 and 6. A: Anterior, P: Posterior. (C-E) Quantification of (C) C4da presynaptic, (D) A08n postsynaptic, and (E) colocalized C4da-A08n synaptic markers in controls or upon *dRUFY*^{RNAi} expression in A08n neurons. Control n = 11, *dRUFY*^{RNAi} n = 11. Horizontal line and error bars represent mean and standard error of mean (SEM), respectively. ***$p < 0.001$, ****$p < 0.0001$, ns $p \geq 0.05$, Mann-Whitney test. (F) Schematic model of the expression of C4da presynaptic (Brp^{short}-mCherry) and A08n postsynaptic (Drep2-GFP) markers (made with BioRender).

3.5 Loss of *dRUFY* in C4da neurons leads to autophagic defects

RUFY4 has been identified as a positive regulator of autophagy, with its upregulation leading to enhanced autophagic flux through interaction with interleukin-4 (IL-4) (Terawaki et al., 2015).

To test for a conserved role of *dRUFY* in autophagy, I utilized a dual fluorescent autophagosome marker, GFP-mCherry-Atg8 (Tan et al., 2024), to examine potential changes in autophagic flux. When autophagosomes merge with lysosomes, the GFP fluorescence is quenched due to the acidic environment within the autolysosomes, whereas the mCherry fluorescence persists. Typically, only mCherry but not GFP-positive puncta can be detected in neurons with normal autophagic flux (Tan et al., 2024).

Expressing the Atg8 reporter in C4da neurons, I could observe few GFP-positive puncta in the soma of control neurons, as well as a significant number of mCherry-positive autophagosomes. However, upon specific knockdown of *dRUFY* in C4da neurons, there was a notable decrease in mCherry-positive puncta within the soma of these neurons. The quantity of GFP-positive puncta remained unchanged in both control and $dRUFY^{RNAi}$ C4da neurons (Fig. 17B-D). Additionally, I assessed Atg8 puncta at C4da axon terminals in the ventral nerve cord (VNC) and observed a substantial reduction in mCherry-positive autophagosomes in neurons lacking *dRUFY* compared to the control, with no differences in GFP-positive puncta (Fig. 17E-G). These findings suggest autophagic processing defects due to the absence of *dRUFY*.

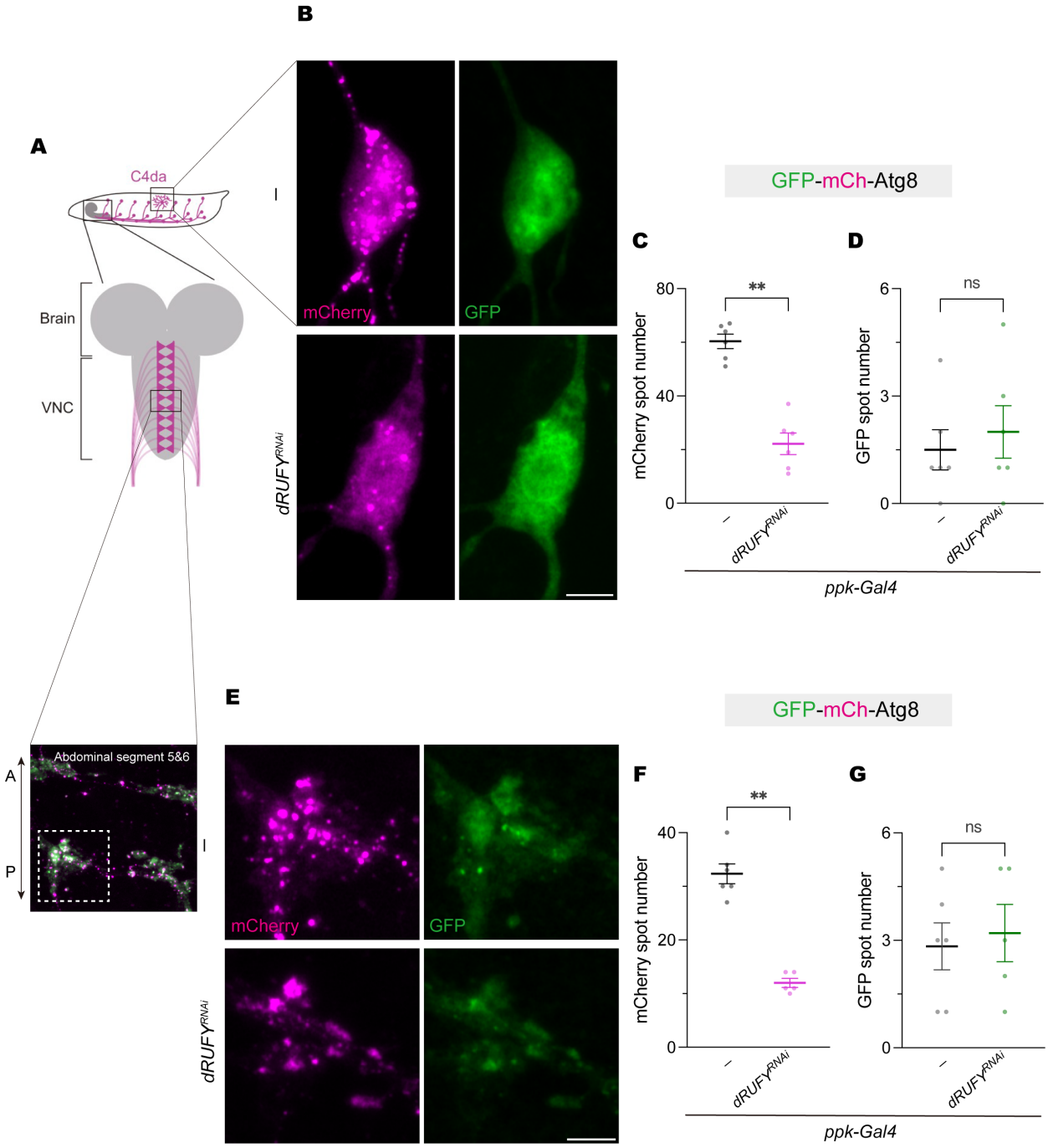
A
C4da
Brain
VNC
Abdominal segment 5&6
A
P
B
mCherry
GFP
dRUFY^RNAi
E
mCherry
GFP
dRUFY^RNAi
GFP-mCh-Atg8
C
mCherry spot number
80
40
0
**
–
dRUFY^RNAi
D
GFP spot number
6
3
0
ns
–
dRUFY^RNAi
ppk-Gal4
GFP-mCh-Atg8
F
mCherry spot number
40
20
0
**
–
dRUFY^RNAi
G
GFP spot number
6
3
0
ns
–
dRUFY^RNAi
ppk-Gal4

Fig. 17: Autophagic anomalies in C4da neurons due to the loss of *dRUFY*. (A) Top, schematic models depicting C4da neurons in third instar larvae (96 h AEL) and their axonal projections in the ventral nerve cord (VNC) (Nakamizo-Dojo et al., 2023). Bottom, example confocal image displaying GFP (green) and mCherry (magenta) dual fluorescence Atg8 autophagosome markers in abdominal segments 5 and 6 (*ppk-Gal4>UAS-GFP-mCherry-Atg8*). A: Anterior, P: Posterior. (B) Confocal microscopy images showing C4da neuron somata in controls and those expressing $dRUFY^{RNAi}$ in C4da neurons using the GFP-mCherry-Atg8 autophagy reporter. Scale bar = 5 µm. (C, D) Analysis of Atg8-containing puncta within C4da neuron somata, with quantification of (C) mCherry-positive puncta and (D) GFP-positive puncta in controls or upon $dRUFY^{RNAi}$ expression in C4da neurons. Control n = 6, $dRUFY^{RNAi}$ n = 6. Horizontal line and error bars represent mean and standard error of mean (SEM), respectively. $^{**}p < 0.01$, ns $p \geq 0.05$, Mann-Whitney test. (E) Confocal microscopy images of hemisegments showing the same GFP-mCherry-Atg8 reporter expression under control conditions and with $dRUFY^{RNAi}$ expression in C4da neurons. Scale bar = 5 µm. (F, G) Quantification of Atg8-containing puncta in hemisegments, (F) mCherry-positive and (G) GFP-positive puncta in control and $dRUFY^{RNAi}$-expressing neurons. Control n = 6, $dRUFY^{RNAi}$ n = 5. Horizontal line and error bars represent mean and standard error of mean (SEM), respectively. $^{**}p < 0.01$, ns $p \geq 0.05$, Mann-Whitney test.

3.6 Testing functional conservation of *dRUFY* and *RUFY4* and the pathogenicity of patient variant

In order to test the functional conservation between *Drosophila dRUFY* and human *RUFY4* as well as the pathogenicity of patient-derived variant, UAS transgenes of the wildtype and patient variant were made and combined with the *dRUFY* RNAi line.

At the synaptic level, I observed a significant increase in numbers of A08n postsynapses and C4da-A08n synaptic connections due to the specific knockdown of *dRUFY* in C4da neurons compared to the controls (Fig. 15). Co-overexpression of human *RUFY4* wild type ($hRUFY4^{WT}$) but not patient-derived variant ($hRUFY4^{Q432*}$) in C4da neurons effectively rescued the increase in A08n postsynapses and C4da-A08n synapses resulting from the absence of *dRUFY* in C4da neurons (Fig. 18B, C). I also found that loss of *dRUFY* in A08n neurons resulted in a reduced number of A08n postsynapses and C4da-A08n synaptic connections (Fig. 16). However, overexpression of $hRUFY4^{WT}$ or the patient variant in A08n neurons did not correct synaptic alterations caused by the loss of *dRUFY* in A08n neurons (Fig. 18E, F). This finding suggests that *RUFY4* can compensate for the loss of *dRUFY* in presynaptic but not postsynaptic compartments, and also shows that the truncated patient variant is nonfunctional in this system.

Synaptic rescue after C4da-specific *dRUFY* knockdown

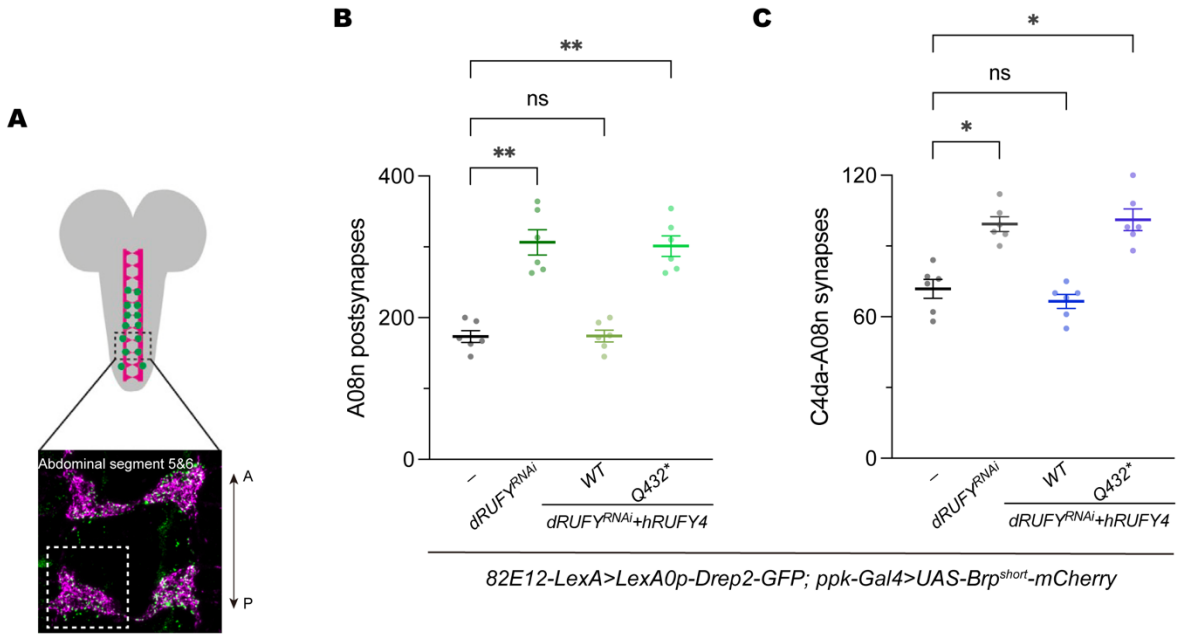

Synaptic rescue after A08n-specific *dRUFY* knockdown

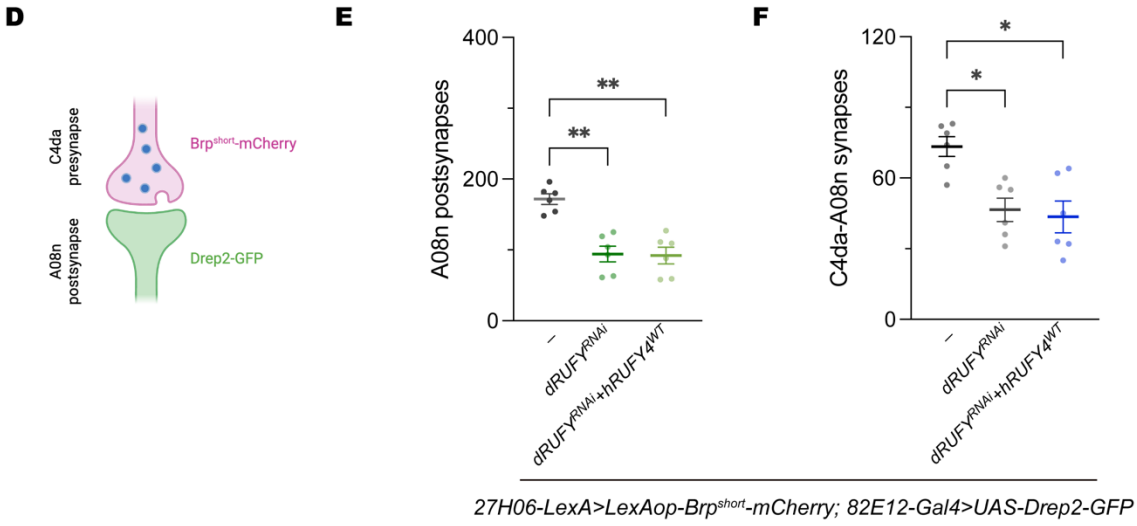

Fig. 18: Synaptic rescue analysis of *dRUFY*^{RNAi}-induced defects by human *RUFY4* in the C4da-A08n neuron circuit. (A) Top, enlarged schematic representation of abdominal segments 5 and 6 (outlined by dotted lines) in the VNC (Yoshino et al., 2017). Bottom, representative confocal image showing C4da presynaptic (magenta) and A08n postsynaptic (green) markers in abdominal segments 5 and 6. A: Anterior, P: Posterior. (B, C) Quantification of (B) A08n postsynaptic and (C) colocalized C4da-A08n synaptic markers in hemisegments following C4da neuron-specific *dRUFY* knockdown, with co-expression of wild-type *hRUFY4* (*hRUFY4*^{WT}) or patient-derived variant (*hRUFY4*^{Q432*}). Each group n = 6. Horizontal line and error bars represent mean and SEM, respectively. **p* < 0.05, ***p* < 0.01, ns *p* ≥ 0.05, Kruskal-Wallis test with Dunn's *post hoc* test. (D) Schematic model of the expression of C4da presynaptic (Brp^{short}-mCherry) and A08n postsynaptic (Drep2-GFP) markers (made with BioRender). (E, F) Quantification of (E) A08n postsynaptic and (F) colocalized C4da-A08n synaptic markers in hemisegments following A08n neuron-specific *dRUFY* knockdown, with co-expression of wild-type *hRUFY4* (*hRUFY4*^{WT}). Each group n = 6. Horizontal line and error bars represent mean and SEM, respectively. **p* < 0.05, ***p* < 0.01, Kruskal-Wallis test with Dunn's *post hoc* test.

The interesting finding that postsynaptic alterations in A08n neurons correlated with sensory behavioral changes upon loss of *dRUFY* in da neurons, prompted further investigations to test if sensory behavioral defects could be ameliorated by *hRUFY4*. Based on my findings that a knockdown of *dRUFY* in C1-4da neurons resulted in reduced rolling latency time in response to noxious heat stimulations (Fig.13F), and optogenetic activation enhanced escape responses (Fig. 13G), I tested if *hRUFY4* could normalize sensory functions. In contrast to patient-derived *hRUFY4*^{Q432*}, overexpression of *hRUFY4*^{WT} in C1-4da neurons completely restored the decreased rolling latency observed in larvae following *dRUFY* loss in da neurons (Fig. 19A). Furthermore, I previously observed increased rolling behavior induced optogenetically by CsChrimson activation in larvae with *dRUFY* knockdown in C4da neurons (Fig. 13G). This phenotype could be restored by overexpression of *hRUFY4*^{WT} but not *hRUFY4*^{Q432*} in C4da neurons, reducing the heightened nociceptive rolling response in larvae with *dRUFY* loss in C4da neurons to control levels (Fig. 19B).

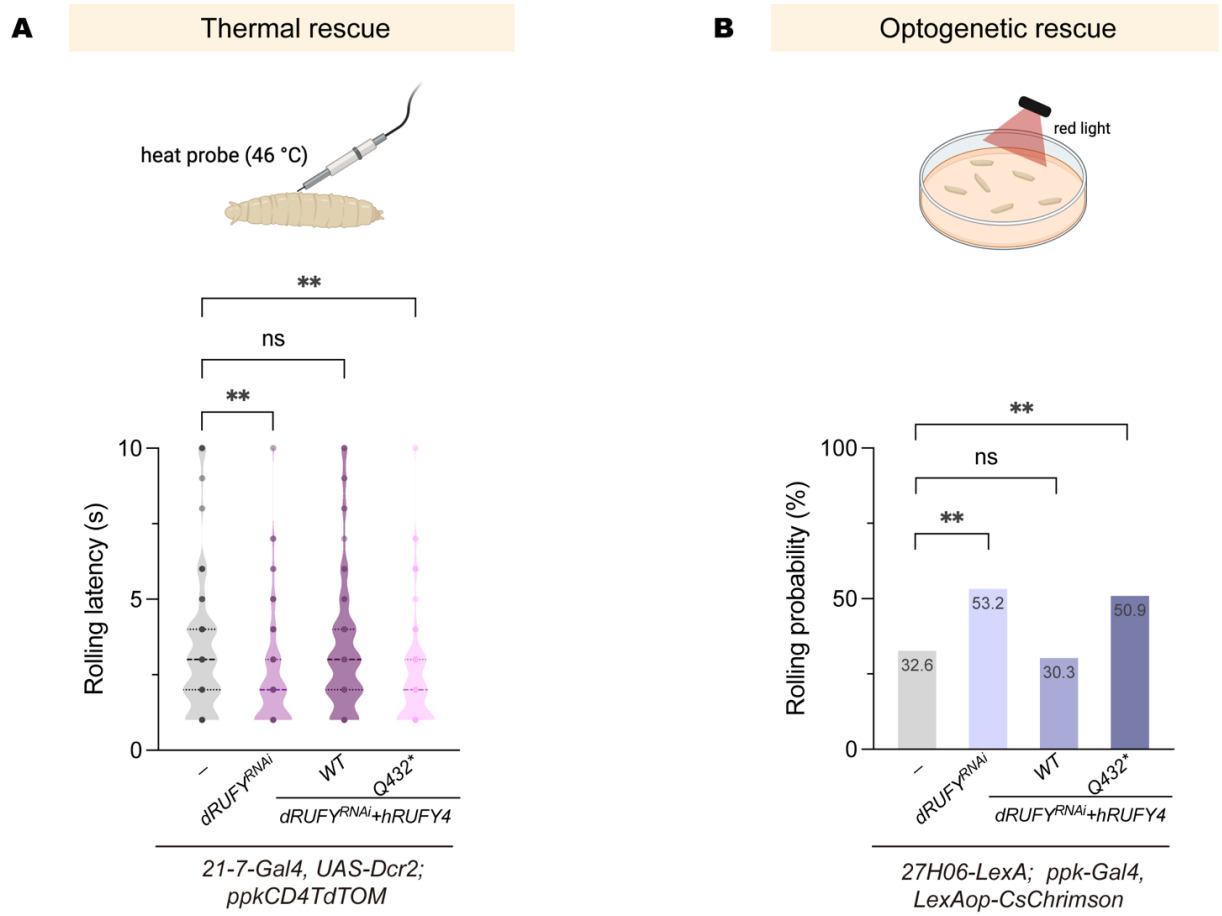

Fig. 19: Sensory behavioral rescue analysis of *dRUFY*^{RNAi}-induced defects by human *RUFY4* in *Drosophila*. (A) Top, schematic diagram showing a third instar larva stimulated by a 46-degree hot probe laterally (made with BioRender). Bottom, thermo-nociceptive rolling latency in third instar larvae following C1-4da neuron-specific knockdown of *dRUFY*, with co-expression of either wild-type *hRUFY4* (*hRUFY4*^{WT}) or patient-derived variant (*hRUFY4*^{Q432*}). Each group n = 80. Thick and thin dotted lines represent median and quartiles, respectively. $^{**}p < 0.01$, ns $p \geq 0.05$, Kruskal-Wallis test with Dunn's *post hoc* test. (B) Top, diagram showing larvae expressing CsChrimson in C4da neurons being stimulated with red light (made with BioRender). Bottom, rolling probability induced by optogenetic activation of C4da neurons in third instar larvae following C4da neuron-specific *dRUFY* knockdown, with co-expression of either wild-type *hRUFY4* (*hRUFY4*^{WT}) or patient-derived variant (*hRUFY4*^{Q432*}). Control n = 119, *dRUFY*^{RNAi} n = 109, *dRUFY*^{RNAi} + *hRUFY4*^{WT} n = 142, *dRUFY*^{RNAi} + *hRUFY4*^{Q432*} n = 110. $^{**}p < 0.01$, ns $p \geq 0.05$, Fisher's exact test with Bonferroni correction.

I further tested if the autophagic changes detected using GFP-mCherry-Atg8, where I observed a reduced number of mCherry-positive Atg8 puncta in the soma or axonal terminals of C4da neurons due to loss of *dRUFY* (Fig. 17) could be rescued by human *RUFY4*. However, overexpressing wild type *hRUFY4* in C4da neurons did not restore the reduced mCherry-positive autophagosomes in C4da neurons induced by *dRUFY*

knockdown, neither in the soma (Fig. 20A) nor the axon terminals (Fig. 20B).

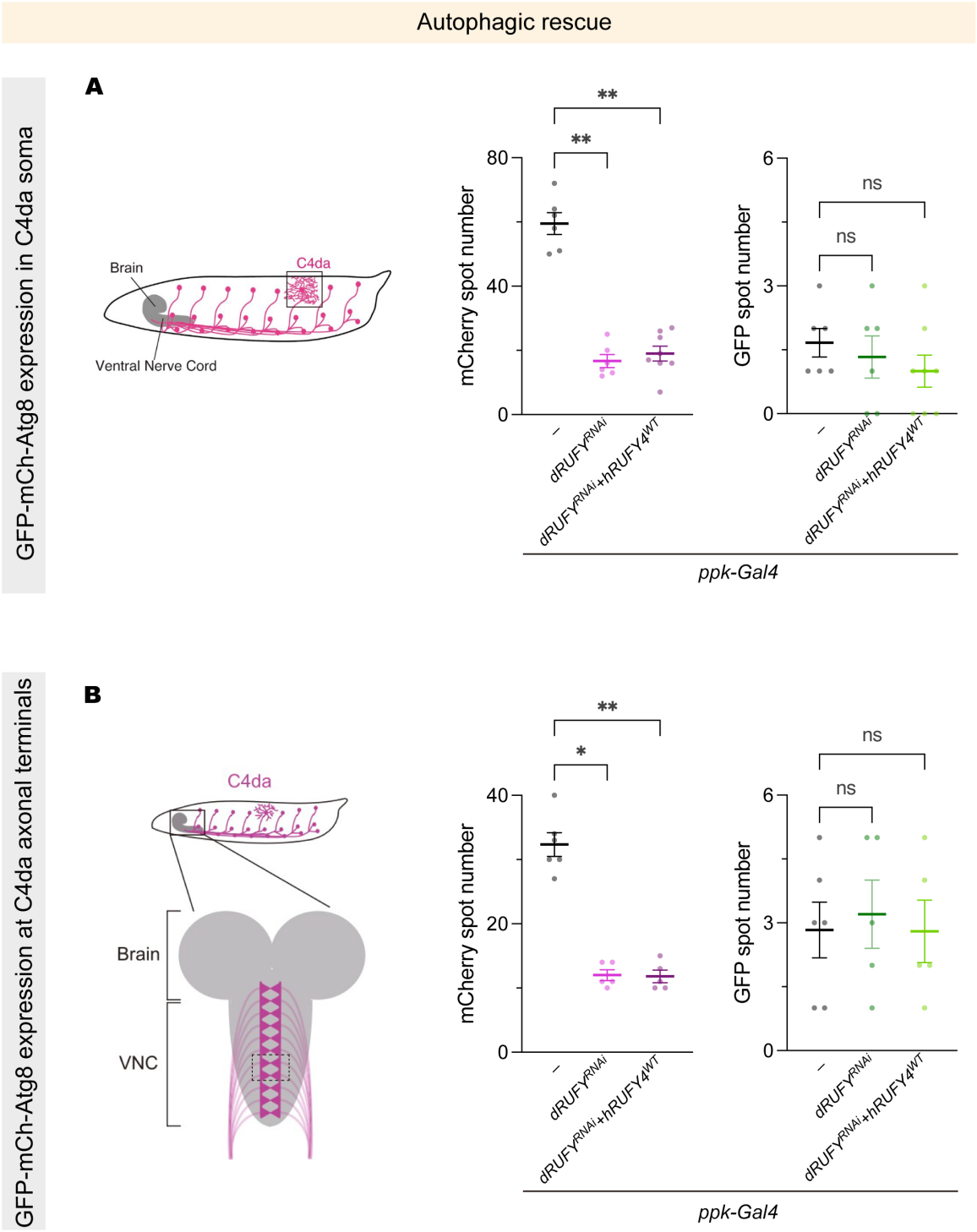

Fig. 20: Autophagic rescue analysis of *dRUFY*^{RNAi}-induced defects by human *RUFY4* in *Drosophila*. (A) Left, schematic lateral view showing dendritic arborization and axonal projections of C4da neurons in third instar larvae (96 h AEL) (Yoshino et al., 2017). Right, quantification of mCherry-positive and GFP-positive Atg8 puncta in C4da neuron somata following C4da neuron-specific knockdown of *dRUFY* and co-expression of *hRUFY4*^{WT}. Control n = 6, *dRUFY*^{RNAi} n = 6, *dRUFY*^{RNAi} + *hRUFY4*^{WT} n = 8. Horizontal line and error bars represent mean and SEM, respectively. $^{**}p < 0.01$, Kruskal-Wallis test with Dunn's *post hoc* test. (B) Left, schematic models depicting C4da neurons in third instar larvae (96 h AEL) and their axonal projections in the VNC. Abdominal segments 5 and 6 are outlined by dotted lines (Nakamizo-Dojo et al., 2023). Right, quantification of mCherry-positive and GFP-positive puncta in hemisegments after C4da neuron-specific knockdown of *dRUFY* and co-expression of *hRUFY4*^{WT}. Control n = 6, *dRUFY*^{RNAi} n = 5, *dRUFY*^{RNAi} + *hRUFY4*^{WT} n = 5. Horizontal line and error bars represent mean and SEM, respectively. $^{*}p < 0.05$, $^{**}p < 0.01$, ns $p \geq 0.05$, Kruskal-Wallis test with Dunn's *post hoc* test.

Overall, these findings confirm that *Drosophila dRUFY* and human *RUFY4* are in part functionally conserved, specifically in regulating synapse alterations and nociceptive behavior mediated by C4da neurons. Interestingly, the patient-derived *hRUFY4* variant was not functional in these assays suggesting it is indeed pathogenic. In addition, no rescue activity was found for human *RUFY4* in controlling synaptic changes caused by *dRUFY* reduction in A08n neurons, or in regulating autophagosome alterations in C4da neurons, suggesting not all of the functions of *dRUFY* can be compensated by *hRUFY4*.

3.7 *dRUFY* functionally interacts with *Rab4*

RUFY proteins play a crucial role in Rab-mediated intracellular membrane trafficking through the RUN domain (Kitagishi and Matsuda, 2013). *RUFY1* has been identified as an effector of *Rab4*, and it influences endosomal dynamics by enlarging early endosomes and modulating the interaction between sorting and recycling endosome proteins when coexpressed with GTP-bound form of *Rab4* (Cormont et al., 2001).

I therefore tested a potential genetic link between *Rab4* and *dRUFY* in flies. In experiments with third instar *Rab4* heterozygous mutant larvae subjected to thermo-nociception assays using a 46 °C hot probe, these animals exhibited increased latency in their rolling response to noxious heat compared to control larvae (Fig. 21). *dRUFY* mutant larvae had a decreased latency in rolling behavior under the same conditions (Fig. 13C). To test for a functional interaction between *dRUFY* and *Rab4*, I combined *Rab4*$^{KO/+}$ with the homozygous *dRUFY*^{KG01739} allele and found that these mutant larvae displayed a

significant increase in rolling latency upon exposure to noxious heat, suggesting a severely impaired nociceptive response (Fig. 21). This outcome supports the hypothesis that *dRUFY* may functionally interact with *Rab4* in flies, providing a link to the endosomal machinery.

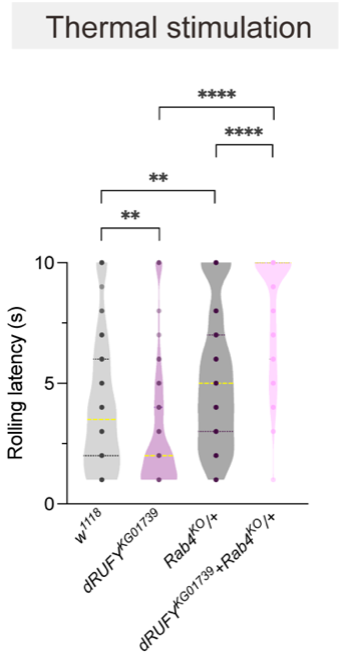

Fig. 21: Genetic interaction of *dRUFY* with *Rab4* in thermo-nociceptive response. Thermo-nociceptive rolling latency in third instar larvae (96 h AEL) across different genetic backgrounds: *dRUFY* mutant ($dRUFY^{KG01739}$), *Rab4* heterozygous mutant ($Rab4^{KO}$/+), and the combined genotypes ($dRUFY^{KG01739}$+ $Rab4^{KO/+}$). Controls used were w^{1118} larvae. Sample sizes for all groups were n = 80. The thick dotted line and the thin dotted lines represent the median and quartiles respectively. Statistical significance was determined using Kruskal-Wallis with Dunn's *post hoc* test, $^{**}p < 0.01$, $^{****}p < 0.0001$.

4 Discussion

Neurodevelopmental disorders (NDDs) encompass a spectrum of conditions marked by significant functional impairments with the onset during development (Morris-Rosendahl et al., 2020). Approximately 15 % of children and adolescents in the US are affected by NDDs, including ADHD, ID, ASD, and developmental delays (Boyle et al., 2011), making them a significant public health concern. ID typically manifests as a central feature across a variety of NDDs, profoundly impacting the affected individuals' quality of life. While environmental factors like infection and malnutrition can contribute to NDDs with ID, genetic anomalies are recognized as the primary drivers, especially in severe cases (van Bokhoven, 2011). Despite substantial advancements in genomic research, the genetic underpinnings of over half of ID cases remain elusive (Rauch et al., 2006), particularly in populations with high rates of consanguineous marriages. These marriages increase the likelihood of autosomal recessive genetic disorders, as closely related parents are more likely to pass on identical alleles of deleterious genes to their offspring, thereby enhancing the risk of NDDs. This feature makes genetic diagnosis especially crucial for consanguineous families. Genetic diagnosis can elucidate the specific subtype of NDDs, the severity and prognosis of the condition, and potential complications. For families with a history of NDDs, genetic insights are indispensable. They can provide preventive strategies for future pregnancies, such as prenatal diagnosis and carrier testing, significantly impacting family planning and disease management.

A challenge in identifying NDDs-associated genes is the difficulties in assessing the pathogenicity of recessive variants, especially missense variants, which account for the majority of such variants (Reuter et al., 2017). Characterization of variants, especially in vivo analysis in mammals, is costly and time-consuming. *Drosophila* offers a cost-effective and efficient alternative for in vivo functional studies of recessive variants of identified conserved candidate genes, which are present in approximately 75% of all cases (Link and Bellen, 2020).

Our collaboration with the Department of Human Genetics at FAU Erlangen aimed to improve the diagnostic yield of genetic tests in NDDs by enhancing the identification of novel NDD-associated genes within a cohort of consanguineous families from Turkey. I

focused on one such candidate gene, *RUFY4*, previously identified by our collaborators. My experimental manipulations in a *Drosophila* model revealed that disruptions in the *Drosophila* homologue of *RUFY4*, *dRUFY*, led to deficits in memory, social interaction, and sensory processing, alongside alterations in synaptic connections and autophagic functions. These phenotypes not only mirror the pathological features commonly observed in NDDs but also underscore a central role for *RUFY4* disruptions in these processes. Furthermore, introducing human *RUFY4* but not the patient variant could rescue some of these deficits, highlighting the functional conservation between human *RUFY4* and *dRUFY*, supporting synaptic dysfunction as a plausible mechanism in the etiology of a *RUFY4*-dependent NDD. Our findings extended the potential for *RUFY4* to serve as a therapeutic target, given its involvement in multiple biological pathways essential for neurodevelopment.

4.1 Role of *dRUFY* in adaptive functions

In this study, various methodologies were employed to examine the adaptive behavioral alterations resulting from the deletion of the *dRUFY* gene in *Drosophila*, encompassing aspects of memory, motor function, and social interactions. First, I evaluated innate preferences for fructose or n-amyl acetate in *dRUFY* mutant larvae. These larvae demonstrated a marked increase in preference for sugar, but not for the odor, compared to control larvae (Fig. 11A, C, D), indicating altered gustatory perception. Subsequently, I utilized odor-taste associative learning assays where fructose was paired with n-amyl acetate to evaluate memory functions. Although an enhanced preference for sugar might aid larvae in better remembering the association, they exhibited a lower learning index (Fig. 11B, F), emphasizing their memory impairments. While motor function of *dRUFY* mutant flies evaluated in climbing assays was normal (Fig. 12A, B), social behavior assayed in food competition assays was impaired in flies lacking *dRUFY* in somatosensory neurons (Fig. 12C, D).

The findings of memory defects and social impairments due to loss of *dRUFY* in flies align with the typical symptoms observed in NDDs patients, who frequently face challenges related to memory, motor skills, and social interaction (Morris-Rosendahl and Crocq, 2020; Mullin et al., 2013). However, whether *RUFY* genes are implicated in motor function

remains unknown.

RUFY family proteins interact with small GTPases like Rab proteins to control endosome dynamics and facilitate membrane trafficking, particularly in related to endocytosis and autophagy (Char and Pierre, 2020). Autophagy is involved in regulating synaptic activity and neurotransmission in the brain, particularly in the hippocampus, which is critical for memory formation and learning (Tripathi et al., 2019). Glatigny et al. revealed that inducing autophagy in the hippocampi of aged mice can reverse the memory deficits, suggesting the importance of autophagy in maintaining cognitive functions (Glatigny et al., 2019). Various studies have also indicated that autophagy pathways play a role in the pathogenesis of ASD (Lee et al., 2013). Kim et al. found that the absence of the autophagy-related gene *Atg7* disrupted the autophagic process, leading to deficits in behavior that are characteristic of ASD, such as impaired social interaction and increased repetitive behaviors (Kim et al., 2017). These studies indicate that the absence of *dRUFY* could contribute to memory deficits and social impairments by impacting the autophagy.

Currently, there is no published data that implicates *RUFY* family proteins in adaptive animal behavior. However, based on the obtained data on *dRUFY* in flies I could show that this gene influences the adaptive capabilities of an organism at a behavioral level, which is likely linked to associated defects in synaptogenesis and/or autophagy.

4.2 Loss of *dRUFY* leads to impairments in the somatosensory system

Sensory impairment is characterized by a reduced ability to process sensory information including touch, taste, smell, vision, hearing, and pain. This impairment can result in diminished sensations and inadequate neural coordination (Battaglia, 2011). Individuals with sensory impairments may experience difficulties in hearing, speaking, seeing, smelling, feeling, or responding to respective sensory inputs. In many NDDs, sensory processing alterations are common. These alterations in sensory behavior could potentially act as early prognostic markers, helping predict future abilities (Hudac et al., 2024).

In this study, I employed three distinct sensory behavioral assays in *Drosophila* larvae: mechanonociception, gentle touch, and thermo-nociception assays, to evaluate their

responses to noxious mechanical stimuli, gentle touch, and noxious heat, respectively. *dRUFY* mutant larvae showed an increased responses in all three assays (Fig. 13A-C), indicating hypersensitivity. When *dRUFY* was specifically knocked down in CI-IVda neurons, there was an increased sensitivity to thermal stimuli (Fig. 13F), but not for mechanical or gentle touch responses (Fig. 13D, E). Additionally, C4da-neuron specific *dRUFY* knockdown increased the rolling frequency following optogenetic activation (Fig. 13G), while the same perturbation in downstream A08n neurons resulted in decreased mechanonociceptive responses (Fig. 13H). This suggests that loss of *dRUFY* affects somatosensory processing. Hertz et al. found that knockout of *RUFY3* in mice resulted in misprojections of tropomyosin receptor kinase A positive (TRKA+) sensory axons (Hertz et al., 2019), indicating the implication of RUFY family protein in the development of sensory circuits.

Sensory dysfunction is frequently observed in NDDs (Michaelson et al., 2018). Approximately 90 % of individuals with ASD display atypical responses to sensory stimuli, such as touch (Robertson and Baron-Cohen, 2017). Tactile hypersensitivity is a common feature of Fragile X Syndrome (FXS), which is a major inheritable cause of ASD/ID (Domanski et al., 2019). Kerner-Rossi et al. noted decreased responses to thermal and mechanical stimuli in a mouse model of Christianson Syndrome, a rare developmental disorder characterized by significant intellectual disability, ataxia, postnatal microcephaly, and hyperkinesis (Kerner-Rossi et al., 2019). Lyons-Warren et al. found that Synaptic Ras GTPase-activating protein 1-related ID patients exhibited high levels of sensory avoiding and seeking (Lyons-Warren et al., 2022). Intriguingly, altering *dRUFY* in either C4da or A08n neurons elicited opposite behavioral consequences, implying that *dRUFY* may play varying roles across different types of neurons. Given that A08n neurons function downstream from C4da neurons, it seems *dRUFY* is crucial for modulating the processing and integration of sensory signals at various levels of the sensory pathway.

Significantly, sociability is not an inherent genetic trait but rather a skill developed through interaction with the social environment. This indicates that sociability develops based on sensory feedback, suggesting that any disruptions in sensory perception, particularly during early development, can affect social abilities. Orefice et al. used mouse models with mutations in genes linked to ASD, including *Mecp2, Gabrb3, Shank3, and Fmr1*. They

found that these mice displayed tactile hypersensitivity and social deficits, and *Mecp2* expression specifically in somatosensory neurons of *Mecp2*-null mice rescued both tactile sensitivity and social interaction deficits (Orefice et al., 2016). Subsequently, they also found that a six-week treatment with a peripherally-restricted $GABA_A$ receptor agonist targeting mechanosensory neurons significantly reduced tactile hypersensitivity and social impairments in *Mecp2* and *Shank3* mutant mice (Orefice et al., 2019). These findings highlight the potential of targeting sensory neurons to mitigate social defects in ASD. Hence, sensory deficits found upon *dRUFY* perturbation could be the reason for the observed social defects in flies lacking *dRUFY* in somatosensory neurons in food competition assays (Fig. 12C).

As this is the first study to describe the effects of *RUFY* on the somatosensory system function at the behavioral level, it remains to be shown if these functions are conserved in *RUFY* family proteins in higher organisms.

4.3 *dRUFY* plays a role in regulating synapse formation in the C4da-A08n circuit

The formation of dendritic spines and synapses marks a critical final phase in brain wiring, crucial for establishing functional communication during brain development. Recent studies have shown that defects in dendrites, synapse formation, synaptic plasticity, and associated molecular mechanisms are observed both in animal models of ID and in post-mortem brain tissues of ID patients (Ford et al., 2023).

Abnormal dendritic polarity and branching in neural networks can result in structural and functional brain anomalies that are associated with NDDs like autism and ID (Ka et al., 2022). I detected no changes in the dendritic characteristics of C4da neurons in third instar larvae with a loss of *dRUFY*, as compared to controls (Fig. 14). While no existing studies have explored the impact of *RUFY* on neuronal dendrites, recent studies indicated its role in axon growth. Wei et al. identified *RUFY3* as an important regulator of axon formation and elongation through interactions with actin-related proteins such as Fascin and Drebrin in the growth cones of mouse hippocampal neurons (Wei et al., 2014). They also suggested that during human embryonic development, *RUFY3* may be expressed in neural tissues similarly as in mice, which may hold significance for studies of human neurodevelopment. Furthermore, Honda et al. characterized *RUFY3* as an essential

adaptor protein in the pathways regulating neuronal polarity and axon growth, specifically through interactions with Rap2, emphasizing the importance of *RUFY* family gene in neurodevelopment and its potential link to various neurological disorders if its function is compromised (Honda et al., 2017). The study by Hertz et al. found that dephosphorylation of *RUFY3* at specific residues was necessary to initiate axon degeneration, suggesting an essential role of *RUFY3* in regulating axon maintenance (Hertz et al., 2019). These findings highlight the importance of *RUFY* family protein in axon formation via various molecular pathways, suggesting a need for additional investigation into possible axon alterations in C4da neurons following the manipulation of *dRUFY*.

Synapses are the functional connections through which electrical or chemical signals are transmitted from a presynaptic neuron to a postsynaptic neuron. Impairments in the development of synapses are thought to be a possible underlying cause for the pathogenesis of NDDs, including ASD (Bagni and Zukin, 2019) and ID (Ford et al., 2023). The selective perturbation of *dRUFY* in C4da neurons led to a significant increase in the number of A08n postsynapses and C4da-A08n synapses (Fig. 15). Conversely, knocking down *dRUFY* specifically in A08n neurons resulted in a significant decrease of A08n postsynaptic and C4da-A08n synaptic numbers (Fig. 16). Neither C4da nor A08n neuron-specific expression of $dRUFY^{RNAi}$ influenced the number of C4da presynaptic puncta (Fig. 15C, 16C). Interestingly, these synaptic alterations align with my previously observed sensory behavioral changes, where *dRUFY* knockdown in da neurons increased larval rolling behavior in response to thermal stimuli or upon optogenetic activation (Fig. 13F, G), whereas its knockdown in A08n neurons reduced escape responses to noxious mechanical stimuli (Fig. 13H). This suggests that altered synaptogenesis might contribute to sensory impairments triggered by disruption of *dRUFY*. Disruption of *dRUFY* affected only the number of A08n postsynaptic and C4da-A08n synaptic puncta without impacting C4da presynaptic puncta. Given that post-synaptic neurons utilize dendrites to form synapses for receiving and processing information from pre-synaptic neurons (Ford et al., 2023), additional analysis is needed to explore how *dRUFY* influences the dendrites of A08n neurons.

Ka et al. observed an increased number of excitatory neuronal synapses in *WDR5*-deficient mice, a model for Kabuki syndrome characterized by intellectual disability and

neurodevelopmental delay, compared to control mice (Ka et al., 2022). *ARID1B* gene's haploinsufficiency is linked to ASD and ID and Jung et al. reported an excitation/inhibition imbalance due to reduced GABAergic synapses in the cerebral cortex of mice with *Arid1b* deletion. Additionally, these *Arid1b* heterozygous mice exhibited impaired spatial learning in the Morris water maze test, reduced spatial reference memory in the novel object recognition test, and difficulties in motor learning in the rotarod test. The mutant mice also showed no preference for an unfamiliar stranger mouse in social novelty test and decreased social interaction in open-field test, indicating disrupted social behaviors. Interestingly, the memory and social deficiencies in *Arid1b* knockout mice were rescued through the application of a positive allosteric modulator of the $GABA_A$ receptor, suggesting a link between reduced GABAergic synapses and these impairments (Jung et al., 2017). These findings underscore the significance of synaptic abnormalities in the pathogenesis of NDDs and show that specific synaptic alterations can lead to deficits in cognitive memory and social behavior. Given my previous observations of learning and memory impairments, as well as disrupted social interactions in *dRUFY*-deficient Drosophila, I propose that abnormal synapse formation might contribute to these behavioral changes.

4.4 The role of *dRUFY* in autophagy

Autophagy is a degradation pathway conserved across different species and cell types, transporting organelles or cytoplasmic materials to lysosomes (Morishita and Mizushima, 2019). Cells use autophagy to survive various stressors such as starvation, protein aggregates, damaged mitochondria, or internal bacterial infections (Terawaki et al., 2015). This process is regulated in part by Rab GTPases and depends on the production of phosphatidylinositol-3-phosphate (PtdIns(3)P) for the formation of autophagosomes (Terawaki et al., 2015). Proteins from the RUFY family, featuring a N-terminal RUN domain that binds to small GTPases and a C-terminal FYVE domain that interacts with PtdIns(3)P, are prime candidate effectors for regulating processes like endocytosis or autophagy (Char and Pierre, 2020).

Terawaki et al. identified *RUFY4* as a novel positive regulator of autophagy, with its upregulation playing a role in enhancing autophagic flux through interaction with

interleukin-4 (IL-4). They also noted that *RUFY4* interacted with Rab7 to regulate the positioning of endosomes and autophagosomes in dendritic cells, thus improving immune responses (Terawaki et al., 2015, 2016). Similarly, Pankiv et al. found that *RUFY1*, through its coiled-coil domain, enhanced the movement of autophagic vesicles along microtubules by interacting with Rab7 (Pankiv et al., 2010). Aligning with these studies, my observations showed a decrease in mCherry-positive autophagosomes in both the somas and axon terminals of *dRUFY*-deficient C4da neurons in *Drosophila* larvae (Fig. 17), indicating reduced autophagic activity due to the absence of *dRUFY*.

The RUN domain of *RUFY* family proteins facilitates the interaction between *RUFY* proteins and small GTPases, enhancing the regulation of cell polarity and membrane trafficking across various cellular processes (Kitagishi and Matsuda, 2013). Rab4, a small GTPase associated with endocytosis in all cell types, also performs specialized roles such as receptor recycling to the plasma membrane and antigen processing in specific cell types (Cormont et al., 2001). Cormont et al. revealed that *RUFY1* specifically recognizes and interacts with the active form of Rab4. This interaction enlarged early endosomes and enhanced the colocalization of markers for sorting and recycling endosomes, implicating the interaction between Rab4 and RUFY family protein in regulating endosomal trafficking (Cormont et al., 2001). In this thesis, I established that *dRUFY* genetically interacted with *Rab4*, evidenced by the significantly impaired thermal nociceptive response in larvae carrying both *dRUFY* and *Rab4* mutations (Fig. 21). However, the specific role of *Rab4* in regulating autophagy or endosomal trafficking via *dRUFY* remains unclear, necessitating further investigation.

Autophagy significantly influences synapse formation in *Drosophila*. Shen et al. demonstrated that disrupting autophagy within the mushroom bodies caused a brain-wide increase in synaptic staining for the active zone master scaffold protein Bruchpilot (Brp), a trait typically seen in aged brains (Shen and Ganetzky, 2009). Additionally, research by Kiral et al. indicated that a deficiency in autophagy resulted in the creation of excess synapses and the association with inappropriate postsynaptic partners, leading to less precise synaptic connections in *Drosophila* (Kiral et al., 2020). However, my later findings that *hRUFY4* could rescue altered synapse formation but not autophagic defects suggest that changes in autophagic activity might not contribute to the development of synaptic

anomalies in this system.

4.5 Functional conservation between *Drosophila dRUFY* and human *RUFY4*

In this study, I identified synaptic alterations, autophagic disruptions, and impairments in sensory processing, memory, and social behavior resulting from decreased expression or deletion of *dRUFY* in *Drosophila*. Cell type-specific overexpression of *RUFY4* was able to completely restore synaptic and sensory behavioral defects in specific types of neurons caused by the absence of *Drosophila dRUFY*, indicating significant functional conservation between these genes. Conversely, the patient-derived *RUFY4* variant, which truncates *RUFY4* resulting in a variant lacking the C-terminal FYVE domain, did not ameliorate these defects, suggesting that the mutation compromises the functionality of *RUFY4* protein function.

I discovered that human *RUFY4* could mitigate the synaptic alterations caused by *dRUFY* knockdown in C4da neurons, yet this was not the case for A08n neurons (Fig. 18). This difference may be a result from the distinct roles of *dRUFY* in presynaptic C4da and postsynaptic A08n neurons. *RUFY4* has been confirmed as a positive regulator of autophagy (Terawaki et al., 2015). Autophagy was shown to positively regulate synapse development by modulating the levels of proteins involved in synaptic assembly and maintenance in *Drosophila* (Shen and Ganetzky, 2009). Therefore, human *RUFY4* may restore the synaptic dysfunction resulted from *dRUFY* knockdown in *Drosophila* by regulating autophagy.

Given the increase in postsynaptic puncta following C4da-specific *dRUFY* reduction and the heightened sensory sensitivity resulting from *dRUFY* knockdown in da neurons, I propose that these synaptic changes could contribute to the etiology of somatosensory impairments. This hypothesis gains support from the effective restoration of normal nociceptive reactions by human *RUFY4,* likely by rescuing synaptic functions and connectivity of C4da neurons (Fig. 19). Moreover, referencing Jung et al.'s findings of a direct link between synaptic alterations and memory and sociability impairments in a mouse model of ASD and ID (Jung et al., 2017), it becomes imperative to further investigate whether the memory and social deficits we observed can also be rescued by human *RUFY4*.

Autophagy is a pathway conserved across species and its disruption is associated with neurodevelopmental disorders in humans. Recent research indicates that autophagy significantly contributes to synapse formation in *Drosophila* (Kiral et al., 2020; Shen and Ganetzky, 2009). However, introducing human *RUFY4* wild type into *dRUFY*-lacking C4da neurons did not restore autophagic dysfunction based on reduced Atg8-positive structures (Fig. 20). This suggests that autophagic dysfunction might not be directly involved in the synaptic anomalies resulting from the loss of *dRUFY* in our model. Further investigation is required to elucidate the mechanisms behind the observed synaptic changes.

Exploring the functional conservation between *dRUFY* and *RUFY4* enriches the understanding of crucial neurobiological mechanisms and identifies potential therapeutic targets. Although there are notable functional similarities, particularly in synapse formation and sensory responses, significant differences in autophagic functions highlight the complexity of gene functionality across different species. The inability of human *RUFY4* to rescue autophagic defects suggests a need to explore whether *Drosophila dRUFY* is also conserved with other human *RUFY* family members in this regard. Based on the closer homology between *dRUFY* and *RUFY2*, future research employing rescue studies using other human *RUFY* family members in *Drosophila* could reveal the extent of functional conservation and the differences between these orthologous genes.

4.6 Limitations

In this study, I employed the *Drosophila* model system, utilizing well-established experimental approaches such as associative learning, climbing, social interaction, sensory behavior, as well as the analysis of dendritic and synaptic morphology, and autophagic flux, to investigate the function of the *dRUFY* gene in neuronal development and related behaviors. Nonetheless, recent research underscores the challenges of using such animal models for studying Fragile X Syndrome (FXS), highlighting the need for careful interpretation and application of findings from animal models to human conditions (Jacquemont et al., 2014).

NDDs encompass a heterogeneous group of conditions, most of which are characterized by ID (Reuter et al., 2017). The diagnosis of ID heavily relies on the IQ test and learning capabilities, with memory assessment being a key component of the IQ test (Androschuk

et al., 2015). Various paradigms have been employed to examine learning and memory in *Drosophila*, such as olfactory conditioning, visual operant learning, and courtship memory (Bolduc and Tully, 2009). In this study, I evaluated the short-term memory capabilities of *dRUFY* mutant larvae using odor-taste associative learning assays, wherein larvae were tested on their ability to link the odor of n-amyl acetate with a positive reinforcement (fructose). These mutant larvae exhibited compromised memory functions. For this study, incorporating an additional behavioral paradigm such as olfactory and courtship conditioning might provide a deeper understanding of the role of *dRUFY* in learning and memory.

The partial rescue of *dRUFY* deficiency by *hRUFY4* might be attributed to the non-specific defects caused by off-target effects of the *RUFY* RNAi line. Furthermore, considering the closer homology between *dRUFY* and *RUFY2*, it would be advisable to conduct future rescue experiments with human *RUFY2*. Additionally, since the *dRUFY* mutant allele has not been characterized at the molecular level, it is not clear if and how strongly RUFY expression levels are affected by this allele. Some phenotypes might also result from background mutations in this allele, so additional experiments are needed to evaluate the specificity.

4.7 Outlook

4.7.1 *RUFY* genes have a high potential in the etiology of NDDs

To confirm a candidate gene as the causative gene for NDDs/ID, the key is to identify mutations in the same gene across multiple unrelated affected individuals who exhibit similar phenotypes, while these mutations are not present in the control group (Ataei et al., 2019; Vissers et al., 2016). Hu et al. performed whole exome and whole genome sequencing in 404 consanguineous Iranian families, each having at least two affected children. They found that mutations in 26 genes appeared in at least two different consanguineous families who had no connection with each other (Hu et al., 2019). In addition, it is also very important to conduct confirmatory functional studies in animal models that explore both the gene and its mutations (Ataei et al., 2019; Vissers et al., 2016).

In this study, I manipulated the human *RUFY* gene homolog, *Drosophila dRUFY*, revealing that its loss of function resulted in cognitive and social deficits, sensory impairments, synaptic malformation, and autophagic defects. I also confirmed the functional conservation between human *RUFY4* and *Drosophila dRUFY*. Interestingly, Bofill-De Ros et al. found that *RUFY2* was downregulated in the hippocampi of Ts65Dn mice, a model for Down syndrome, and its expression was restored in treated Ts65Dn mice (Bofill-De Ros et al., 2015). This suggests a possible role for *RUFY2* in Down syndrome, which is the most common chromosomal anomaly associated with ID. These findings underscore the significant potential of *RUFY* genes in the etiology of ID, indicating the necessity for further functional studies to explore and validate their roles in ID and NDDs

4.7.2 Affected pathways are important targets for the development of therapeutic approaches

For a long time, it has been believed that ID cannot be cured, with no drugs or gene therapies available to prevent or treat the condition. Treatments have primarily focused on managing behavior and providing physical therapies (Jung et al., 2017). However, this situation has been improved over the past few years due to the increasing understanding of the neuronal biology of affected genes in ID pathogenesis (Vissers et al., 2016). Apparently, the development for therapeutic approaches of ID will mainly have to target common dysfunctional pathways and networks instead of specific genes, given the genetic heterogeneity of the condition which makes it impractical to target treatments at the level of individual genes (Ataei et al., 2019; Vissers et al., 2016).

Recent discoveries have begun to unveil various molecular networks involving genes associated with ID leading to synaptic changes (van Bokhoven, 2011). For instance, research by McBride and colleagues, as well as Choi et al., has discovered that impaired synaptic plasticity in models of Fragile X Syndrome (FXS) in *Drosophila* and mice is due to increased metabotropic glutamate receptor (mGluR) signaling (Choi et al., 2011; McBride et al., 2005). They also found that antagonists of mGluR could reverse these synaptic changes and also ameliorate memory deficits in these ID models. Additionally, disruptions in GABAergic signaling within presynaptic vesicles have been identified in both FXS and Rett syndrome, pointing to potential targets for therapeutic interventions (Braat and Kooy, 2015). These studies indicate that disruption in both excitatory glutamatergic

and inhibitory GABAergic signaling pathways can lead to synaptic abnormalities and associated behavioral issues in conditions related to ID. The *GDI1* gene on the X chromosome, which is the first gene linked to non-syndromic ID. It encodes for GDIα, which helps maintaining a reservoir of inactive Rab proteins by binding and retrieving Rab-GDP (van Bokhoven, 2011). *GDI1* knockout mice displayed alterations in synaptic vesicle pools and short-term synaptic plasticity, along with deficits in short-term memory and learning abilities (Bianchi et al., 2009).

In this work, I have identified synaptic anomalies that I believe are linked to the detected impairments in sensation, memory, and social functions, resulting from the absence of the *dRUFY* gene. Future studies in this project could aim to uncover the underlying mechanisms that drive these anatomical, functional, and behavioral changes. This could include exploring the regulation of membrane trafficking, in which RUFY family proteins are extensively involved, through various signaling pathways, such as mTOR, AMPK, and PI3K pathways (He and Klionsky, 2009).

4.8 Conclusion

This study has significantly advanced our understanding of the role of *RUFY* genes in neurodevelopment and function. Utilizing *Drosophila* as a model with established experimental techniques, I discovered that reduction or deletion of *dRUFY* (the *Drosophila* homolog of *RUFY*) resulted in synaptic abnormalities, sensory impairments, autophagic disruptions, and changes in memory and social behavior. Importantly, the introduction of human *RUFY4*—but not the patient-derived variant—successfully ameliorated some of these deficits, underscoring the functional conservation between *Drosophila dRUFY* and human *RUFY4* and highlighting the pathogenic nature of the patient variant.

This study elucidates potential links between synaptic dysfunction and the observed deficits in sensation, memory, and social skills, thereby expanding the understanding of the genetic underpinnings of NDDs. Moreover, this study reinforces the value of the *Drosophila* model in NDD research, offering a viable avenue for rapid, cost-effective initial screening of genetic and pharmacological modifications before more extensive mammalian studies. As the molecular basis of NDDs further unravel, the insights gained from this study will enhance the development of more precise and effective treatments.

In summary, these findings not only advance the understanding of the genetic basis of NDDs but also pave the way for future research that could lead to novel therapeutic approaches for treating such challenging conditions.

5 Abstract

Neurodevelopmental disorders (NDDs) encompass a heterogeneous group of complex conditions, most of which are characterized by intellectual disability (ID). ID arises from both environmental and genetic causes, with most severe forms predominantly attributed to genetic factors. Notably, most genes associated with ID exhibit an autosomal recessive inheritance pattern, particularly prevalent in the ID cases in consanguineous populations. Despite technological advancements in gene discovery, most autosomal recessive ID genes remain unidentified. This is likely due to high genetic heterogeneity and challenges in proving pathogenicity of variants. *Drosophila melanogaster* offers a cost-effective and efficient model for in vivo functional studies of recessive variants of the identified conserved candidate genes, which are present in approximately 75% of all cases.

The focus of this study was on *RUFY4*, one of the NDDs candidate genes identified through our collaboration with the Human Genetics apartment at the FAU Erlangen. *RUFY* proteins are essential in intracellular membrane trafficking and cytoskeleton dynamics, but have not been extensively studied at the organismal level and in the nervous system. I identified a single fly *RUFY* homolog (*CG31064*/*dRUFY*), which I analyzed functionally in *Drosophila*. Manipulating the *Drosophila* homolog of human *RUFY* genes revealed that its disruption resulted in various phenotypes which mirror the common features of NDDs. Loss of *dRUFY* led to decreased number of autophagosomes, synaptic abnormalities within the nociceptive circuits, as well as aberrant somatosensory functions. In addition, *dRUFY*-deficient *Drosophila* displayed memory dysfunction in associative learning test, and reduced social interaction in food competition assays. Importantly, I discovered that reintroducing human *RUFY4*, but not the patient-derived variant, could rescue some of these deficits, including synaptic alterations and somatosensory hypersensitivity caused by loss of *dRUFY* in sensory neurons. These findings validate the functional conservation between *Drosophila dRUFY* and human *RUFY4* and confirming the pathogenic nature of the patient-derived variant. This study illuminates the crucial role of *RUFY4* in neuronal development and behavior, enhancing our understanding of NDD pathogenesis.

6 List of Figures

7 References

Aberg KA, Dean B, Shabalin AA, Chan RF, Han LKM, Zhao M, van Grootheest G, Xie LY, Milaneschi Y, Clark SL, Turecki G, Penninx BWJH, van den Oord EJCG. Methylome-wide association findings for major depressive disorder overlap in blood and brain and replicate in independent brain samples. Mol Psychiatry 2020; 25(6): 1344-1354

Alkuraya FS. Impact of new genomic tools on the practice of clinical genetics in consanguineous populations: the Saudi experience. Clin Genet 2013; 84(3): 203-208

Androschuk A, Al-Jabri B, Bolduc FV. From Learning to Memory: What Flies Can Tell Us about Intellectual Disability Treatment. Front Psychiatry 2015; 6: 85

Antolini G, Colizzi M. Where Do Neurodevelopmental Disorders Go? Casting the Eye Away from Childhood towards Adulthood. Healthcare (Basel) 2023; 11(7): 1015

Ao X, Zou L, Wu Y. Regulation of autophagy by the Rab GTPase network. Cell Death Differ 2014; 21(3): 348-358

Arosio A, Sala G, Rodriguez-Menendez V, Grana D, Gerardi F, Lunetta C, Ferrarese C, Tremolizzo L. MEF2D and MEF2C pathways disruption in sporadic and familial ALS patients. Mol Cell Neurosci 2016; 74: 10-17

Ataei R, Khoshbakht S, Beheshtian M, Abedini SS, Behravan H, Esmaeili Dizghandi S, Godratpour F, Mirzaei S, Bahrami F, Akbari M, Keshavarzi F, Kahrizi K, Najmabadi H. Contribution of Iran in Elucidating the Genetic Causes of Autosomal Recessive Intellectual Disability. Arch Iran Med 2019; 22(8): 461-471

Bagni C, Zukin RS. A Synaptic Perspective of Fragile X Syndrome and Autism Spectrum Disorders. Neuron 2019; 101(6): 1070-1088

Bassett AR, Liu JL. CRISPR/Cas9 and genome editing in Drosophila. J Genet Genomics

2014; 41(1): 7-19

Battaglia A. Sensory impairment in mental retardation: a potential role for NGF. Arch Ital Biol 2011; 149(2): 193-203

Bellen HJ, Yamamoto S. Morgan's legacy: fruit flies and the functional annotation of conserved genes. Cell 2015; 163(1): 12-14

Ben Itzchak E, Lahat E, Burgin R, Zachor AD. Cognitive, behavior and intervention outcome in young children with autism. Res Dev Disabil 2008; 29(5): 447-458

Benítez-Bribiesca L, De la Rosa-Alvarez I, Mansilla-Olivares A. Dendritic spine pathology in infants with severe protein-calorie malnutrition. Pediatrics 1999; 104(2): e21

Berkel S, Marshall CR, Weiss B, Howe J, Roeth R, Moog U, Endris V, Roberts W, Szatmari P, Pinto D, Bonin M, Riess A, Engels H, Sprengel R, Scherer SW, Rappold GA. Mutations in the SHANK2 synaptic scaffolding gene in autism spectrum disorder and mental retardation. Nat Genet 2010; 42(6): 489-491

Bianchi V, Farisello P, Baldelli P, Meskenaite V, Milanese M, Vecellio M, Mühlemann S, Lipp HP, Bonanno G, Benfenati F, Toniolo D, D'Adamo P. Cognitive impairment in Gdi1-deficient mice is associated with altered synaptic vesicle pools and short-term synaptic plasticity, and can be corrected by appropriate learning training. Hum Mol Genet 2009; 18(1): 105-117

Bier E, Harrison MM, O'Connor-Giles KM, Wildonger J. Advances in Engineering the Fly Genome with the CRISPR-Cas System. Genetics 2018; 208(1): 1-18

Bier E. Drosophila, the golden bug, emerges as a tool for human genetics. Nat Rev Genet 2005; 6(1): 9-23

Bofill-De Ros X, Santos M, Vila-Casadesús M, Villanueva E, Andreu N, Dierssen M, Fillat

C. Genome-wide miR-155 and miR-802 target gene identification in the hippocampus of Ts65Dn Down syndrome mouse model by miRNA sponges. BMC Genomics 2015; 16: 907

Bolduc FV, Tully T. Fruit flies and intellectual disability. Fly (Austin) 2009; 3(1): 91-104

Boyle CA, Boulet S, Schieve LA, Cohen RA, Blumberg SJ, Yeargin-Allsopp M, Visser S, Kogan MD. Trends in the prevalence of developmental disabilities in US children, 1997-2008. Pediatrics 2011; 127(6): 1034-1042

Braat S, Kooy RF. The GABAA Receptor as a Therapeutic Target for Neurodevelopmental Disorders. Neuron 2015; 86(5): 1119-1130

Brand AH, Perrimon N. Targeted gene expression as a means of altering cell fates and generating dominant phenotypes. Development 1993; 118(2): 401-415

Callebaut I, de Gunzburg J, Goud B, Mornon JP. RUN domains: a new family of domains involved in Ras-like GTPase signaling. Trends Biochem Sci 2001; 26(2): 79-83

Char R, Pierre P. The RUFYs, a Family of Effector Proteins Involved in Intracellular Trafficking and Cytoskeleton Dynamics. Front Cell Dev Biol 2020; 8: 779

Choi CH, Schoenfeld BP, Bell AJ, Hinchey P, Kollaros M, Gertner MJ, Woo NH, Tranfaglia MR, Bear MF, Zukin RS, McDonald TV, Jongens TA, McBride SM. Pharmacological reversal of synaptic plasticity deficits in the mouse model of fragile X syndrome by group II mGluR antagonist or lithium treatment. Brain Res 2011; 1380: 106-119

Cordero ME, D'Acuña E, Benveniste S, Prado R, Nuñez JA, Colombo M. Dendritic development in neocortex of infants with early postnatal life undernutrition. Pediatr Neurol 1993; 9(6): 457-464

Cormont M, Mari M, Galmiche A, Hofman P, Le Marchand-Brustel Y. A FYVE-finger-

containing protein, Rabip4, is a Rab4 effector involved in early endosomal traffic. Proc Natl Acad Sci USA 2001; 98(4): 1637-1642

Dan Z, Mao X, Liu Q, Guo M, Zhuang Y, Liu Z, Chen K, Chen J, Xu R, Tang J, Qin L, Gu B, Liu K, Su C, Zhang F, Xia Y, Hu Z, Liu X. Altered gut microbial profile is associated with abnormal metabolism activity of Autism Spectrum Disorder. Gut Microbes 2020; 11(5): 1246-1267

Dankert H, Wang L, Hoopfer ED, Anderson DJ, Perona P. Automated monitoring and analysis of social behavior in Drosophila. Nat Methods 2009; 6(4): 297-303

D'Arrigo S, Gavazzi F, Alfei E, Zuffardi O, Montomoli C, Corso B, Buzzi E, Sciacca FL, Bulgheroni S, Riva D, Pantaleoni C. The Diagnostic Yield of Array Comparative Genomic Hybridization Is High Regardless of Severity of Intellectual Disability/Developmental Delay in Children. J Child Neurol 2016; 31(6): 691-699

DeLong GR. Effects of nutrition on brain development in humans. Am J Clin Nutr 1993; 57(2 Suppl): 286-290

Domanski APF, Booker SA, Wyllie DJA, Isaac JTR, Kind PC. Cellular and synaptic phenotypes lead to disrupted information processing in Fmr1-KO mouse layer 4 barrel cortex. Nat Commun 2019; 10(1): 4814

Filipello F, Morini R, Corradini I, Zerbi V, Canzi A, Michalski B, Erreni M, Markicevic M, Starvaggi-Cucuzza C, Otero K, Piccio L, Cignarella F, Perrucci F, Tamborini M, Genua M, Rajendran L, Menna E, Vetrano S, Fahnestock M, Paolicelli RC, Matteoli M. The Microglial Innate Immune Receptor TREM2 Is Required for Synapse Elimination and Normal Brain Connectivity. Immunity 2018; 48(5): 979-991

Ford TJL, Jeon BT, Lee H, Kim WY. Dendritic spine and synapse pathology in chromatin modifier-associated autism spectrum disorders and intellectual disability. Front Mol Neurosci 2023; 15: 1048713

Freeman RD, Fast DK, Burd L, Kerbeshian J, Robertson MM, Sandor P. An international perspective on Tourette syndrome: selected findings from 3,500 individuals in 22 countries. Dev Med Child Neurol 2000; 42(7): 436-447

Fyke W, Velinov M. FMR1 and Autism, an Intriguing Connection Revisited. Genes (Basel) 2021; 12(8): 1218

Gerber B, Biernacki R, Thum J. Odor-taste learning assays in Drosophila larvae. Cold Spring Harb Protoc 2013; 2013(3): pdb.prot071639

Gidziela A, Ahmadzadeh YI, Michelini G, Allegrini AG, Agnew-Blais J, Lau LY, Duret M, Procopio F, Daly E, Ronald A, Rimfeld K, Malanchini M. A meta-analysis of genetic effects associated with neurodevelopmental disorders and co-occurring conditions. Nat Hum Behav 2023; 7(4): 642-656

Glatigny M, Moriceau S, Rivagorda M, Ramos-Brossier M, Nascimbeni AC, Lante F, Shanley MR, Boudarene N, Rousseaud A, Friedman AK, Settembre C, Kuperwasser N, Friedlander G, Buisson A, Morel E, Codogno P, Oury F. Autophagy Is Required for Memory Formation and Reverses Age-Related Memory Decline. Curr Biol 2019; 29(3): 435-448

Gropman AL, Batshaw ML. Epigenetics, copy number variation, and other molecular mechanisms underlying neurodevelopmental disabilities: new insights and diagnostic approaches. J Dev Behav Pediatr 2010; 31(7): 582-591

Grueber WB, Jan LY, Jan YN. Tiling of the Drosophila epidermis by multidendritic sensory neurons. Development 2002; 129(12): 2867-2878

Gupta N. Deciphering Intellectual Disability. Indian J Pediatr 2023; 90(2): 160-167

Hales KG, Korey CA, Larracuente AM, Roberts DM. Genetics on the Fly: A Primer on the Drosophila Model System. Genetics 2015; 201(3): 815-842

Halter MJ, Rolin-Kenny D, Dzurec LC. An overview of the DSM-5: changes, controversy, and implications for psychiatric nursing. J Psychosoc Nurs Ment Health Serv 2013; 51(4): 30-39

Hamamy H. Consanguineous marriages : Preconception consultation in primary health care settings. J Community Genet 2012; 3(3): 185-192

Han VX, Jones HF, Patel S, Mohammad SS, Hofer MJ, Alshammery S, Maple-Brown E, Gold W, Brilot F, Dale RC. Emerging evidence of Toll-like receptors as a putative pathway linking maternal inflammation and neurodevelopmental disorders in human offspring: A systematic review. Brain Behav Immun 2022; 99: 91-105

Han VX, Patel S, Jones HF, Dale RC. Maternal immune activation and neuroinflammation in human neurodevelopmental disorders. Nat Rev Neurol 2021; 17(9): 564-579

Hannon GJ. RNA interference. Nature 2002; 418(6894): 244-251

Hansen BH, Oerbeck B, Skirbekk B, Petrovski BÉ, Kristensen H. Neurodevelopmental disorders: prevalence and comorbidity in children referred to mental health services. Nord J Psychiatry 2018; 72(4): 285-291

Hayakawa A, Hayes S, Leonard D, Lambright D, Corvera S. Evolutionarily conserved structural and functional roles of the FYVE domain. Biochem Soc Symp 2007; (74): 95-105

He C, Klionsky DJ. Regulation mechanisms and signaling pathways of autophagy. Annu Rev Genet 2009; 43:67-93

Hertz NT, Adams EL, Weber RA, Shen RJ, O'Rourke MK, Simon DJ, Zebroski H, Olsen O, Morgan CW, Mileur TR, Hitchcock AM, Sinnott Armstrong NA, Wainberg M, Bassik MC, Molina H, Wells JA, Tessier-Lavigne M. Neuronally Enriched RUFY3 Is Required for Caspase-Mediated Axon Degeneration. Neuron 2019; 103(3): 412-422

Homberg JR, Kyzar EJ, Nguyen M, Norton WH, Pittman J, Poudel MK, Gaikwad S, Nakamura S, Koshiba M, Yamanouchi H, Scattoni ML, Ullman JF, Diamond DM, Kaluyeva AA, Parker MO, Klimenko VM, Apryatin SA, Brown RE, Song C, Gainetdinov RR, Gottesman II, Kalueff AV. Understanding autism and other neurodevelopmental disorders through experimental translational neurobehavioral models. Neurosci Biobehav Rev 2016; 65: 292-312

Honda A, Usui H, Sakimura K, Igarashi M. Rufy3 is an adapter protein for small GTPases that activates a Rac guanine nucleotide exchange factor to control neuronal polarity. J Biol Chem 2017; 292(51): 20936-20946

Hoyer N, Petersen M, Tenedini F, Soba P. Assaying Mechanonociceptive Behavior in Drosophila Larvae. Bio Protoc 2018; 8(4): e2736

Hu C, Kanellopoulos AK, Richter M, Petersen M, Konietzny A, Tenedini FM, Hoyer N, Cheng L, Poon CLC, Harvey KF, Windhorst S, Parrish JZ, Mikhaylova M, Bagni C, Calderon de Anda F, Soba P. Conserved Tao Kinase Activity Regulates Dendritic Arborization, Cytoskeletal Dynamics, and Sensory Function in Drosophila. J Neurosci 2020; 40(9): 1819-1833

Hu C, Petersen M, Hoyer N, Spitzweck B, Tenedini F, Wang D, Gruschka A, Burchardt LS, Szpotowicz E, Schweizer M, Guntur AR, Yang CH, Soba P. Sensory integration and neuromodulatory feedback facilitate Drosophila mechanonociceptive behavior. Nat Neurosci 2017; 20(8): 1085-1095

Hu H, Kahrizi K, Musante L, Fattahi Z, Herwig R, Hosseini M, Oppitz C, Abedini SS, Suckow V, Larti F, Beheshtian M, Lipkowitz B, Akhtarkhavari T, Mehvari S, Otto S, Mohseni M, Arzhangi S, Jamali P, Mojahedi F, Taghdiri M, Papari E, Soltani Banavandi MJ, Akbari S, Tonekaboni SH, Dehghani H, Ebrahimpour MR, Bader I, Davarnia B, Cohen M, Khodaei H, Albrecht B, Azimi S, Zirn B, Bastami M, Wieczorek D, Bahrami G, Keleman K, Vahid LN, Tzschach A, Gärtner J, Gillessen-Kaesbach G, Varaghchi JR, Timmermann B, Pourfatemi F, Jankhah A, Chen W, Nikuei P, Kalscheuer VM, Oladnabi M, Wienker TF,

Ropers HH, Najmabadi H. Genetics of intellectual disability in consanguineous families. Mol Psychiatry 2019; 24(7): 1027-1039

Hudac CM, Friedman NR, Ward VR, Estreicher RE, Dorsey GC, Bernier RA, Kurtz-Nelson EC, Earl RK, Eichler EE, Neuhaus E. Characterizing Sensory Phenotypes of Subgroups with a Known Genetic Etiology Pertaining to Diagnoses of Autism Spectrum Disorder and Intellectual Disability. J Autism Dev Disord 2024; 54(6): 2386-2401

Jacquemont ML, Sanlaville D, Redon R, Raoul O, Cormier-Daire V, Lyonnet S, Amiel J, Le Merrer M, Heron D, de Blois MC, Prieur M, Vekemans M, Carter NP, Munnich A, Colleaux L, Philippe A. Array-based comparative genomic hybridisation identifies high frequency of cryptic chromosomal rearrangements in patients with syndromic autism spectrum disorders. J Med Genet 2006; 43(11): 843-849

Jacquemont S, Berry-Kravis E, Hagerman R, von Raison F, Gasparini F, Apostol G, Ufer M, Des Portes V, Gomez-Mancilla B. The challenges of clinical trials in fragile X syndrome. Psychopharmacology (Berl) 2014; 231(6): 1237-1250

Jung EM, Moffat JJ, Liu J, Dravid SM, Gurumurthy CB, Kim WY. Arid1b haploinsufficiency disrupts cortical interneuron development and mouse behavior. Nat Neurosci 2017; 20(12): 1694-1707

Ka M, Kim HG, Kim WY. WDR5-HOTTIP Histone Modifying Complex Regulates Neural Migration and Dendrite Polarity of Pyramidal Neurons via Reelin Signaling. Mol Neurobiol 2022; 59(8): 5104-5120

Kaneko T, Macara AM, Li R, Hu Y, Iwasaki K, Dunnings Z, Firestone E, Horvatic S, Guntur A, Shafer OT, Yang CH, Zhou J, Ye B. Serotonergic Modulation Enables Pathway-Specific Plasticity in a Developing Sensory Circuit in Drosophila. Neuron 2017; 95(3): 623-638

Kanellopoulos AK, Mariano V, Spinazzi M, Woo YJ, McLean C, Pech U, Li KW, Armstrong JD, Giangrande A, Callaerts P, Smit AB, Abrahams BS, Fiala A, Achsel T, Bagni C. Aralar

Sequesters GABA into Hyperactive Mitochondria, Causing Social Behavior Deficits. Cell 2020; 180(6): 1178-1197

Keren-Kaplan T, Sarić A, Ghosh S, Williamson CD, Jia R, Li Y, Bonifacino JS. RUFY3 and RUFY4 are ARL8 effectors that promote coupling of endolysosomes to dynein-dynactin. Nat Commun 2022; 13(1): 1506

Kernan M, Cowan D, Zuker C. Genetic dissection of mechanosensory transduction: mechanoreception-defective mutations of Drosophila. Neuron 1994; 12(6): 1195-1206

Kerner-Rossi M, Gulinello M, Walkley S, Dobrenis K. Pathobiology of Christianson syndrome: Linking disrupted endosomal-lysosomal function with intellectual disability and sensory impairments. Neurobiol Learn Mem 2019; 165: 106867

Khan MU, Aslani P. A Review of Factors Influencing the Three Phases of Medication Adherence in People with Attention-Deficit/Hyperactivity Disorder. J Child Adolesc Psychopharmacol 2019; 29(6): 398-418

Kilo L, Stürner T, Tavosanis G, Ziegler AB. Drosophila Dendritic Arborisation Neurons: Fantastic Actin Dynamics and Where to Find Them. Cells 2021; 10(10): 2777

Kim HJ, Cho MH, Shim WH, Kim JK, Jeon EY, Kim DH, Yoon SY. Deficient autophagy in microglia impairs synaptic pruning and causes social behavioral defects. Mol Psychiatry 2017; 22(11): 1576-1584

Kim M, Park JH, Go M, Lee N, Seo J, Lee H, Kim D, Ha H, Kim T, Jeong MS, Kim S, Kim T, Kim HS, Kang D, Shim H, Lee SY. RUFY4 deletion prevents pathological bone loss by blocking endo-lysosomal trafficking of osteoclasts. Bone Res 2024; 12(1): 29

Kiral FR, Linneweber GA, Mathejczyk T, Georgiev SV, Wernet MF, Hassan BA, von Kleist M, Hiesinger PR. Autophagy-dependent filopodial kinetics restrict synaptic partner choice during Drosophila brain wiring. Nat Commun 2020; 11(1): 1325

Kitagishi Y, Matsuda S. RUFY, Rab and Rap Family Proteins Involved in a Regulation of Cell Polarity and Membrane Trafficking. Int J Mol Sci 2013; 14(3): 6487-6498

Klapoetke NC, Murata Y, Kim SS, Pulver SR, Birdsey-Benson A, Cho YK, Morimoto TK, Chuong AS, Carpenter EJ, Tian Z, Wang J, Xie Y, Yan Z, Zhang Y, Chow BY, Surek B, Melkonian M, Jayaraman V, Constantine-Paton M, Wong GK, Boyden ES. Independent optical excitation of distinct neural populations. Nat Methods 2014; 11(3): 338-346

Kochinke K, Zweier C, Nijhof B, Fenckova M, Cizek P, Honti F, Keerthikumar S, Oortveld MA, Kleefstra T, Kramer JM, Webber C, Huynen MA, Schenck A. Systematic Phenomics Analysis Deconvolutes Genes Mutated in Intellectual Disability into Biologically Coherent Modules. Am J Hum Genet 2016; 98(1): 149-164

Koemans TS, Oppitz C, Donders RAT, van Bokhoven H, Schenck A, Keleman K, Kramer JM. Drosophila Courtship Conditioning As a Measure of Learning and Memory. J Vis Exp 2017; (124): 55808

Kohrs FE, Daumann IM, Pavlovic B, Jin EJ, Kiral FR, Lin SC, Port F, Wolfenberg H, Mathejczyk TF, Linneweber GA, Chan CC, Boutros M, Hiesinger PR. Systematic functional analysis of rab GTPases reveals limits of neuronal robustness to environmental challenges in flies. Elife 2021; 10: e59594

Kunkle BW, Vardarajan BN, Naj AC, Whitehead PL, Rolati S, Slifer S, Carney RM, Cuccaro ML, Vance JM, Gilbert JR, Wang LS, Farrer LA, Reitz C, Haines JL, Beecham GW, Martin ER, Schellenberg GD, Mayeux RP, Pericak-Vance MA. Early-Onset Alzheimer Disease and Candidate Risk Genes Involved in Endolysosomal Transport. JAMA Neurol 2017; 74(9): 1113-1122

Kutateladze T, Overduin M. Structural mechanism of endosome docking by the FYVE domain. Science 2001; 291(5509): 1793-1796

Lai SL, Lee T. Genetic mosaic with dual binary transcriptional systems in Drosophila. Nat

Neurosci 2006; 9(5): 703-709

Lamb CA, Longatti A, Tooze SA. Rabs and GAPs in starvation-induced autophagy. Small GTPases 2016; 7(4): 265-269

Langemeyer L, Fröhlich F, Ungermann C. Rab GTPase Function in Endosome and Lysosome Biogenesis. Trends Cell Biol 2018; 28(11): 957-970

LaSalle JM, Yasui DH. Evolving role of MeCP2 in Rett syndrome and autism. Epigenomics 2009; 1(1): 119-130

Laumonnier F, Bonnet-Brilhault F, Gomot M, Blanc R, David A, Moizard MP, Raynaud M, Ronce N, Lemonnier E, Calvas P, Laudier B, Chelly J, Fryns JP, Ropers HH, Hamel BC, Andres C, Barthélémy C, Moraine C, Briault S. X-linked mental retardation and autism are associated with a mutation in the NLGN4 gene, a member of the neuroligin family. Am J Hum Genet 2004; 74(3): 552-557

Lee KM, Hwang SK, Lee JA. Neuronal autophagy and neurodevelopmental disorders. Exp Neurobiol 2013; 22(3): 133-142

Lee PJ, Ridout D, Walter JH, Cockburn F. Maternal phenylketonuria: report from the United Kingdom Registry 1978-97. Arch Dis Child 2005; 90(2): 143-146

Leyfer OT, Folstein SE, Bacalman S, Davis NO, Dinh E, Morgan J, Tager-Flusberg H, Lainhart JE. Comorbid psychiatric disorders in children with autism: interview development and rates of disorders. J Autism Dev Disord 2006; 36(7): 849-861

Link N, Bellen HJ. Using Drosophila to drive the diagnosis and understand the mechanisms of rare human diseases. Development 2020; 147(21): dev191411

Lyons-Warren AM, McCormack MC, Holder JL Jr. Sensory Processing Phenotypes in Phelan-McDermid Syndrome and SYNGAP1-Related Intellectual Disability. Brain Sci

2022; 12(2): 137

Ma M, Moulton MJ, Lu S, Bellen HJ. 'Fly-ing' from rare to common neurodegenerative disease mechanisms. Trends Genet 2022; 38(9): 972-984

Maenner MJ, Warren Z, Williams AR, Amoakohene E, Bakian AV, Bilder DA, Durkin MS, Fitzgerald RT, Furnier SM, Hughes MM, Ladd-Acosta CM, McArthur D, Pas ET, Salinas A, Vehorn A, Williams S, Esler A, Grzybowski A, Hall-Lande J, Nguyen RHN, Pierce K, Zahorodny W, Hudson A, Hallas L, Mancilla KC, Patrick M, Shenouda J, Sidwell K, DiRienzo M, Gutierrez J, Spivey MH, Lopez M, Pettygrove S, Schwenk YD, Washington A, Shaw KA. Prevalence and Characteristics of Autism Spectrum Disorder Among Children Aged 8 Years - Autism and Developmental Disabilities Monitoring Network, 11 Sites, United States, 2020. MMWR Surveill Summ 2023; 72(2): 1-14

Manjila SB, Hasan G. Flight and Climbing Assay for Assessing Motor Functions in Drosophila. Bio Protoc 2018; 8(5): e2742

Mari M, Macia E, Le Marchand-Brustel Y, Cormont M. Role of the FYVE finger and the RUN domain for the subcellular localization of Rabip4. J Biol Chem 2001; 276(45): 42501-42508

Matson JL, Shoemaker M. Intellectual disability and its relationship to autism spectrum disorders. Res Dev Disabil 2009; 30(6): 1107-1114

McBride SM, Choi CH, Wang Y, Liebelt D, Braunstein E, Ferreiro D, Sehgal A, Siwicki KK, Dockendorff TC, Nguyen HT, McDonald TV, Jongens TA. Pharmacological rescue of synaptic plasticity, courtship behavior, and mushroom body defects in a Drosophila model of fragile X syndrome. Neuron 2005; 45(5): 753-764

McClain MB, Hasty Mills AM, Murphy LE. Inattention and hyperactivity/impulsivity among children with attention-deficit/hyperactivity-disorder, autism spectrum disorder, and intellectual disability. Res Dev Disabil 2017; 70: 175-184

Miao D, Shi J, Xiong Z, Xiao W, Meng X, Lv Q, Xie K, Yang H, Zhang X. As a prognostic biomarker of clear cell renal cell carcinoma RUFY4 predicts immunotherapy responsiveness in a PDL1-related manner. Cancer Cell Int 2022; 22(1): 66

Michaelson SD, Ozkan ED, Aceti M, Maity S, Llamosas N, Weldon M, Mizrachi E, Vaissiere T, Gaffield MA, Christie JM, Holder JL Jr, Miller CA, Rumbaugh G. SYNGAP1 heterozygosity disrupts sensory processing by reducing touch-related activity within somatosensory cortex circuits. Nat Neurosci 2018; 21(12):1-13

Moeschler JB, Shevell M; Committee on Genetics. Comprehensive evaluation of the child with intellectual disability or global developmental delays. Pediatrics 2014; 134(3): e903-918

Mori T, Wada T, Suzuki T, Kubota Y, Inagaki N. Singar1, a novel RUN domain-containing protein, suppresses formation of surplus axons for neuronal polarity. J Biol Chem 2007; 282(27): 19884-19893

Morishita H, Mizushima N. Diverse Cellular Roles of Autophagy. Annu Rev Cell Dev Biol 2019; 35: 453-475

Morris-Rosendahl DJ, Crocq MA. Neurodevelopmental disorders-the history and future of a diagnostic concept. Dialogues Clin Neurosci 2020; 22(1): 65-72

Muller HJ. Genetic Variability, Twin Hybrids and Constant Hybrids, in a Case of Balanced Lethal Factors. Genetics 1918; 3(5): 422-499

Mullin AP, Gokhale A, Moreno-De-Luca A, Sanyal S, Waddington JL, Faundez V. Neurodevelopmental disorders: mechanisms and boundary definitions from genomes, interactomes and proteomes. Transl Psychiatry 2013; 3(12): e329

Musante L, Ropers HH. Genetics of recessive cognitive disorders. Trends Genet 2014; 30(1): 32-39

Nakamizo-Dojo M, Ishii K, Yoshino J, Tsuji M, Emoto K. Descending GABAergic pathway links brain sugar-sensing to peripheral nociceptive gating in Drosophila. Nat Commun 2023; 14(1): 6515

Nascimbeni AC, Codogno P, Morel E. Phosphatidylinositol-3-phosphate in the regulation of autophagy membrane dynamics. FEBS J 2017; 284(9): 1267-1278

Ohyama T, Schneider-Mizell CM, Fetter RD, Aleman JV, Franconville R, Rivera-Alba M, Mensh BD, Branson KM, Simpson JH, Truman JW, Cardona A, Zlatic M. A multilevel multimodal circuit enhances action selection in Drosophila Nature 2015; 520(7549): 633-639

Oortveld MA, Keerthikumar S, Oti M, Nijhof B, Fernandes AC, Kochinke K, Castells-Nobau A, van Engelen E, Ellenkamp T, Eshuis L, Galy A, van Bokhoven H, Habermann B, Brunner HG, Zweier C, Verstreken P, Huynen MA, Schenck A. Human intellectual disability genes form conserved functional modules in Drosophila. PLoS Genet 2013; 9(10): e1003911

Orefice LL, Mosko JR, Morency DT, Wells MF, Tasnim A, Mozeika SM, Ye M, Chirila AM, Emanuel AJ, Rankin G, Fame RM, Lehtinen MK, Feng G, Ginty DD. Targeting Peripheral Somatosensory Neurons to Improve Tactile-Related Phenotypes in ASD Models. Cell 2019; 178(4): 867-886

Orefice LL, Zimmerman AL, Chirila AM, Sleboda SJ, Head JP, Ginty DD. Peripheral Mechanosensory Neuron Dysfunction Underlies Tactile and Behavioral Deficits in Mouse Models of ASDs. Cell 2016; 166(2): 299-313

Palmer EE, Sachdev R, Macintosh R, Melo US, Mundlos S, Righetti S, Kandula T, Minoche AE, Puttick C, Gayevskiy V, Hesson L, Idrisoglu S, Shoubridge C, Thai MHN, Davis RL, Drew AP, Sampaio H, Andrews PI, Lawson J, Cardamone M, Mowat D, Colley A, Kummerfeld S, Dinger ME, Cowley MJ, Roscioli T, Bye A, Kirk E. Diagnostic Yield of Whole Genome Sequencing After Nondiagnostic Exome Sequencing or Gene Panel in

Developmental and Epileptic Encephalopathies. Neurology 2021; 96(13): e1770-e1782

Pandey UB, Nichols CD. Human disease models in Drosophila melanogaster and the role of the fly in therapeutic drug discovery. Pharmacol Rev 2011; 63(2): 411-436

Pankiv S, Alemu EA, Brech A, Bruun JA, Lamark T, Overvatn A, Bjørkøy G, Johansen T. FYCO1 is a Rab7 effector that binds to LC3 and PI3P to mediate microtubule plus end-directed vesicle transport. J Cell Biol 2010; 188(2): 253-269

Papuc SM, Abela L, Steindl K, Begemann A, Simmons TL, Schmitt B, Zweier M, Oneda B, Socher E, Crowther LM, Wohlrab G, Gogoll L, Poms M, Seiler M, Papik M, Baldinger R, Baumer A, Asadollahi R, Kroell-Seger J, Schmid R, Iff T, Schmitt-Mechelke T, Otten K, Hackenberg A, Addor MC, Klein A, Azzarello-Burri S, Sticht H, Joset P, Plecko B, Rauch A. The role of recessive inheritance in early-onset epileptic encephalopathies: a combined whole-exome sequencing and copy number study. Eur J Hum Genet 2019; 27(3): 408-421

Parker-Athill EC, Ehrhart J, Tan J, Murphy TK. Cytokine correlations in youth with tic disorders. J Child Adolesc Psychopharmacol 2015; 25(1): 86-92

Patel DR, Cabral MD, Ho A, Merrick J. A clinical primer on intellectual disability. Transl Pediatr 2020; 9(Suppl 1): S23-S35

Patel DR, Greydanus DE, Calles JL Jr, Pratt HD. Developmental disabilities across the lifespan. Dis Mon 2010; 56(6): 304-397

Petersen M, Tenedini F, Hoyer N, Kutschera F, Soba P. Assaying Thermo-nociceptive Behavior in Drosophila Larvae. Bio Protoc 2018; 8(4): e2737

Pfeiffer BE, Huber KM. Fragile X mental retardation protein induces synapse loss through acute postsynaptic translational regulation. J Neurosci 2007; 27(12): 3120-3130

Piton A, Redin C, Mandel JL. XLID-causing mutations and associated genes challenged in light of data from large-scale human exome sequencing. Am J Hum Genet 2013; 93(2): 368-383

Rajan A, Perrimon N. Of flies and men: insights on organismal metabolism from fruit flies. BMC Biol 2013; 11: 38

Rauch A, Hoyer J, Guth S, Zweier C, Kraus C, Becker C, Zenker M, Hüffmeier U, Thiel C, Rüschendorf F, Nürnberg P, Reis A, Trautmann U. Diagnostic yield of various genetic approaches in patients with unexplained developmental delay or mental retardation. Am J Med Genet A 2006; 140(19): 2063-2074

Reiter LT, Potocki L, Chien S, Gribskov M, Bier E. A systematic analysis of human disease-associated gene sequences in Drosophila melanogaster. Genome Res 2001; 11(6): 1114-1125

Reuter MS, Tawamie H, Buchert R, Hosny Gebril O, Froukh T, Thiel C, Uebe S, Ekici AB, Krumbiegel M, Zweier C, Hoyer J, Eberlein K, Bauer J, Scheller U, Strom TM, Hoffjan S, Abdelraouf ER, Meguid NA, Abboud A, Al Khateeb MA, Fakher M, Hamdan S, Ismael A, Muhammad S, Abdallah E, Sticht H, Wieczorek D, Reis A, Abou Jamra R. Diagnostic Yield and Novel Candidate Genes by Exome Sequencing in 152 Consanguineous Families With Neurodevelopmental Disorders. JAMA Psychiatry 2017; 74(3): 293-299

Robertson CE, Baron-Cohen S. Sensory perception in autism. Nat Rev Neurosci 2017; 18(11): 671-684

Rojas-Charry L, Nardi L, Methner A, Schmeisser MJ. Abnormalities of synaptic mitochondria in autism spectrum disorder and related neurodevelopmental disorders. J Mol Med (Berl) 2021; 99(2): 161-178

Ropers HH. Genetics of early onset cognitive impairment. Annu Rev Genomics Hum Genet 2010; 11: 161-187

Rubin GM, Spradling AC. Genetic transformation of Drosophila with transposable element vectors. Science 1982; 218(4570): 348-353

Sandweiss AJ, Brandt VL, Zoghbi HY. Advances in understanding of Rett syndrome and MECP2 duplication syndrome: prospects for future therapies. Lancet Neurol 2020; 19(8): 689-698

Saxena R, Babadi M, Namvarhaghighi H, Roullet FI. Role of environmental factors and epigenetics in autism spectrum disorders. Prog Mol Biol Transl Sci 2020; 173: 35-60

Sebat J, Lakshmi B, Malhotra D, Troge J, Lese-Martin C, Walsh T, Yamrom B, Yoon S, Krasnitz A, Kendall J, Leotta A, Pai D, Zhang R, Lee YH, Hicks J, Spence SJ, Lee AT, Puura K, Lehtimäki T, Ledbetter D, Gregersen PK, Bregman J, Sutcliffe JS, Jobanputra V, Chung W, Warburton D, King MC, Skuse D, Geschwind DH, Gilliam TC, Ye K, Wigler M. Strong association of de novo copy number mutations with autism. Science 2007; 316(5823): 445-449

Şentürk M, Bellen HJ. Genetic strategies to tackle neurological diseases in fruit flies. Curr Opin Neurobiol 2018; 50: 24-32

Sharma SR, Gonda X, Tarazi FI. Autism Spectrum Disorder: Classification, diagnosis and therapy. Pharmacol Ther 2018; 190: 91-104

Shen L, Zhang K, Feng C, Chen Y, Li S, Iqbal J, Liao L, Zhao Y, Zhai J. iTRAQ-Based Proteomic Analysis Reveals Protein Profile in Plasma from Children with Autism. Proteomics Clin Appl 2018; 12(3): e1700085

Shen W, Ganetzky B. Autophagy promotes synapse development in Drosophila. J Cell Biol 2009; 187(1): 71-79

Shih J, Hodge R, Andrade-Navarro MA. Comparison of inter- and intraspecies variation in humans and fruit flies. Genom Data 2014; 3: 49-54

Srour M, Shevell M. Genetics and the investigation of developmental delay/intellectual disability. Arch Dis Child 2014; 99(4): 386-389

St Pierre SE, Ponting L, Stefancsik R, McQuilton P; FlyBase Consortium. FlyBase 102--advanced approaches to interrogating FlyBase. Nucleic Acids Res 2014; 42(Database issue): D780-8

Stenmark H. Rab GTPases as coordinators of vesicle traffic. Nat Rev Mol Cell Biol 2009; 10(8): 513-525

Strati F, Cavalieri D, Albanese D, De Felice C, Donati C, Hayek J, Jousson O, Leoncini S, Renzi D, Calabrò A, De Filippo C. New evidences on the altered gut microbiota in autism spectrum disorders. Microbiome 2017; 5(1): 24

Tan JYK, Chew LY, Juhász G, Yu F. Interplay between autophagy and CncC regulates dendrite pruning in Drosophila. Proc Natl Acad Sci USA 2024; 121(10): e2310740121

Tenedini FM, Sáez González M, Hu C, Pedersen LH, Petruzzi MM, Spitzweck B, Wang D, Richter M, Petersen M, Szpotowicz E, Schweizer M, Sigrist SJ, Calderon de Anda F, Soba P. Maintenance of cell type-specific connectivity and circuit function requires Tao kinase. Nat Commun 2019; 10(1): 3506

Terawaki S, Camosseto V, Pierre P, Gatti E. RUFY4: Immunity piggybacking on autophagy? Autophagy 2016; 12(3): 598-600

Terawaki S, Camosseto V, Prete F, Wenger T, Papadopoulos A, Rondeau C, Combes A, Rodriguez Rodrigues C, Vu Manh TP, Fallet M, English L, Santamaria R, Soares AR, Weil T, Hammad H, Desjardins M, Gorvel JP, Santos MA, Gatti E, Pierre P. RUN and FYVE domain-containing protein 4 enhances autophagy and lysosome tethering in response to Interleukin-4. J Cell Biol 2015; 210(7): 1133-1152

Thomas R, Sanders S, Doust J, Beller E, Glasziou P. Prevalence of attention-

deficit/hyperactivity disorder: a systematic review and meta-analysis. Pediatrics 2015; 135(4): e994-1001

Tripathi T, Kalita P, Martins R, Bharadwaj P. Autophagy Promotes Memory Formation. ACS Chem Neurosci 2019; 10(8): 3337-3339

van Bokhoven H. Genetic and epigenetic networks in intellectual disabilities. Annu Rev Genet 2011; 45: 81-104

van der Voet M, Nijhof B, Oortveld MA, Schenck A. Drosophila models of early onset cognitive disorders and their clinical applications. Neurosci Biobehav Rev 2014; 46 Pt 2: 326-342

Vissers LE, Gilissen C, Veltman JA. Genetic studies in intellectual disability and related disorders. Nat Rev Genet 2016; 17(1): 9-18

Vogelstein JT, Park Y, Ohyama T, Kerr RA, Truman JW, Priebe CE, Zlatic M. Discovery of brainwide neural-behavioral maps via multiscale unsupervised structure learning. Science 2014; 344(6182): 386-392

Wang C, Geng H, Liu W, Zhang G. Prenatal, perinatal, and postnatal factors associated with autism: A meta-analysis. Medicine (Baltimore) 2017; 96(18): e6696

Wei Z, Sun M, Liu X, Zhang J, Jin Y. Rufy3, a protein specifically expressed in neurons, interacts with actin-bundling protein Fascin to control the growth of axons. J Neurochem 2014; 130(5): 678-692

Weiss LA, Shen Y, Korn JM, Arking DE, Miller DT, Fossdal R, Saemundsen E, Stefansson H, Ferreira MA, Green T, Platt OS, Ruderfer DM, Walsh CA, Altshuler D, Chakravarti A, Tanzi RE, Stefansson K, Santangelo SL, Gusella JF, Sklar P, Wu BL, Daly MJ; Autism Consortium. Association between microdeletion and microduplication at 16p11.2 and autism. N Engl J Med 2008; 358(7): 667-675

Wu Y, Bolduc FV, Bell K, Tully T, Fang Y, Sehgal A, Fischer JA. A Drosophila model for Angelman syndrome. Proc Natl Acad Sci U S A 2008; 105(34): 12399-12404

Yang J, Kim O, Wu J, Qiu Y. Interaction between tyrosine kinase Etk and a RUN domain- and FYVE domain-containing protein RUFY1. A possible role of ETK in regulation of vesicle trafficking. J Biol Chem 2002; 277(33): 30219-30226

Yoshida, H.; Kitagishi, Y.; Okumura, N.; Murakami, M.; Nishimura, Y.; Matsuda, S. How do you RUN on? FEBS Lett 2011; 585: 1707–1710

Yoshino J, Morikawa RK, Hasegawa E, Emoto K. Neural Circuitry that Evokes Escape Behavior upon Activation of Nociceptive Sensory Neurons in Drosophila Larvae. Curr Biol 2017; 27(16): 2499-2504

Zahir F, Friedman JM. The impact of array genomic hybridization on mental retardation research: a review of current technologies and their clinical utility. Clin Genet 2007; 72(4): 271-287

Zelaya MV, Pérez-Valderrama E, de Morentin XM, Tuñon T, Ferrer I, Luquin MR, Fernandez-Irigoyen J, Santamaría E. Olfactory bulb proteome dynamics during the progression of sporadic Alzheimer's disease: identification of common and distinct olfactory targets across Alzheimer-related co-pathologies. Oncotarget 2015; 6(37): 39437-39456

Zhou Y, Sharma J, Ke Q, Landman R, Yuan J, Chen H, Hayden DS, Fisher JW 3rd, Jiang M, Menegas W, Aida T, Yan T, Zou Y, Xu D, Parmar S, Hyman JB, Fanucci-Kiss A, Meisner O, Wang D, Huang Y, Li Y, Bai Y, Ji W, Lai X, Li W, Huang L, Lu Z, Wang L, Anteraper SA, Sur M, Zhou H, Xiang AP, Desimone R, Feng G, Yang S. Atypical behaviour and connectivity in SHANK3-mutant macaques. Nature 2019; 570(7761): 326-331

8 Acknowledgements

I would like to show my gratitude to my supervisor, Prof. Dr. Peter Soba, for giving me the opportunity to pursue my PhD in his laboratory. I am very thankful for his guidance, patience, and support throughout my research.

My sincere thanks also go to Prof. Dr. Ilona Grunwald Kadow for her role as the second reviewer of my thesis. I am equally grateful to Prof. Dr. Benjamin Odermatt and Prof. Dr. Claudia Bagni for their invaluable contributions as members of my thesis committee. Their mentorship has been instrumental in my improvement during my doctoral studies.

I am thankful for the camaraderie and assistance of all the lab members, who guided and helped a lot in my fly work.

Lastly, I would like to show gratitude to my family and friends, whose love and support have been my cornerstone. This achievement would not have been possible without them.